



Probing the Dynamics of Soft Matter with Neutrons

Norman J Wagner

Chemical & Biomolecular Engineering,
Physics & Astronomy

University of Delaware, Newark, DE 19716 USA



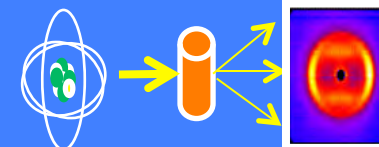
Neutron Measurements for Materials Design & Characterization





Center for Neutron Science

www.cns.che.udel.edu



Measuring the nanoscale to engineer nanomaterials for sustainable energy, protective materials, and improving human health

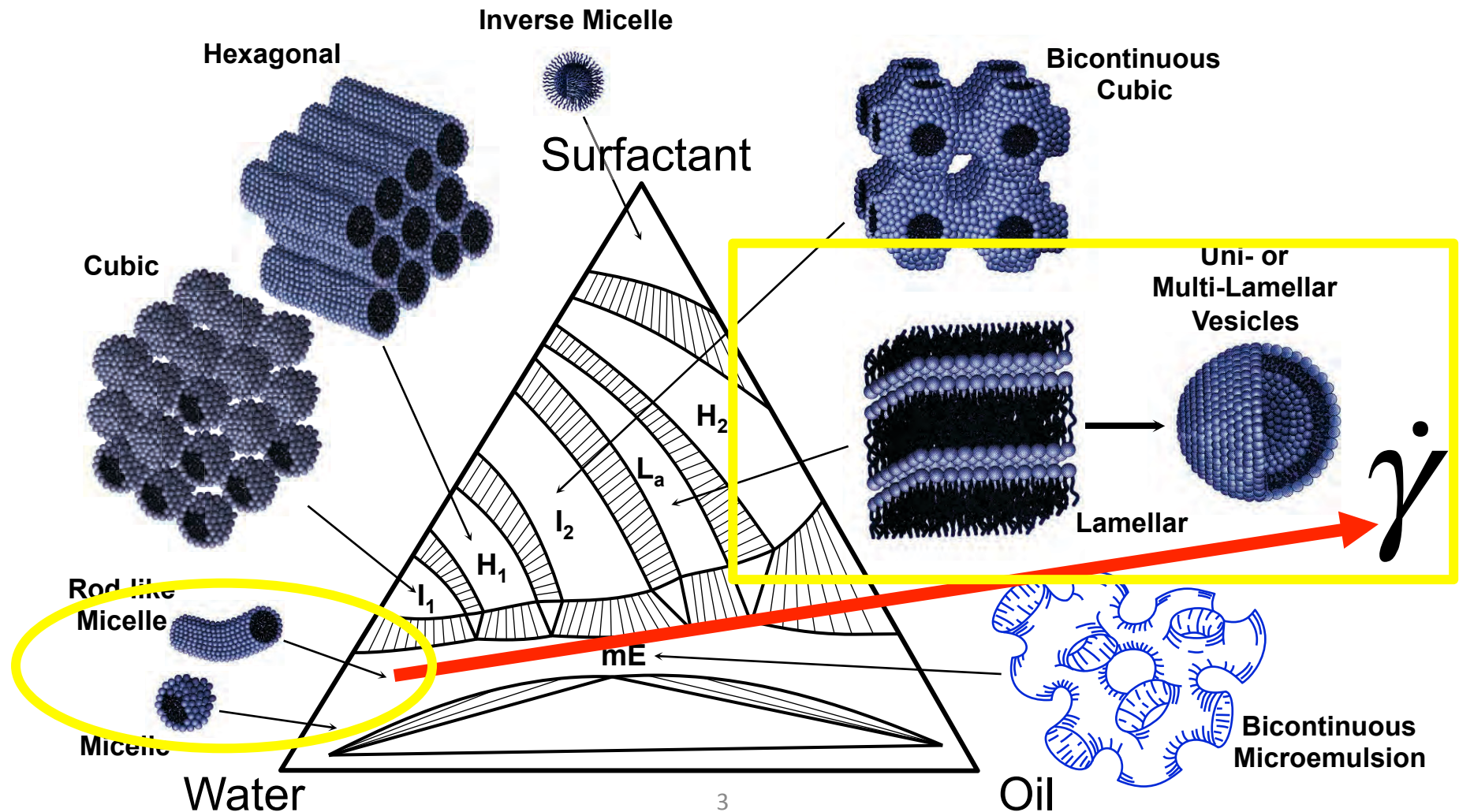
UD's Center for Neutron Science has a mission of exploring and developing new areas of neutron scattering science, with emphasis on strengths in engineering complex fluids, macromolecular science, and soft condensed matter. Our partnership with the **NCNR NIST** enhances the small angle neutron scattering (SANS) capabilities of the United States and make them available to a large scientific user community. It also educates the next generation of neutron scientists and engineers for careers in support of the national nanotechnology initiative.

Surfactant Self-Assembly



Lyophilic
"Oil-loving"

Hydrophilic
"Water-loving"



Applications for Wormlike Micelles (WLM)



- Consumer products
- Emulsifiers/Viscosifiers
- Drag reduction
- Enhanced oil recovery



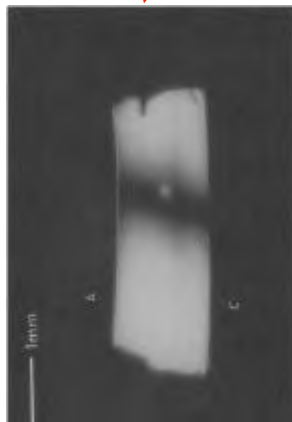
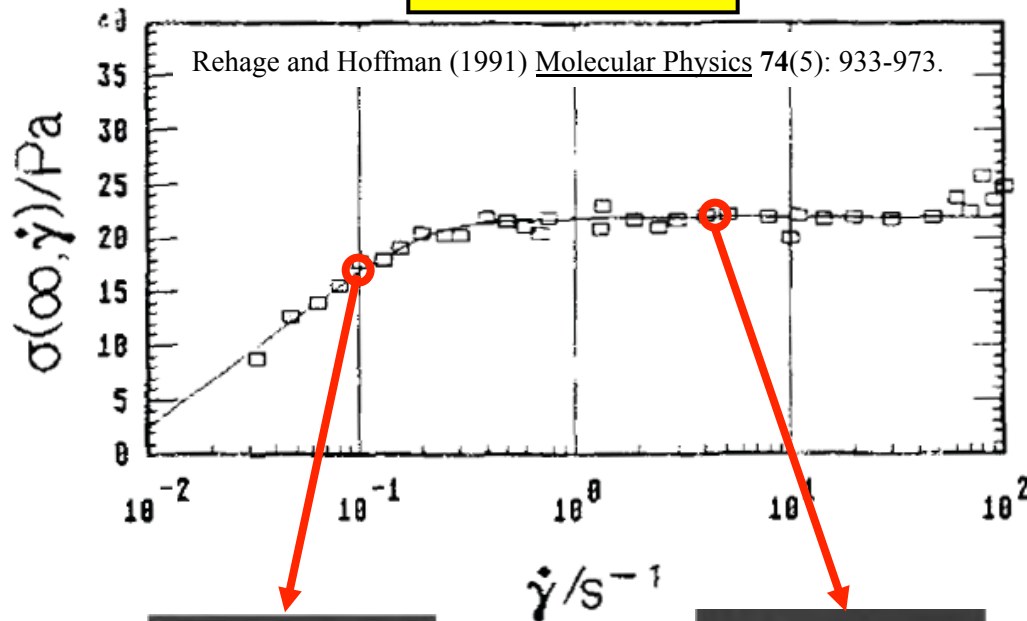
Applications require intimate knowledge of the structure and rheology of WLMs.



Shear banding in wormlike micelles : Summary



Stress plateau

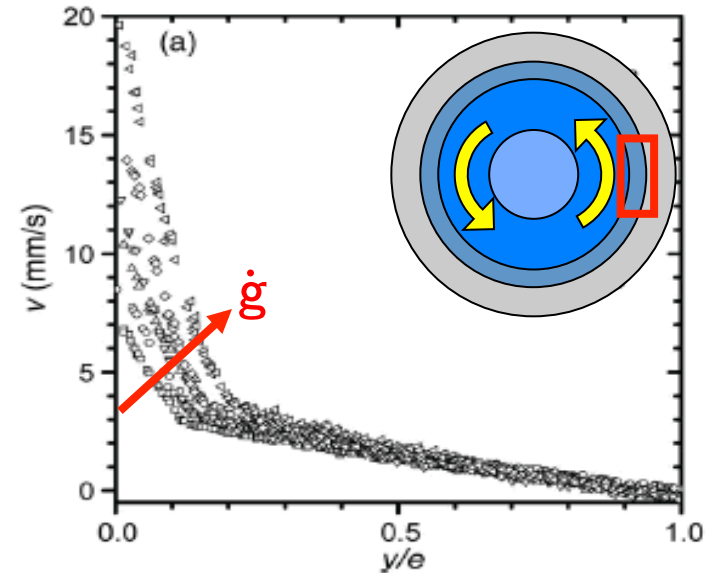


Decruppe et al. (1995) Coll. Polym. Sci. **273**(4): 346-351.

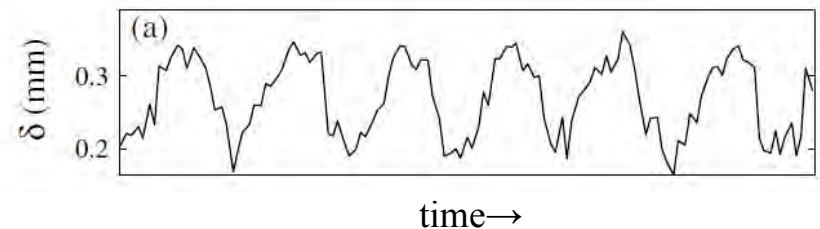
Birefringence banding

Heterogeneous flow

Hu and Lips (2005) J. Rheology **45**(1): 1001-10027.



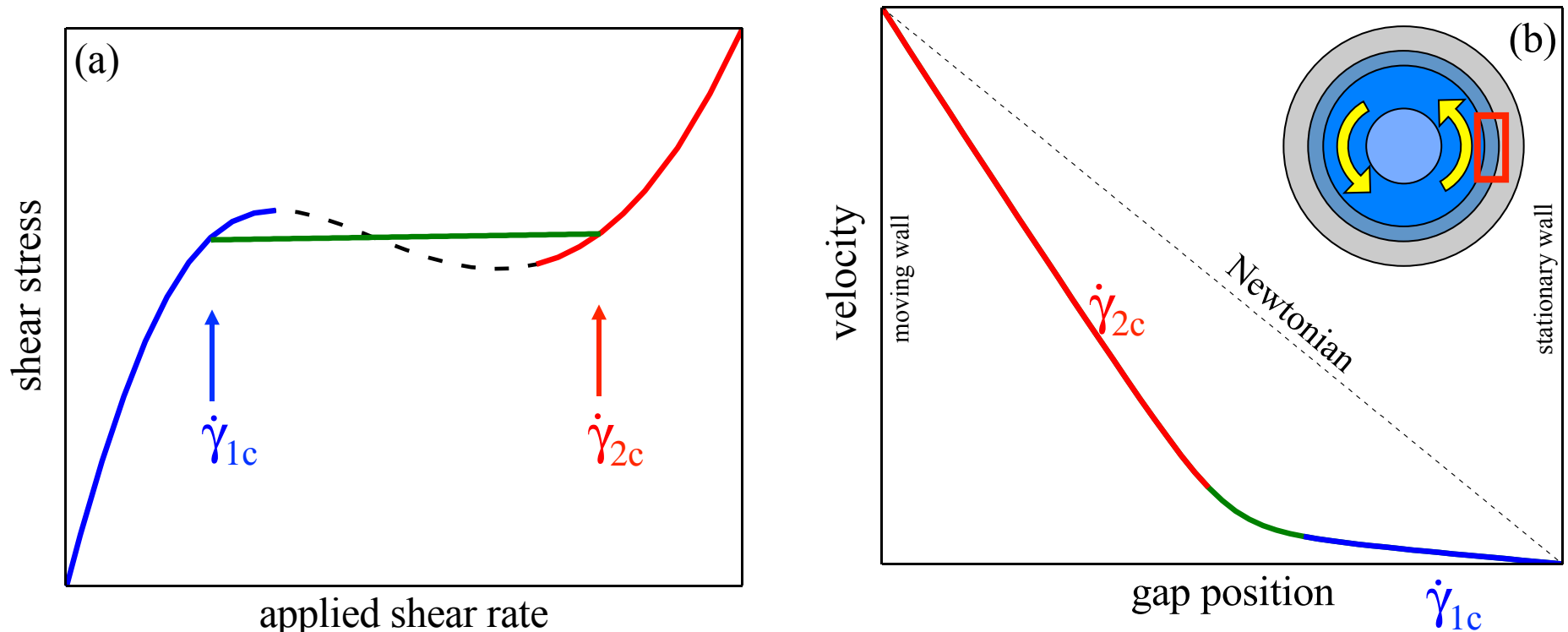
interface position



Becu et al. (2004) Phys Rev. Lett. **93**(1): 1-4

Spatiotemporal fluctuations

Theory of shear banding



Hypothesis: A non-monotonic constitutive relation results in segregation of the flow-field into two distinct shear “states”.

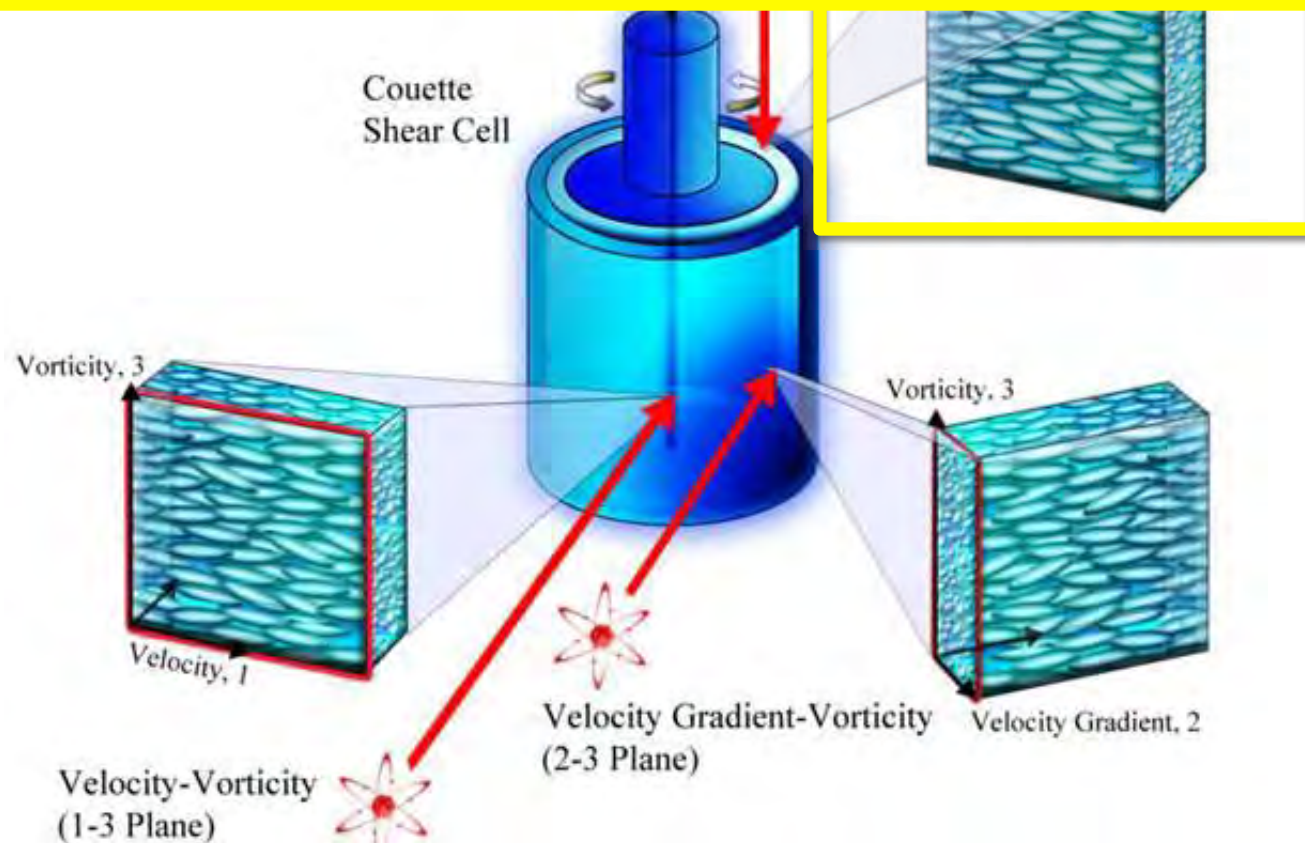
Questions: Are there microstructural changes driving this nonequilibrium instability?
Are there concentration differences between the bands?

Small Angle Neutron Scattering (SANS)

3-D real-space microstructure under shear



Gurnon, A. K., Godfrin, P. D., Wagner, N. J., Eberle, A. P. R., Butler, P., Porcar, L.
Measuring Material Microstructure Under Flow Using 1-2 Plane Flow-Small Angle Neutron Scattering.
J. Vis. Exp. (84), e51068, doi:10.3791/51068 (2014).

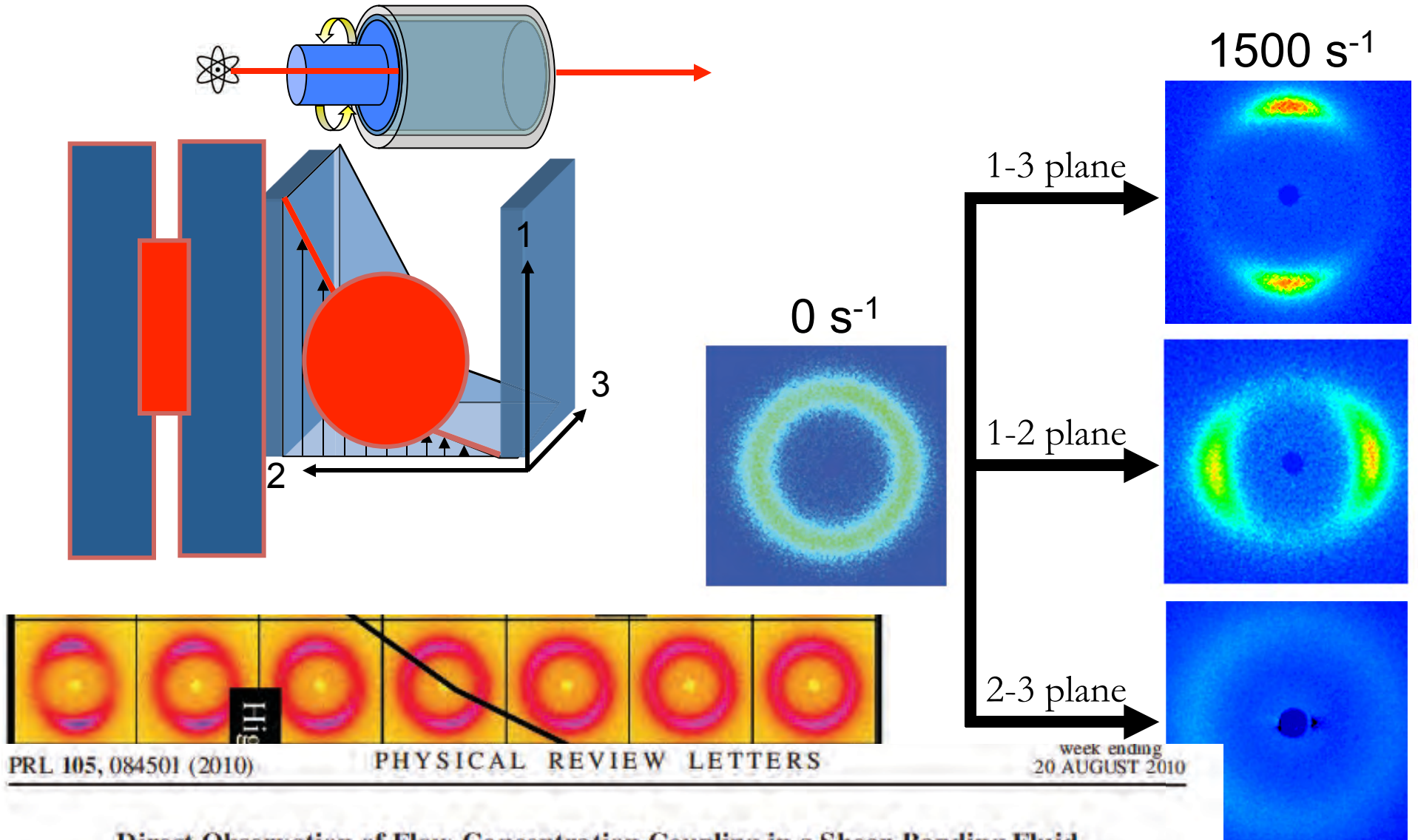


[1] A. Eberle and L. Porcar (2012) *Current Opinion in Colloid and Interface Science* 17(1): 33-43.

[2] [A. Kate Gurnon](#), P. Douglas Godfrin, Norman J. Wagner, Aaron P. R. Eberle, Paul Butler, Lionel Porcar. *Journal of Visualized Experiments*. 84, e51068 (2014).

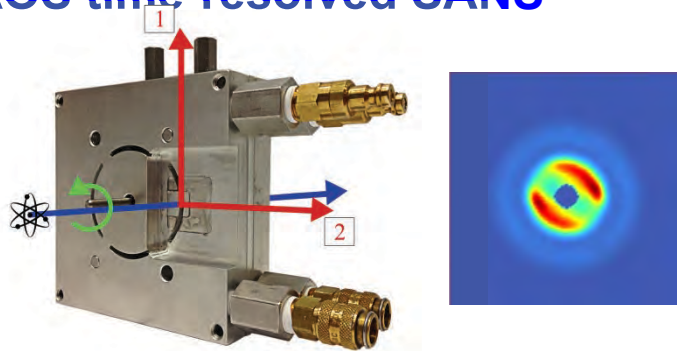
[3] M. Liberatore et al. *Phys. Rev. E* 73, 020504 (2006).

Spatial Resolution - SNAFUSANS: Scanning Narrow Aperture (SNA) Flow-U-SANS

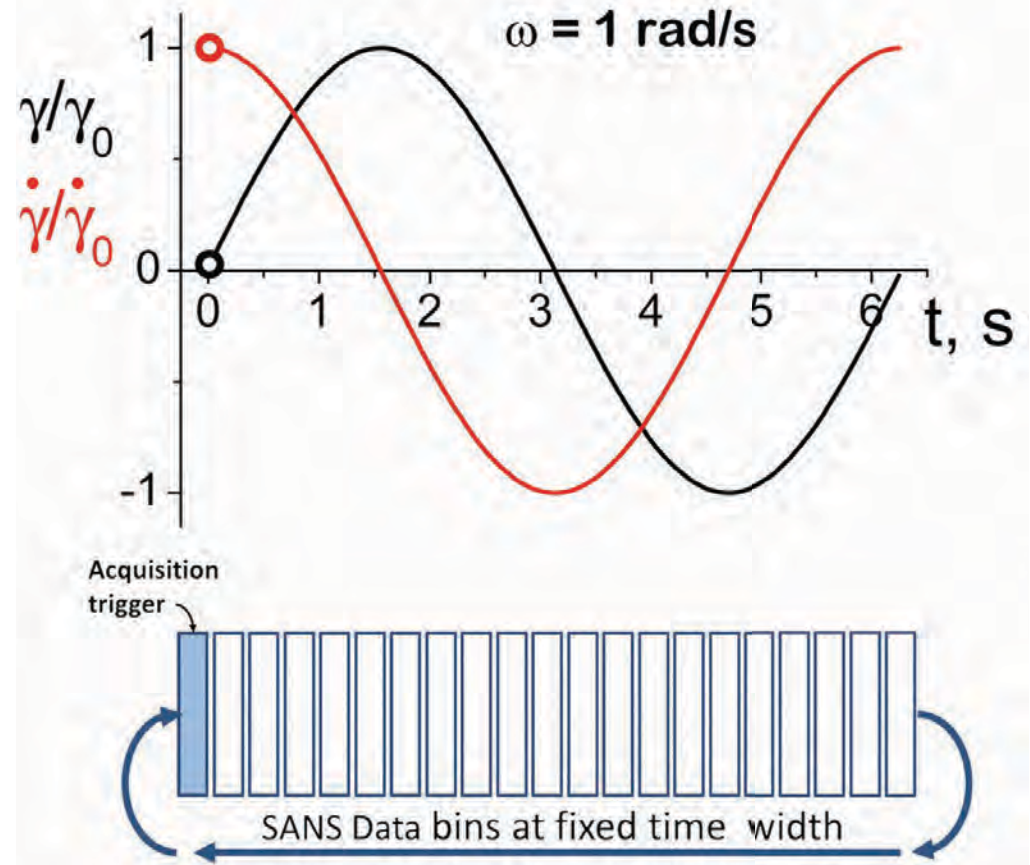
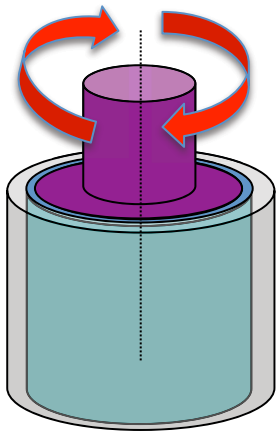


Time Resolution: LAOS + Stroboscopic SANS

velocity- velocity gradient plane
LAOS time-resolved SANS



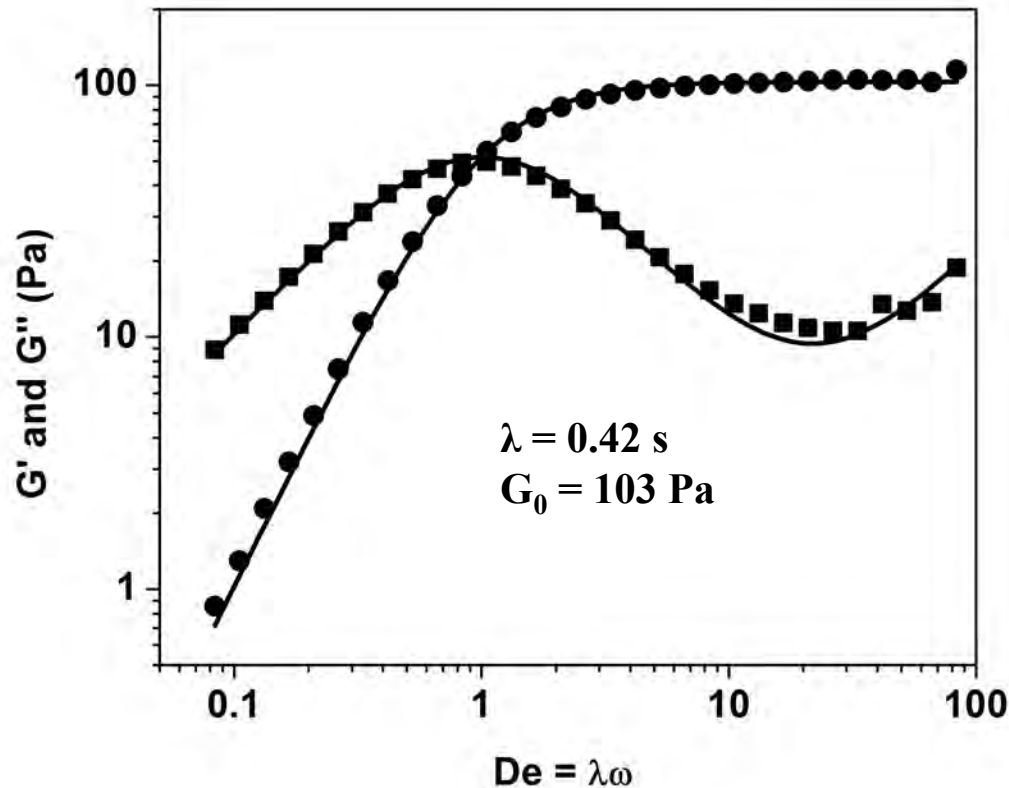
A. Kate Gurnon, P. Douglas Godfrin, Norman J. Wagner, Aaron P. R. Eberle, Paul Butler, Lionel Porcar. "Measuring Material Microstructure under flow using 1-2 plane flow- Small Angle Neutron Scattering," JOVE (2014).



Kim et al. *JOR* (2014), Gurnon et al. *Soft Matter* (2013)
Lopez-Barron et al. *Physical Review Letters*, 108, 258301 (2012).
Rogers, et al. *Soft Matter*, (2012), 8, 3831

Relevant length- and time- scales:

5.1% w/w cetylpyridinium chloride and 1.1% w/w sodium salicylate
(2:1 molar ratio) in a 0.5 M NaCl and D₂O brine



Dimensionless groups:

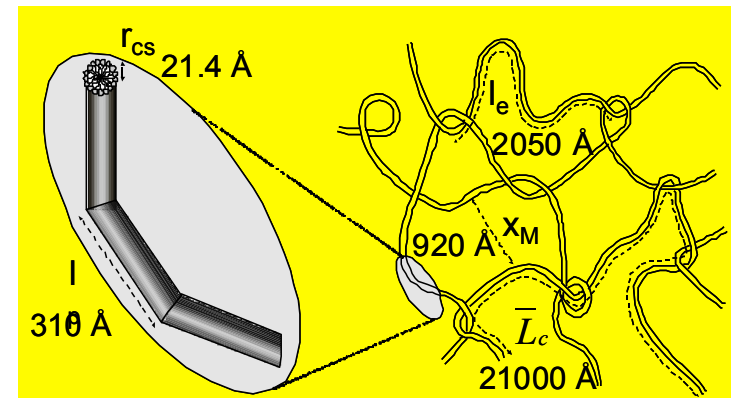
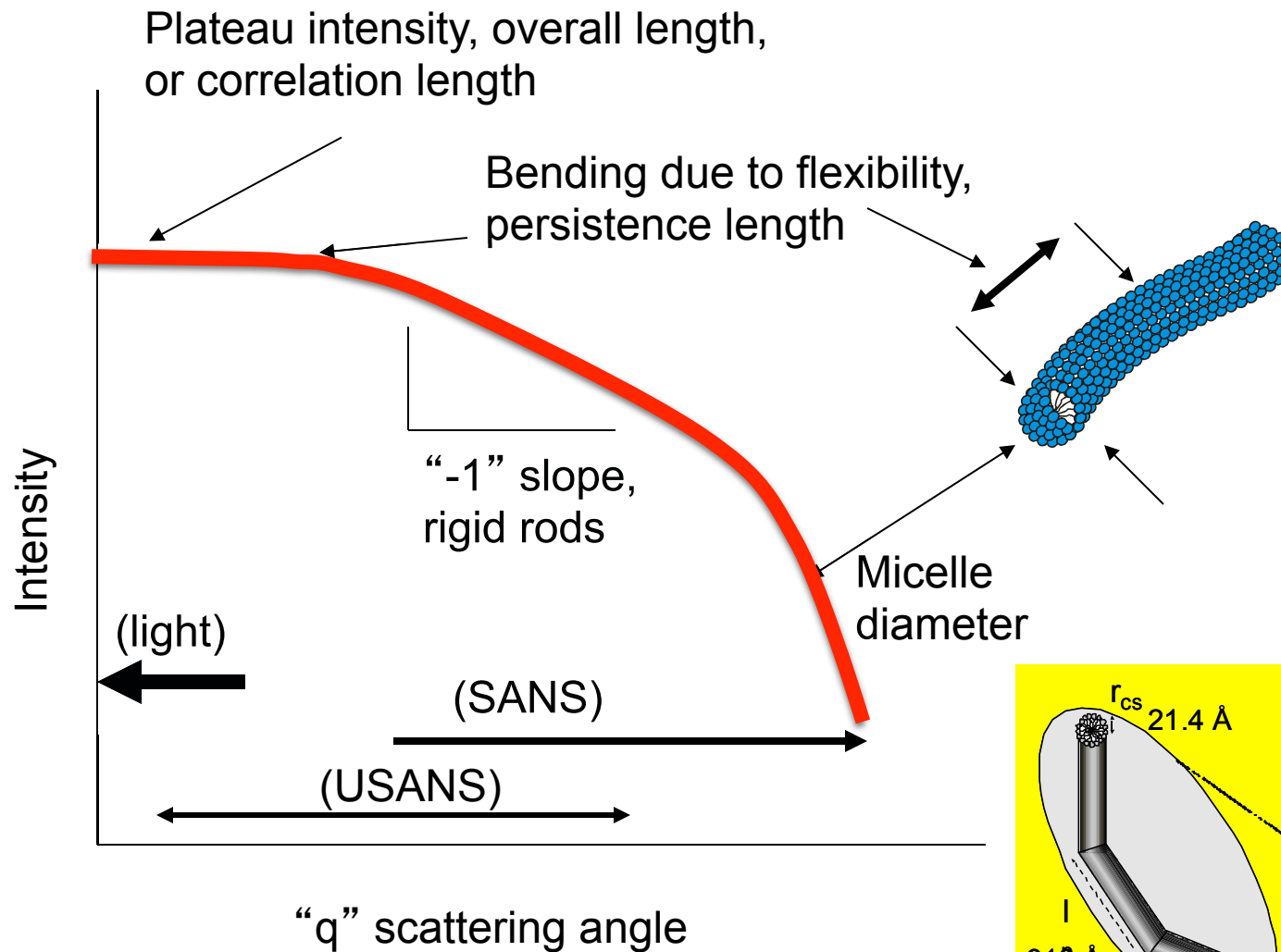
Deborah Number: $De = \lambda\omega = 0.23$ and 2.3

Weissenberg Number: $Wi = \lambda\omega\gamma_0 = 1.2, 2.3$ and 23

x_m [nm]	34 ± 5	$(k_b T / G_0)^{1/3}$
l_p [nm]	24 ± 3	from birefringence measurements ²
l_e [nm]	43 ± 15	$x_m^{5/3} / l_p^{2/3}$
L_c [nm]	334 ± 100	$G''_{\min} / G_0 = l_e / L_c$
r_{cs} [nm]	1.8 ± 0.1	From SANS model fit
Δ_{SLD}	$6.08 \cdot 10^{-6}$	$\rho_{SLD, PLM} - \rho_{SLD, solvent}$

² F. Nettesheim, M. W. Liberatore, M. E. Helgeson, P. A. Vasquez, P. Cook, Y. T. Hu, N. J. Wagner, L. Porcar. Microstructural mechanisms for shear banding in semi-dilute wormlike micellar solutions. (*in preparation*).

Scattering angle “ q ” $\propto 1/\text{Length}$

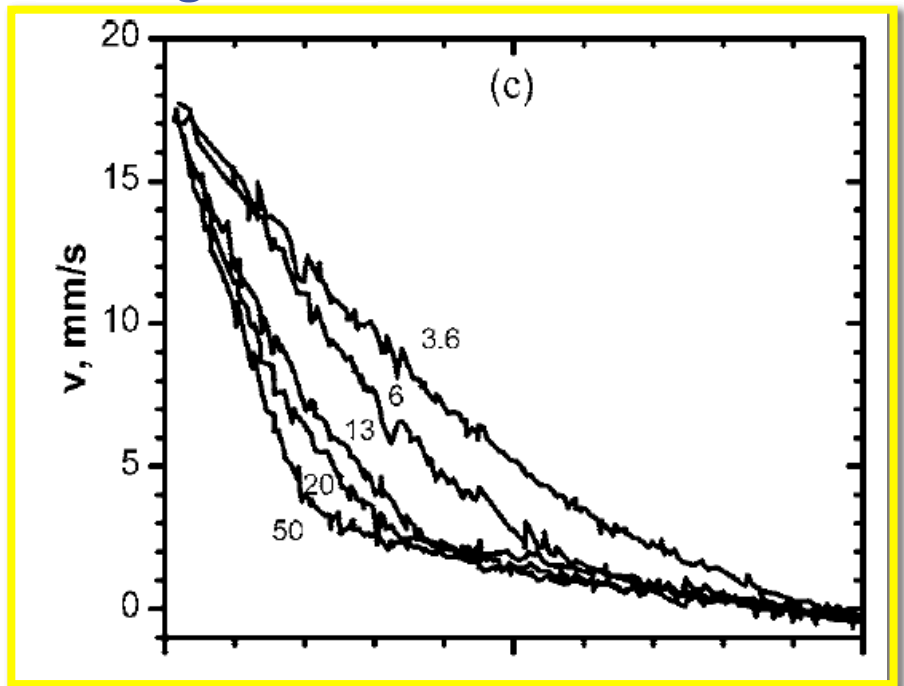


Conflicting Mechanisms Proposed for Shear Banding

Shear-induced Nematic
transition

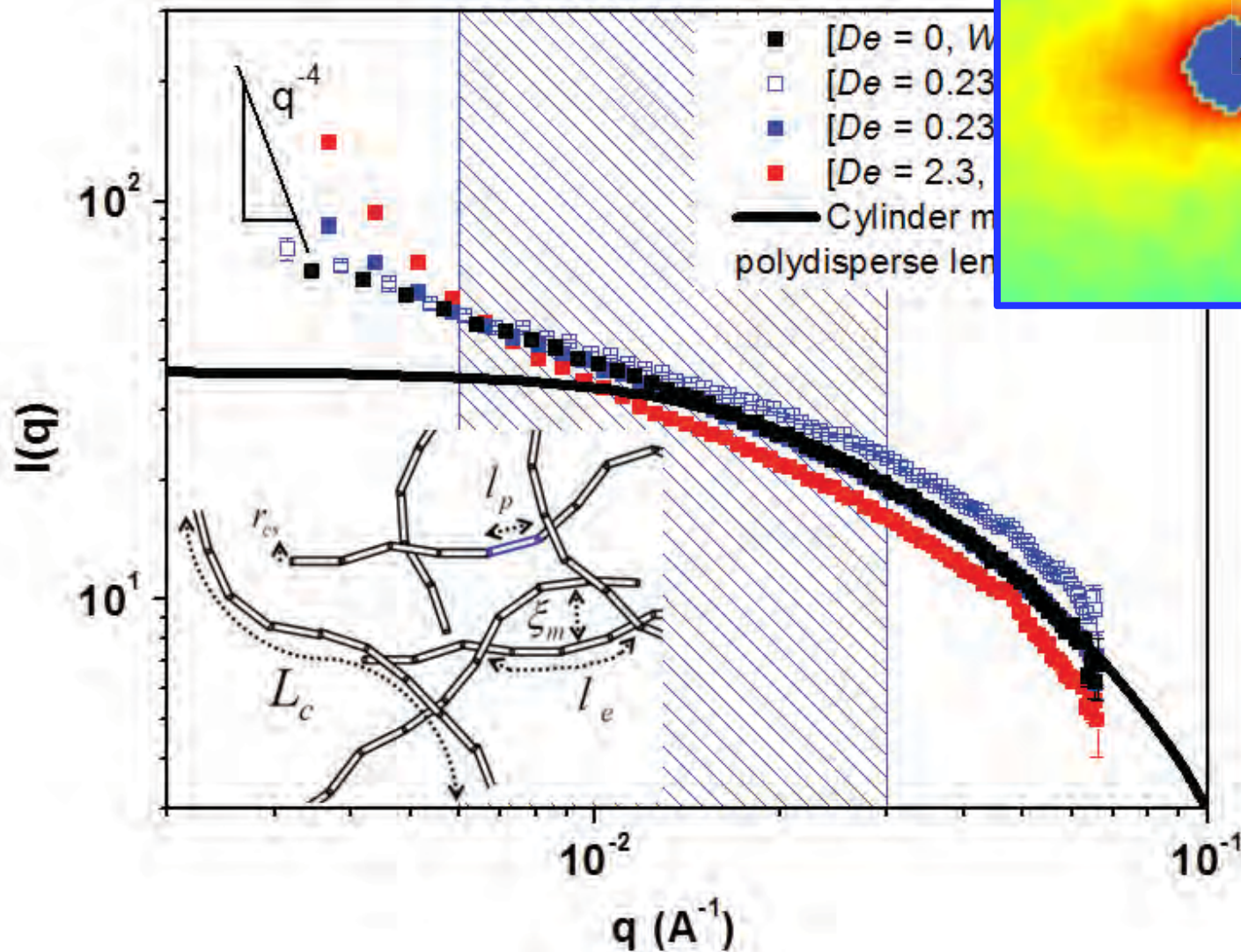


Disentanglement-re-
entanglement



Relevant length- and time- scales:

5.1% w/w cetylpyridinium chloride and 1.1% w/w sodium salicylate
(2:1 molar ratio) in a 0.5 M NaCl and D₂O brine

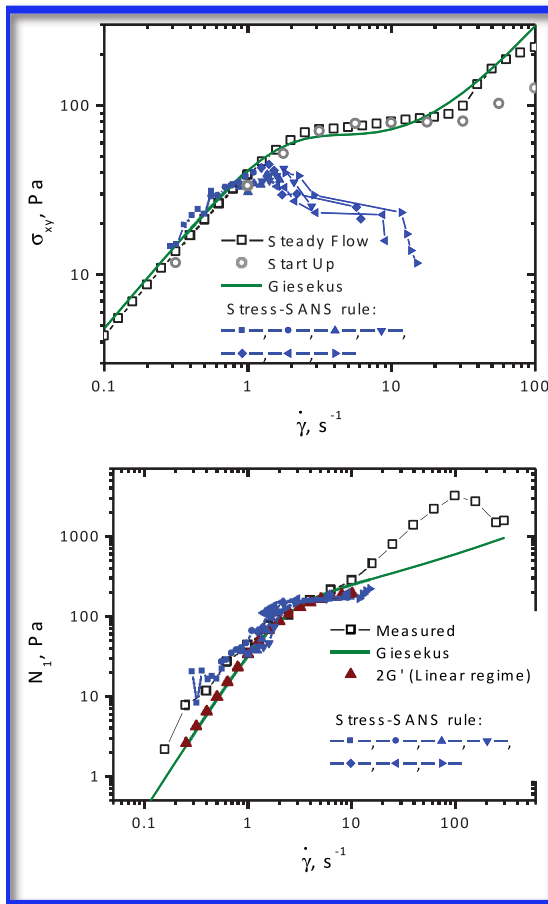
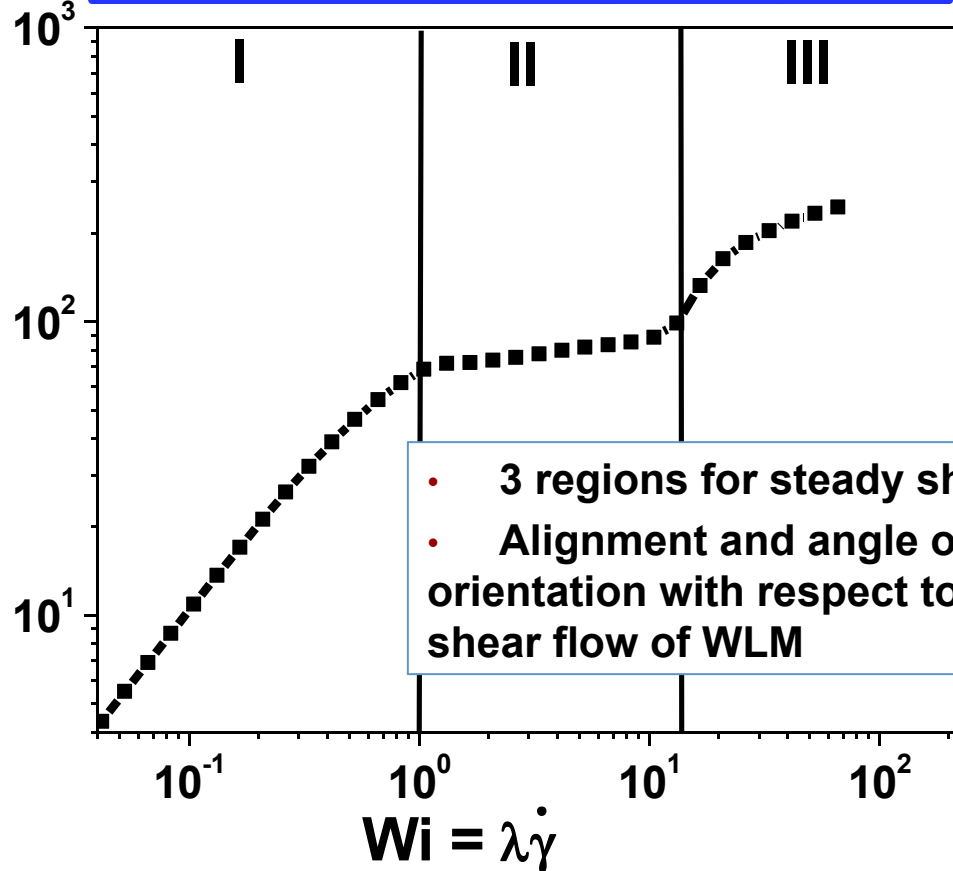
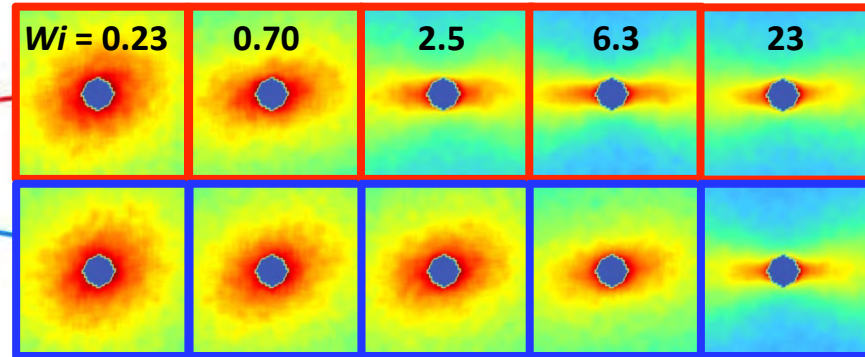
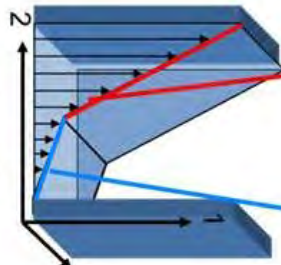


The WLMs persist for steady and oscillatory shear conditions.

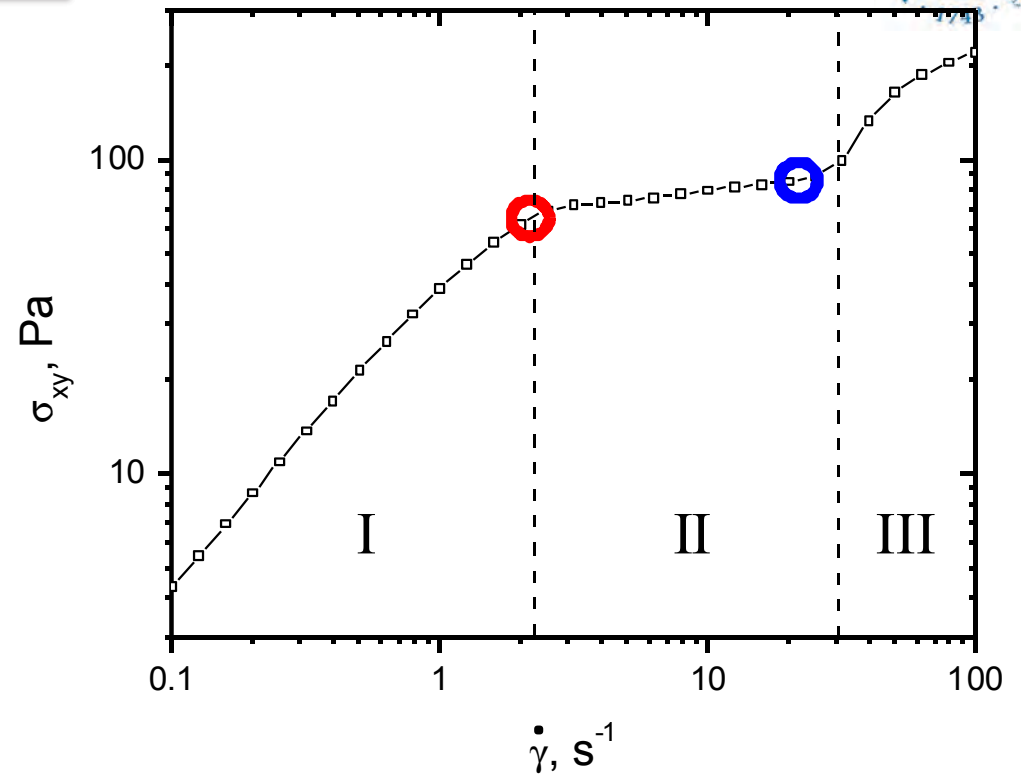
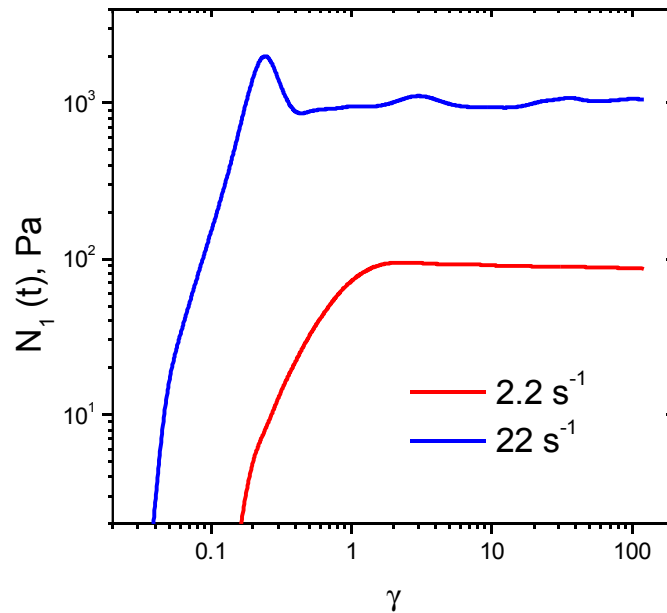
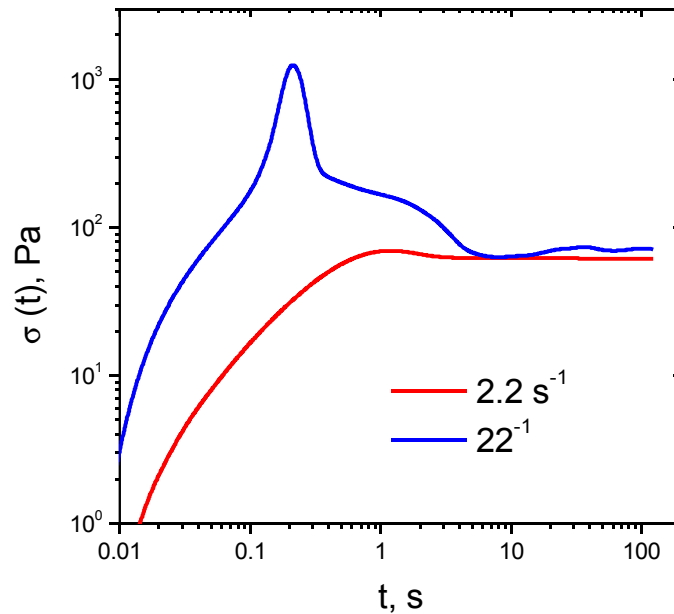
Shear banding microstructure during steady shear flow: Stress-SANS rule

$$\sigma = G_0 (CA_f)^{1/2} \sin(2\phi)$$

Planes of shear



Transient (start-up) flows

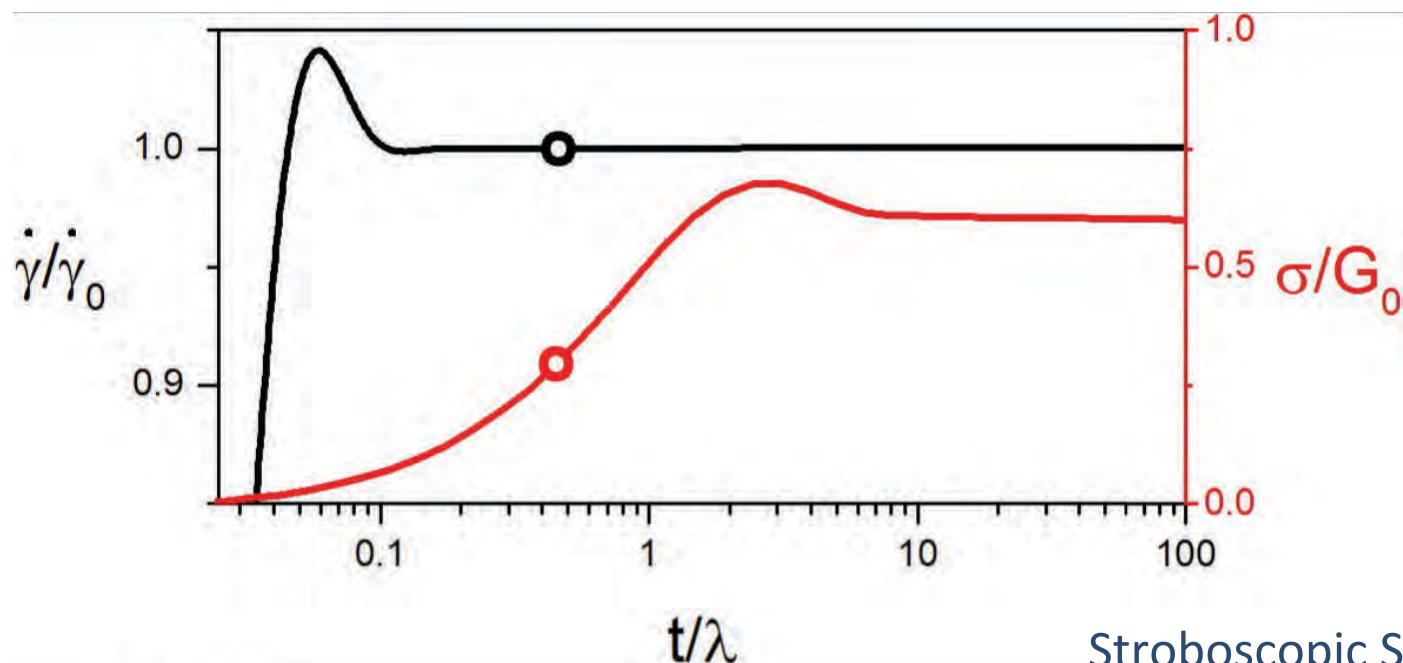


Shear rates:

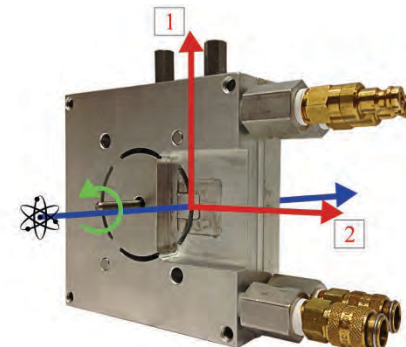
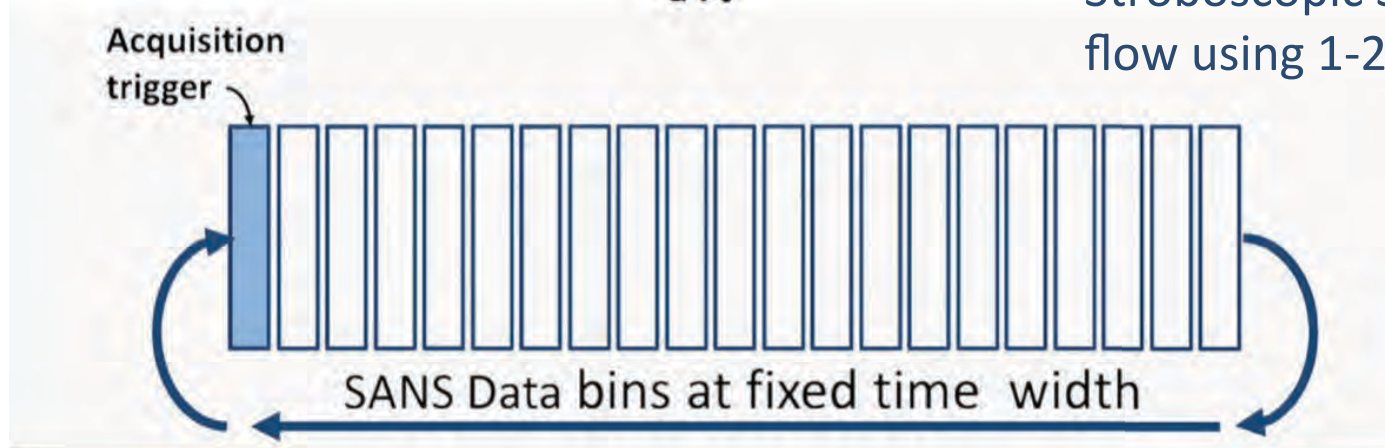
2.2 s^{-1} limit of shear regions I and II

22 s^{-1} deep into shear region II

Spatial and Temporal resolved flow-SANS

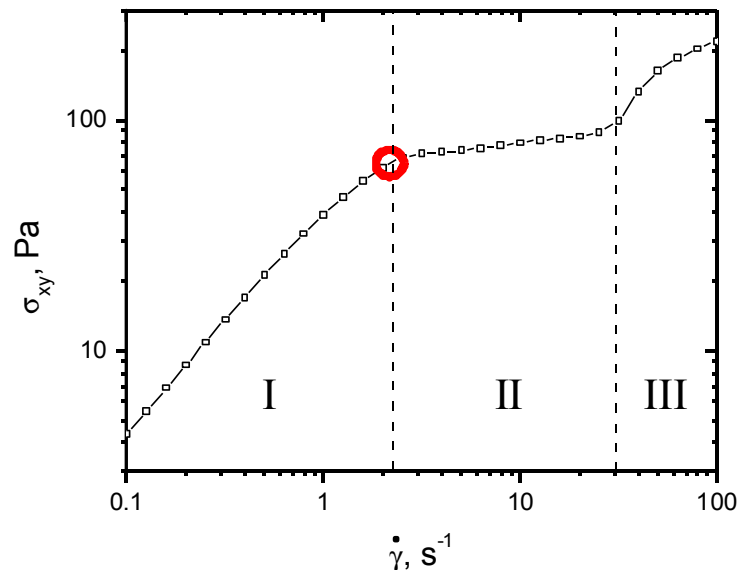


Stroboscopic SANS during start-up flow using 1-2 shear cell



[1] C. Lopez-Barron *et al.* *Physical Review Letters*, 108, 258301 (2012).

Transient (start-up) “slow” flow



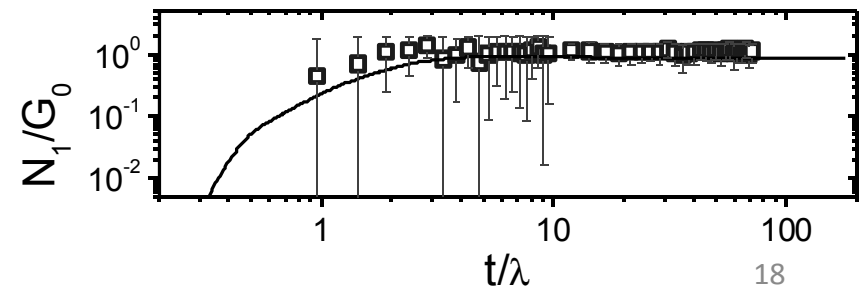
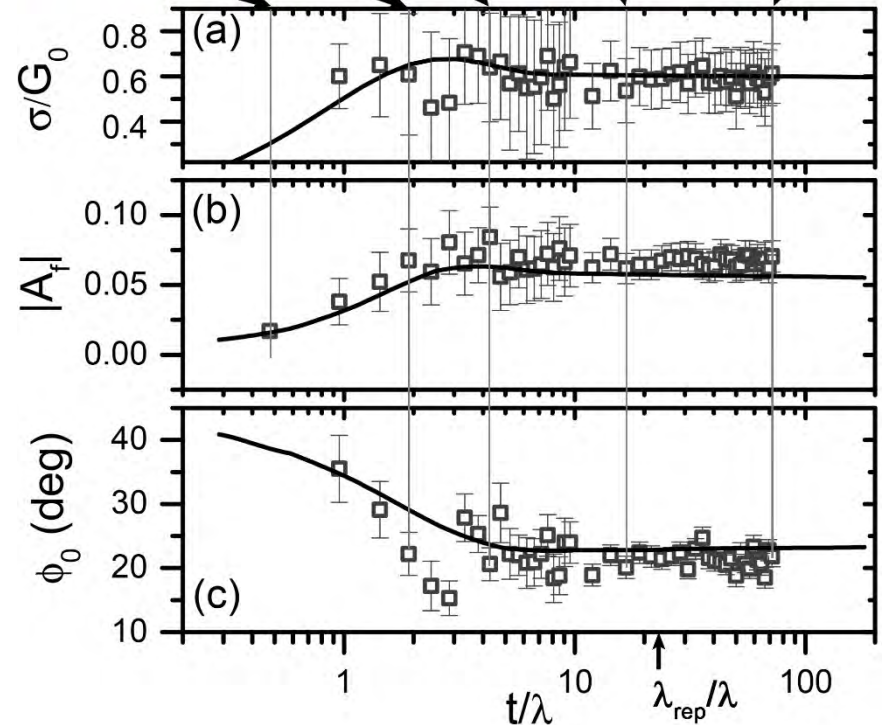
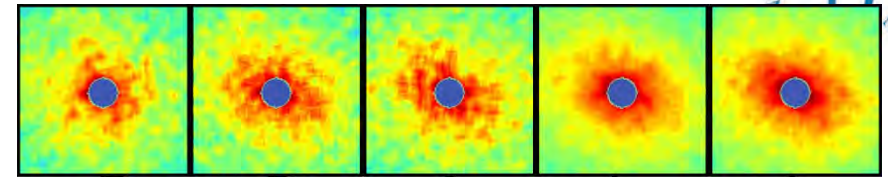
Shear rate = 2.2 s^{-1}

- Homogeneous flow
- Both s and N_1 well predicted by SSR (with $C_1 = 11.2$)

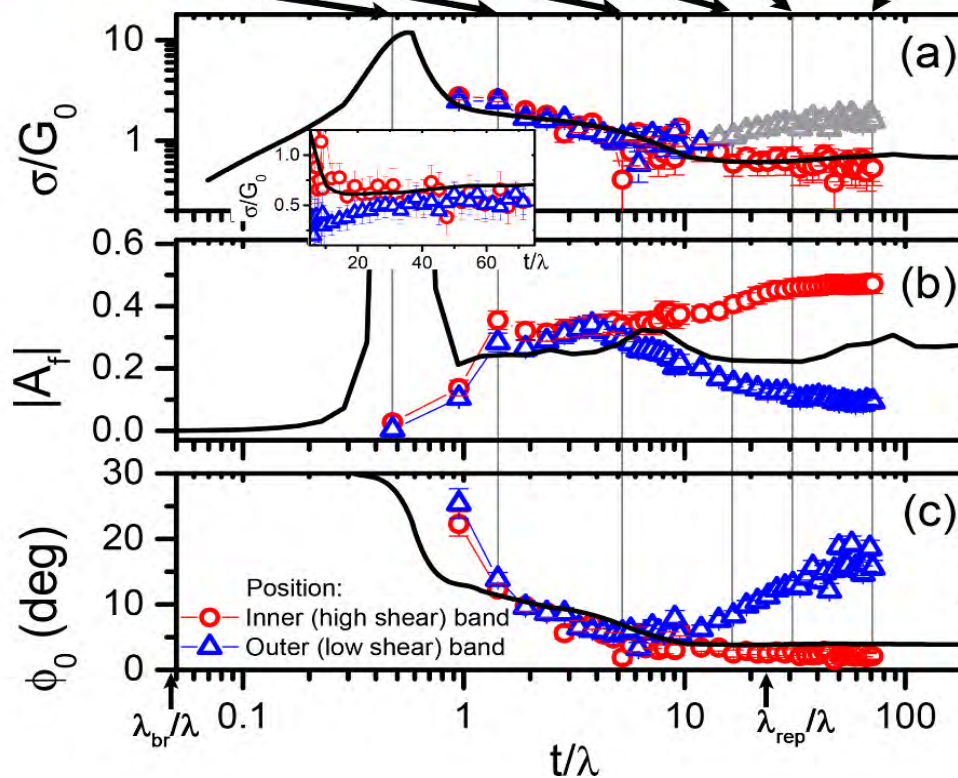
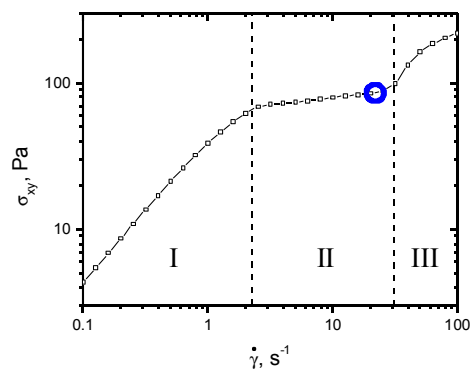
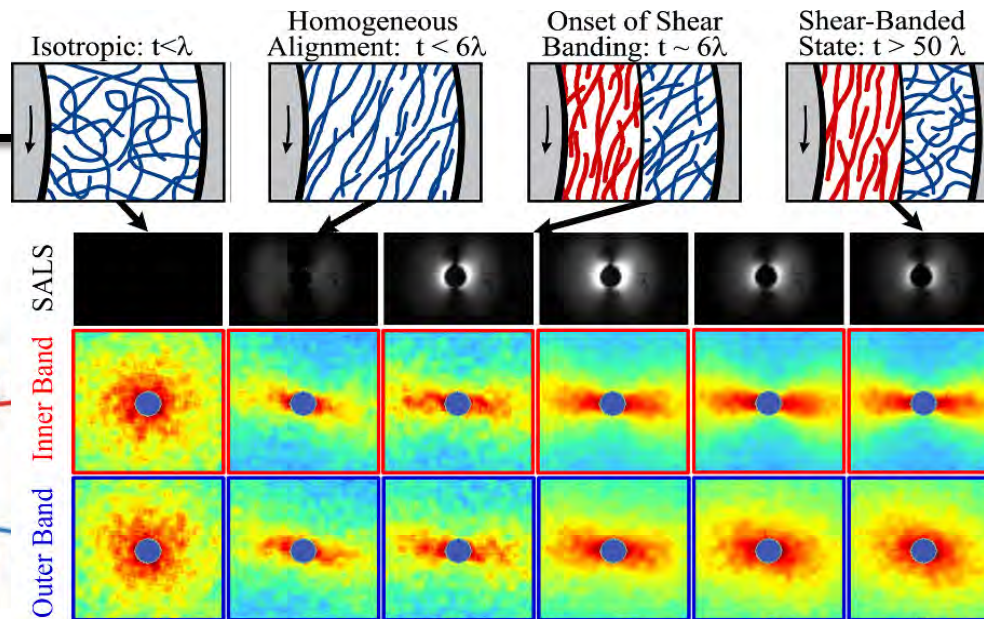
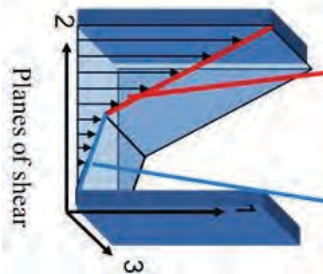
$$\sigma = G_0 (C_1 A_f)^{1/2} \sin(2\phi_0)$$

$$N_1 = G_0 (C_1 A_f)^{1/2} \cos(2\phi_0)$$

- A_f and Φ_0 are also well predicted by SSR from measured stress and N_1 .

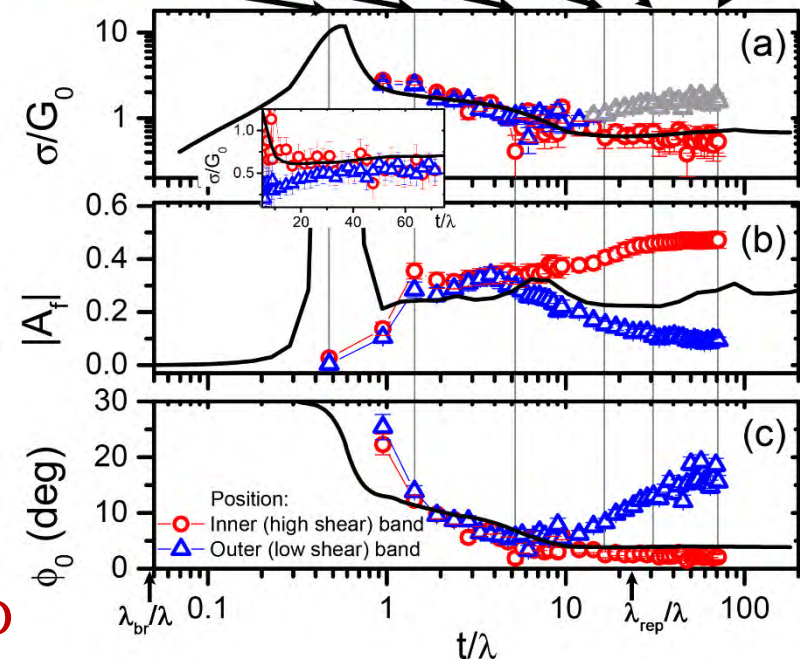
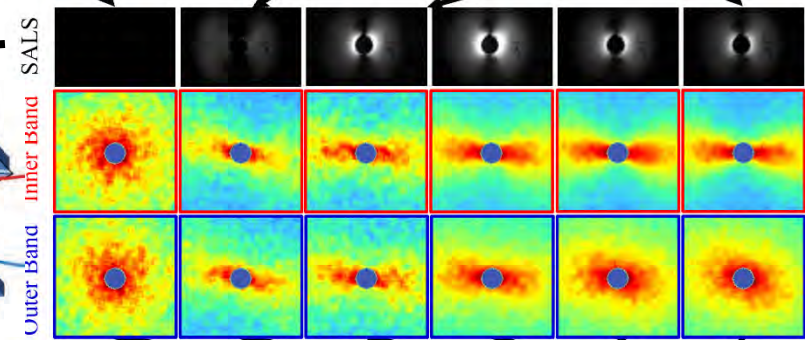
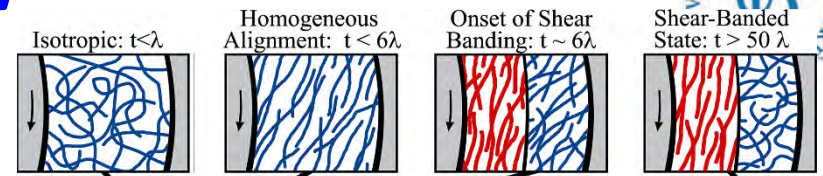
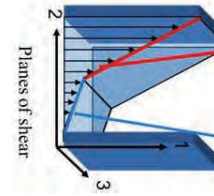
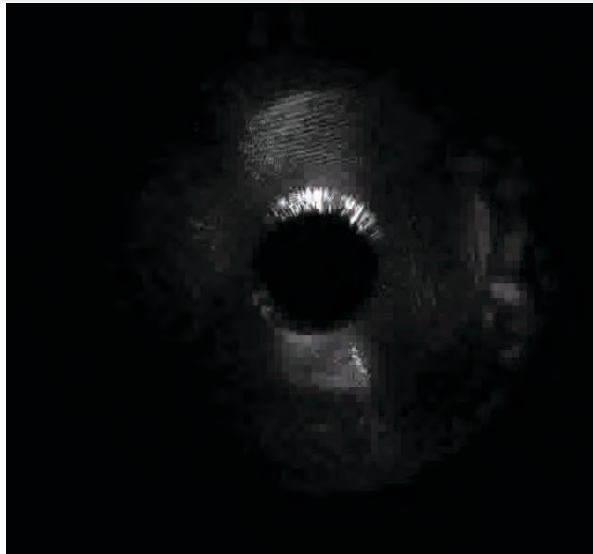


Transient (start-up) “fast” flow



Transient (start-up) “fast” flow

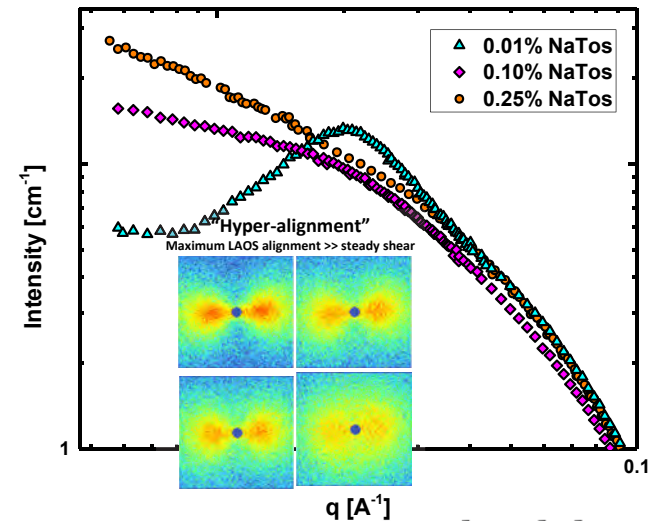
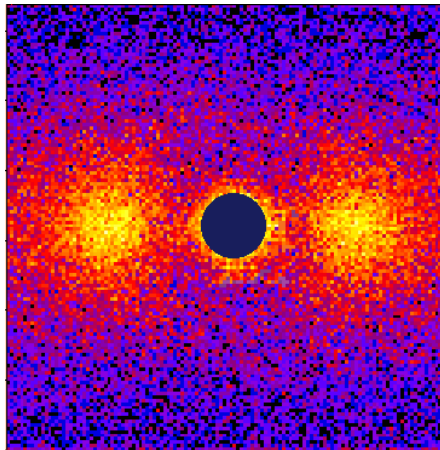
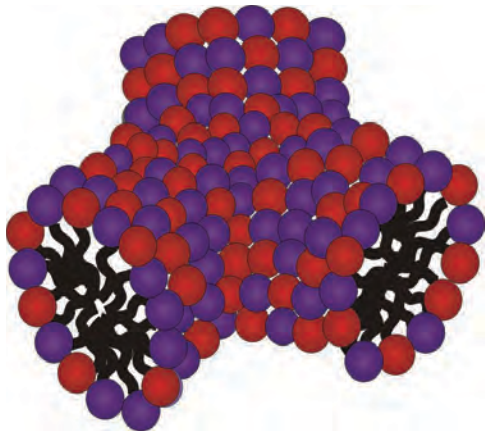
SALS
(1-3 plane)



Shear rate = 22 s^{-1}

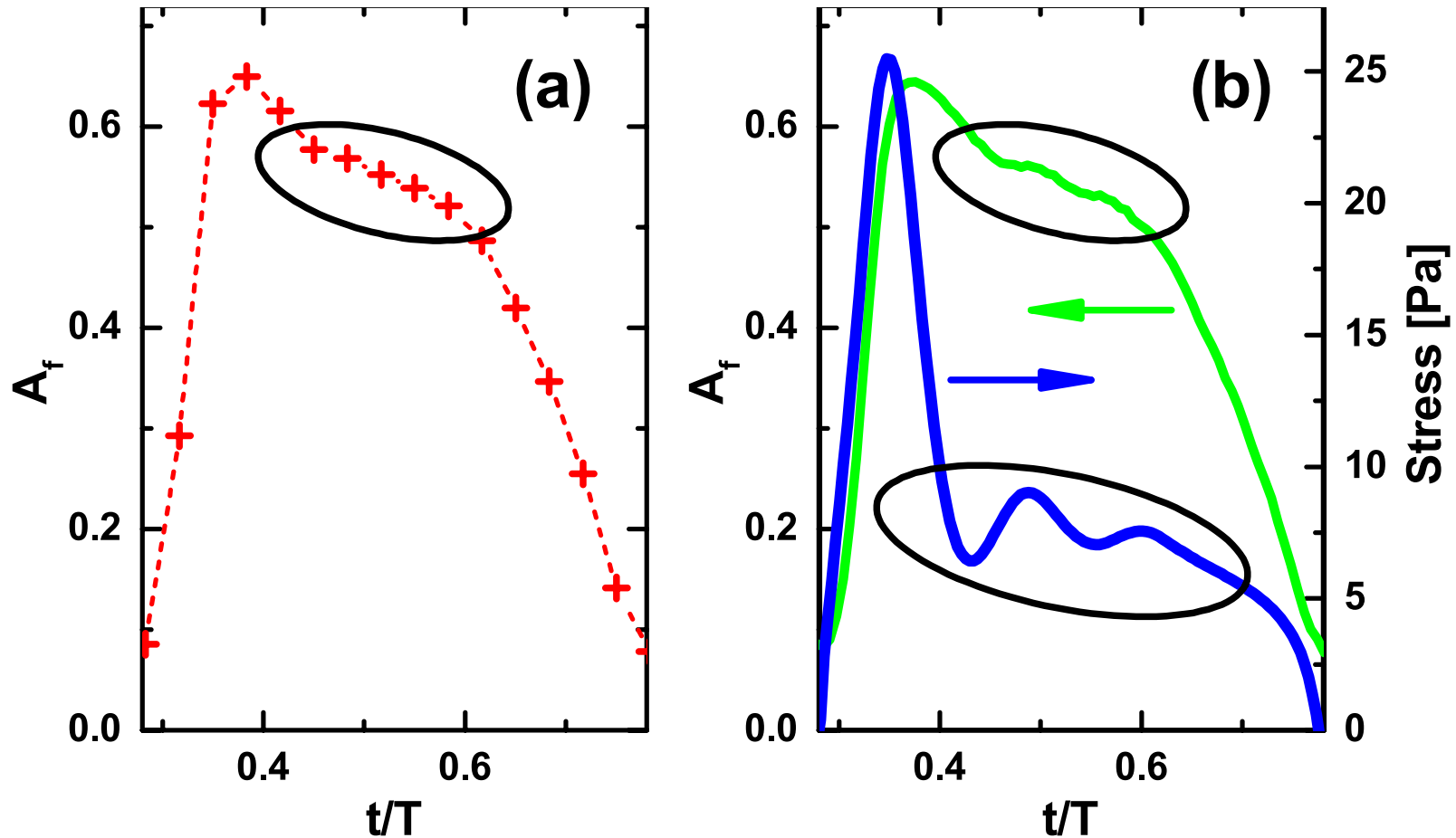
- Butterfly (BF) SALS patterns:
 - Appear after stress overshoot, i.e., no SID during initial elastic response.
 - Oscillation in BF intensity at $\lambda < t < 25\lambda$
 - Steady BF intensity at $t > 25\lambda$, coincident with onset of SB state.
- Shear banding instability accompanied by SID driven by stress-concentration coupling.

Effects of Micellar Branching: Michelle Calabrese & Dr. Simon Rogers



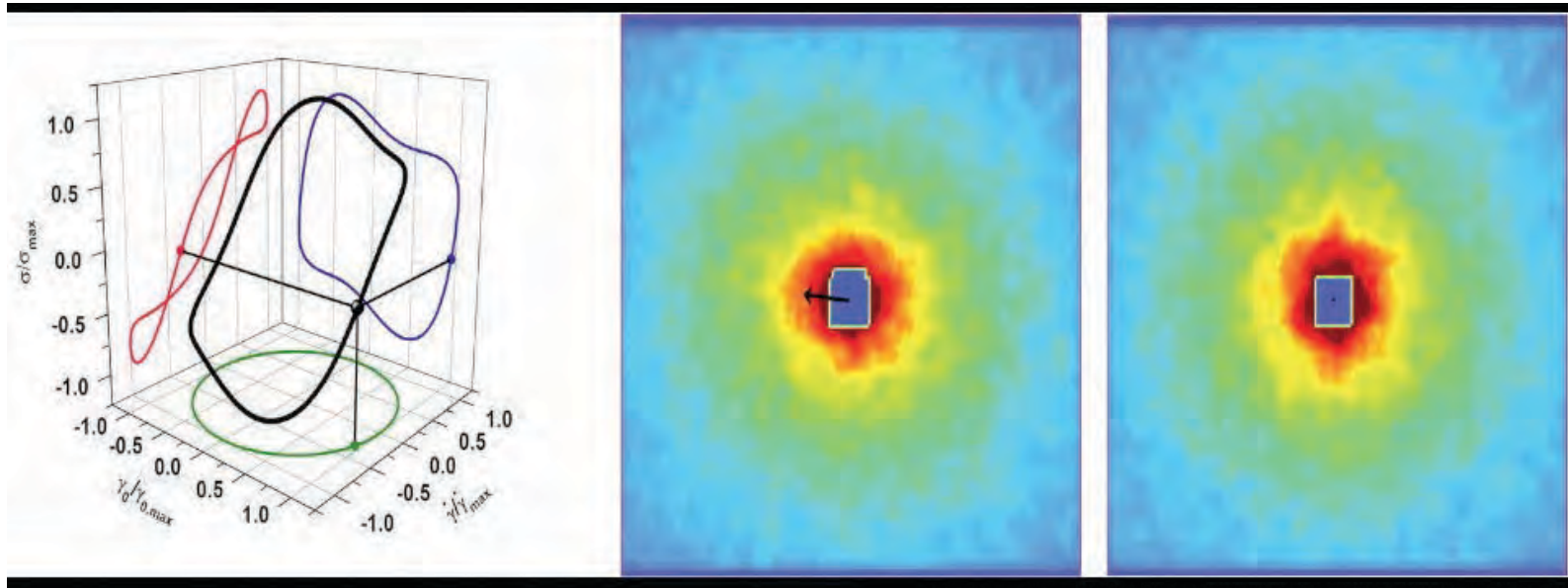
Thareja, P., Hoffmann, I.H., Liberatore, M.W., Helgeson, M.E., Hu, Y.T., Gradzielski, M., and Wagner, N.J., "Shear-induced phase separation (SIPS) with shear banding in solutions of cationic surfactant and salt". *Journal of Rheology*. **55**(6): p. 1375-1397 (2011).

Improvements in Time Resolution < 0.004s possible



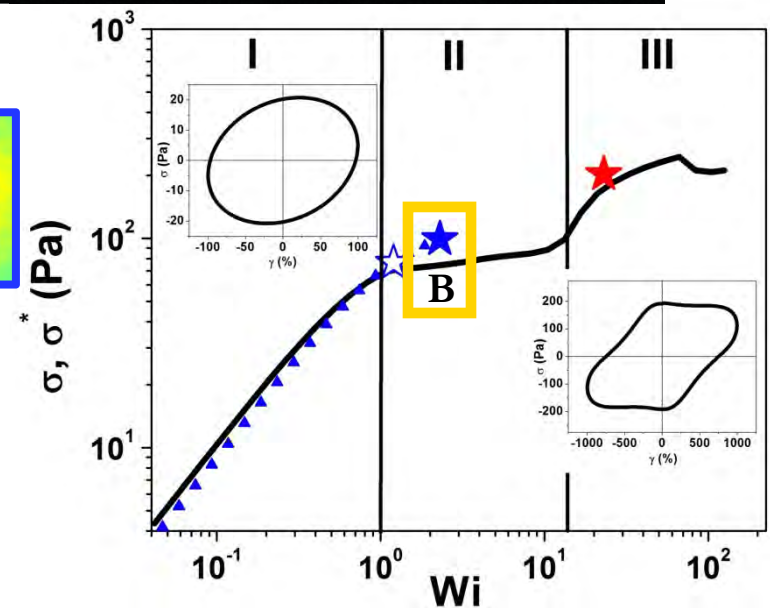
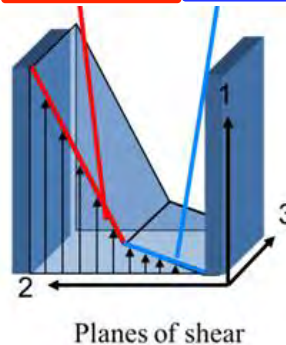
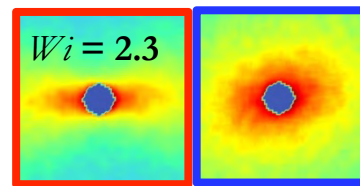
Metastable states of WLMs created with LAOS

[$De = 0.23$, $Wi = 2.3$]



- Steady shear = shear banding
- No banding instead a metastable state created and interrogated using LAOS
- Secondary loops associated with a stress overshoot during LAOS

Gurnon et al. Soft Matter, 2014



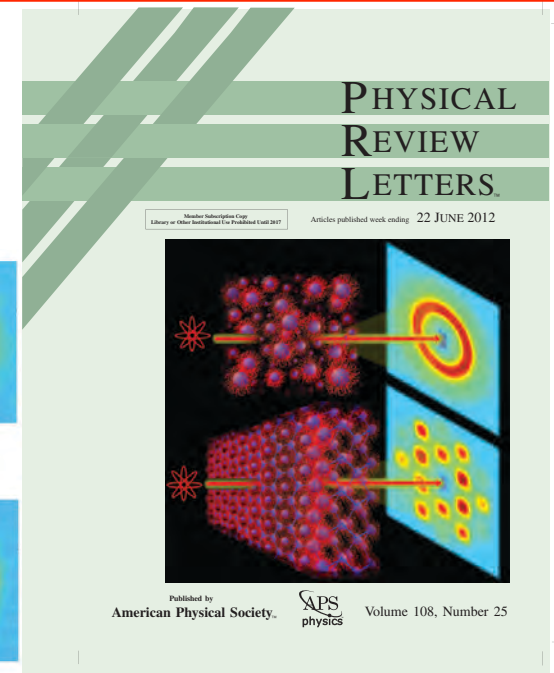
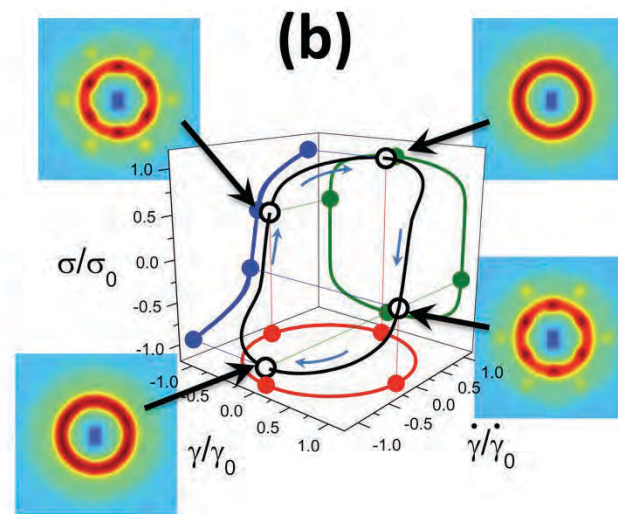
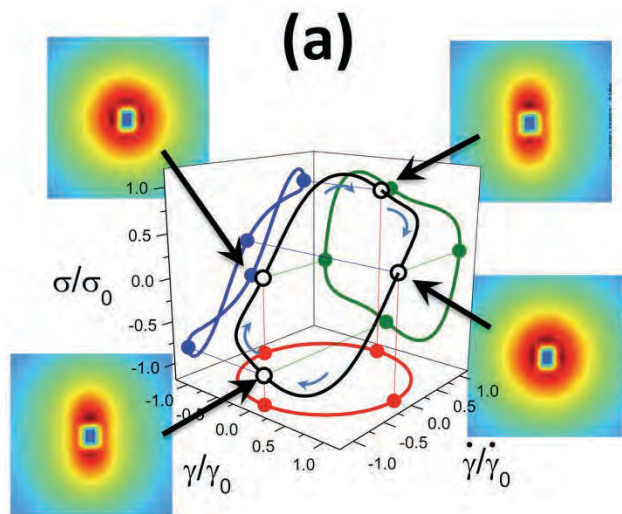
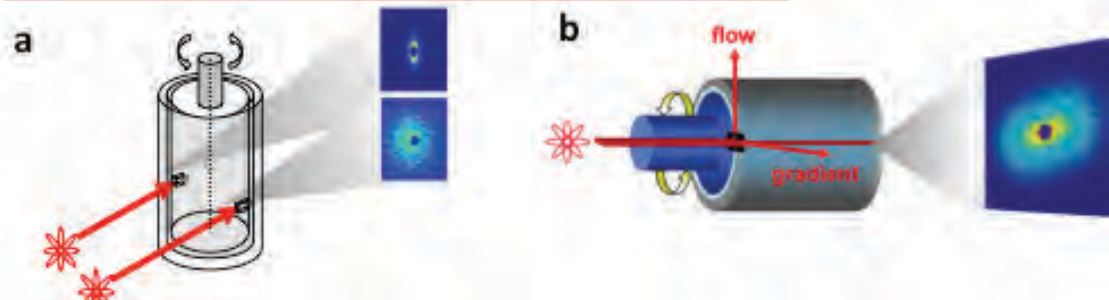
Flow-SANS and Rheo-SANS Applied to Soft Matter

Aaron P.R. Eberle & Lionel Porcar

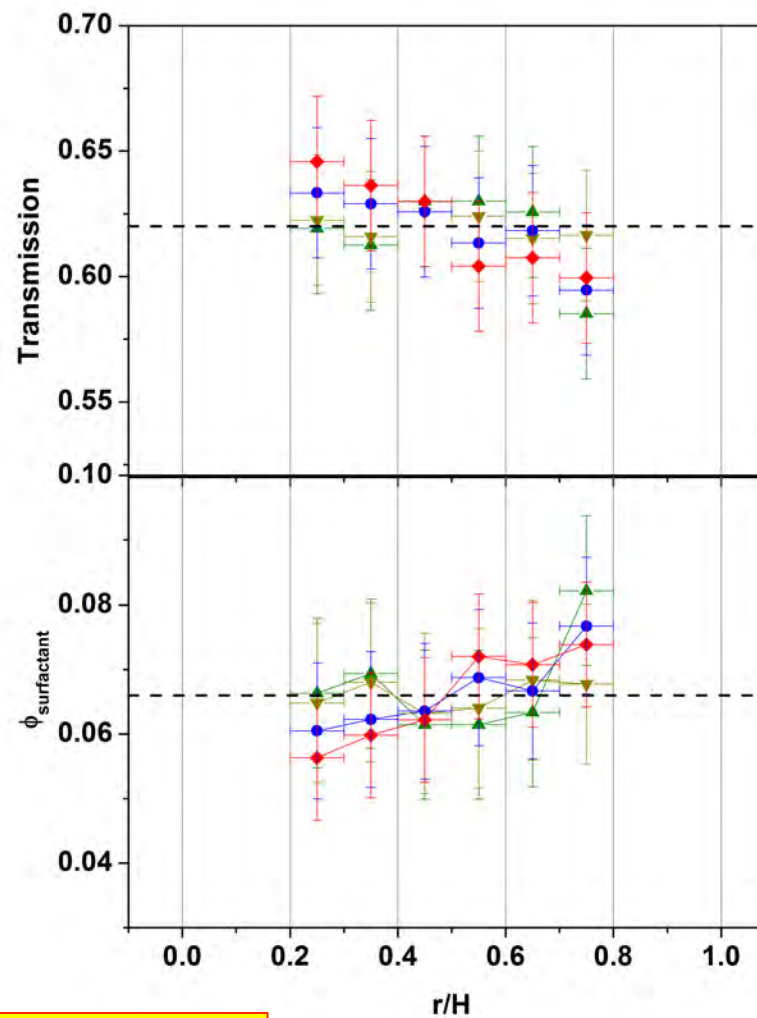
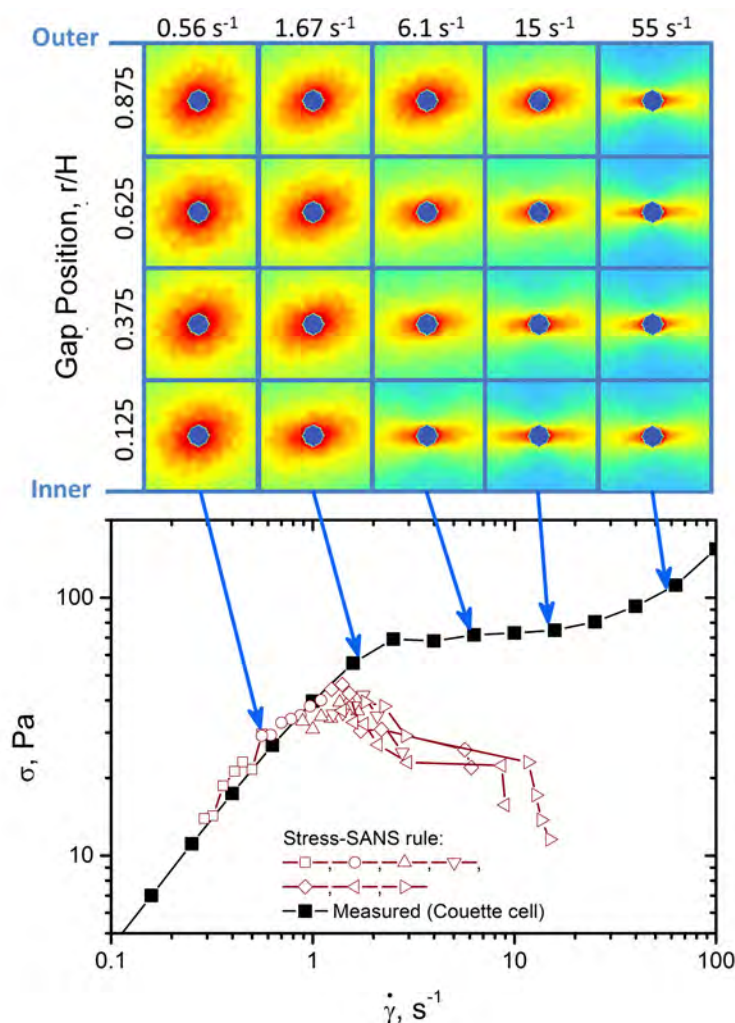
Curr. Opin. Coll. Int. Sci. **17** (2012) 33-43

SOR Rheology Bulletin, July 2012

Lopez-Barron et al. , PRL
108 258301 (2012)

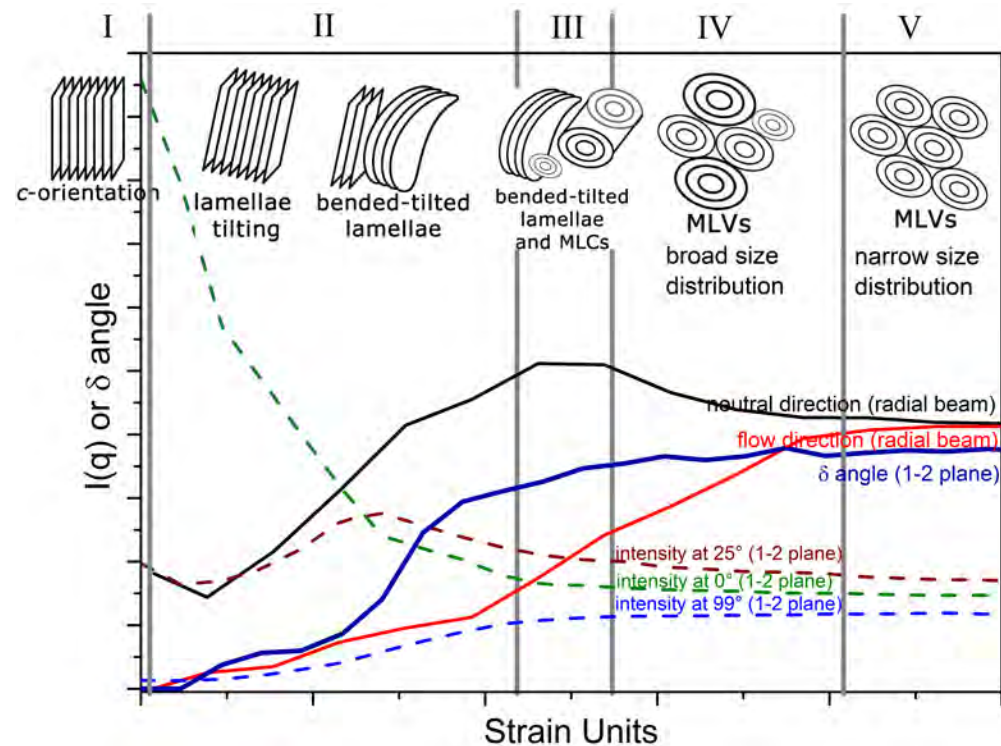
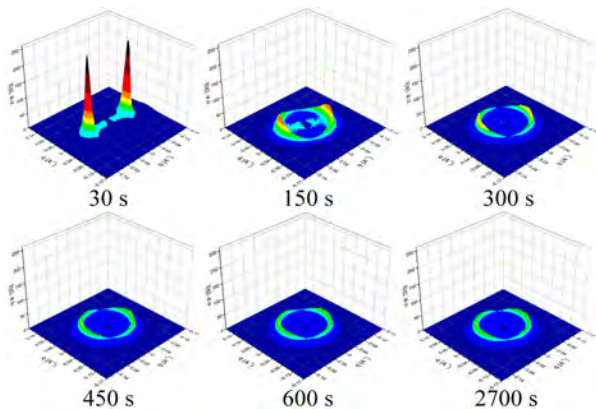
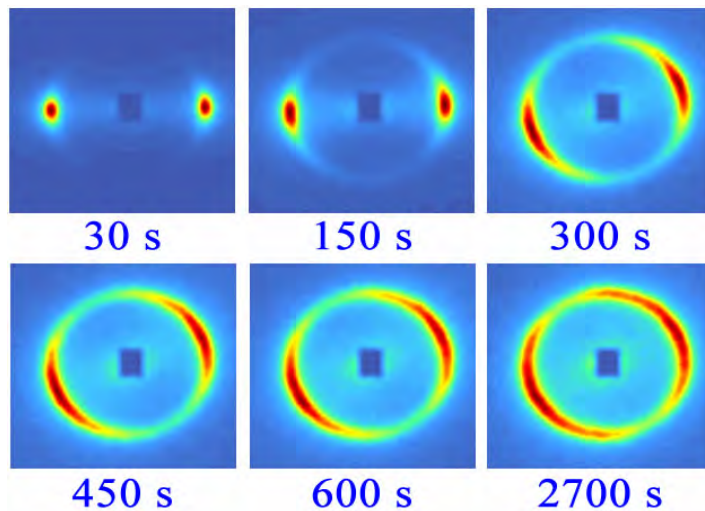


SNAFUSANS-> shows no concentration gradients



Multilamellar Vesicle Formation from a Planar Lamellar Phase under Shear Flow

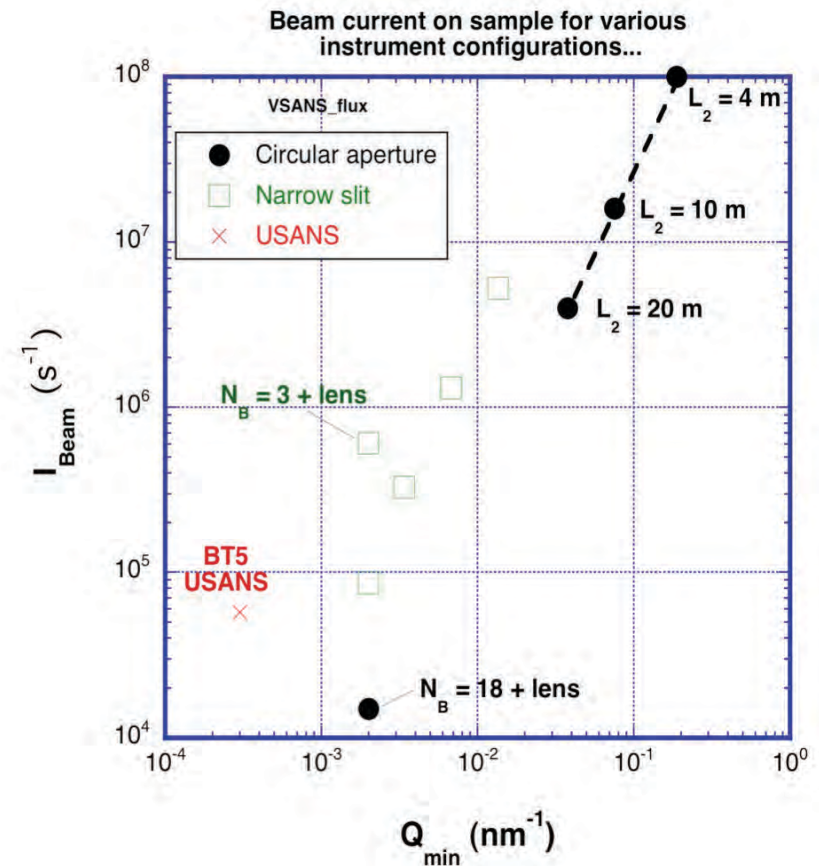
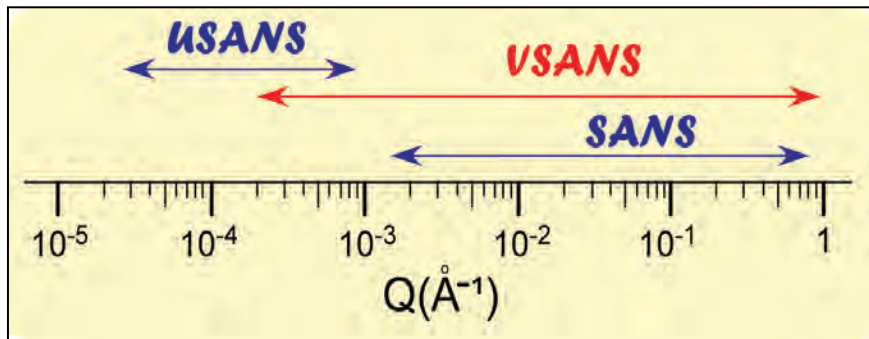
Luigi Gentile^{1,2*}, Manja A. Behrens², Lionel Porcar³, Paul Butler⁴,
Norman J. Wagner^{4,5} and Ulf Olsson²



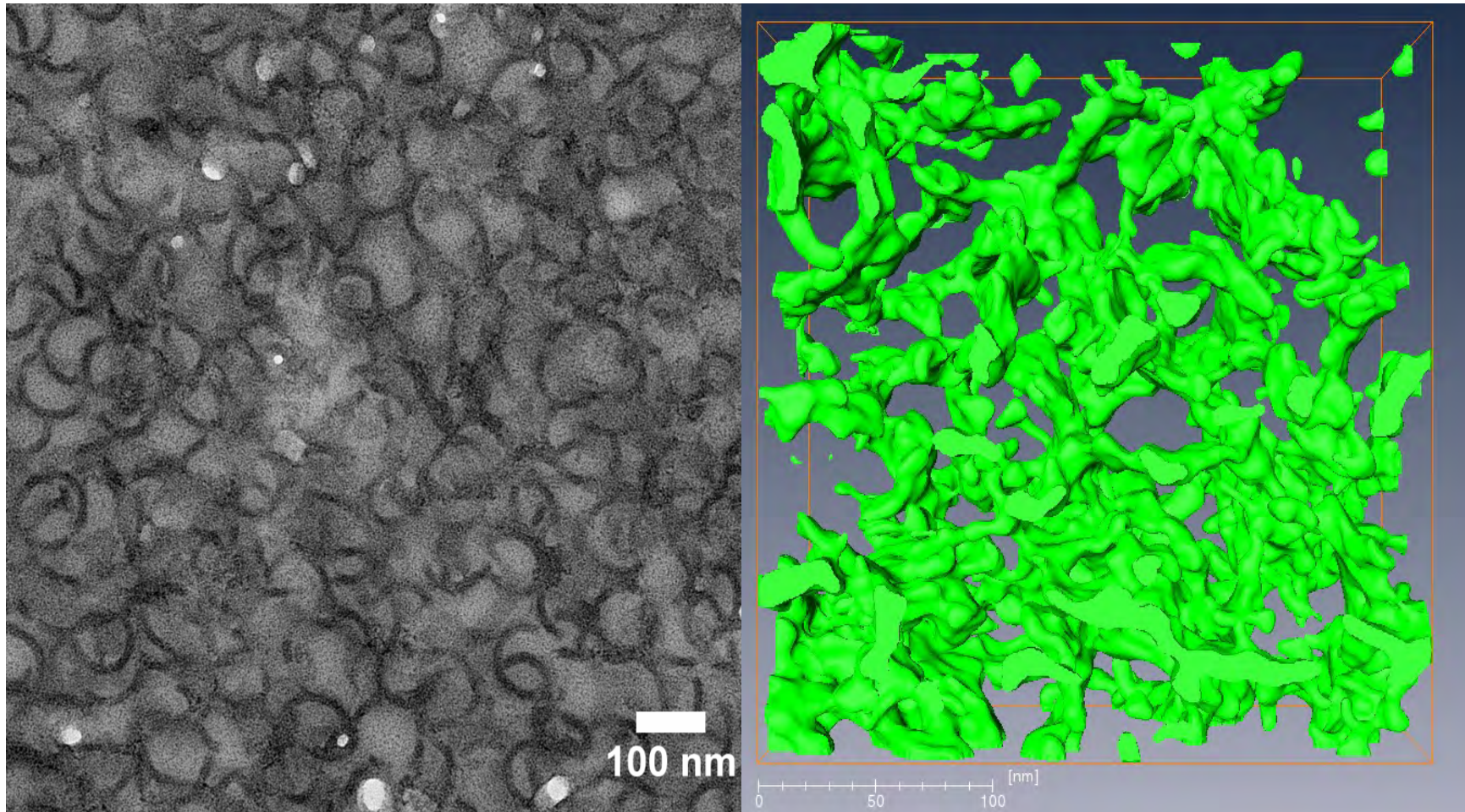
Needs- low q , 2D, high flux

VSANS

Very Small-Angle Neutron
Scattering Diffractometer

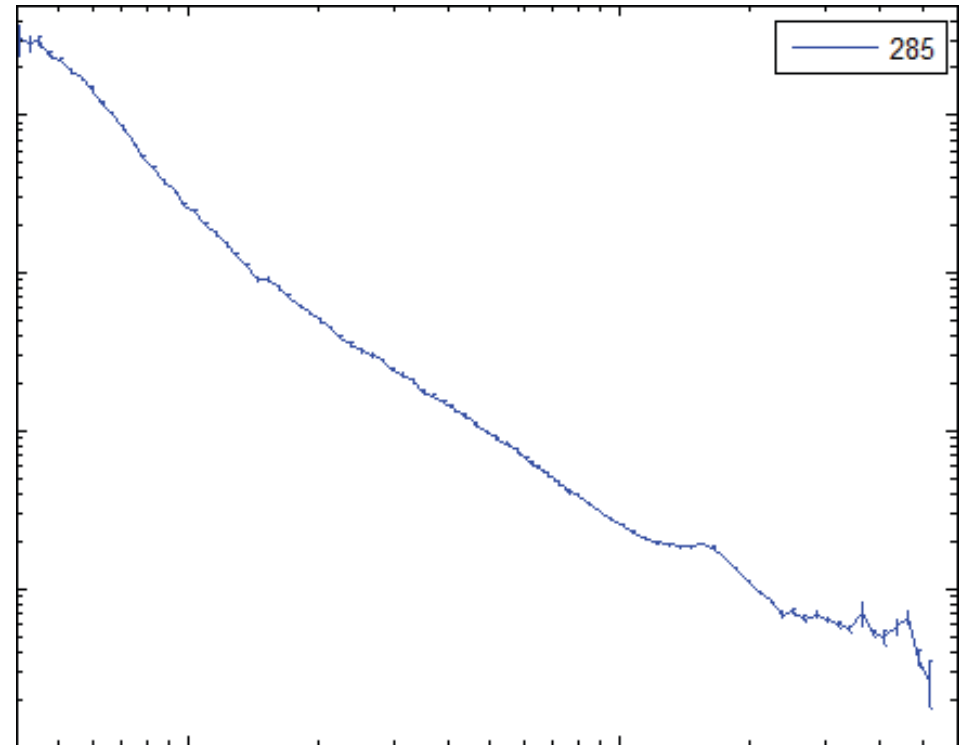
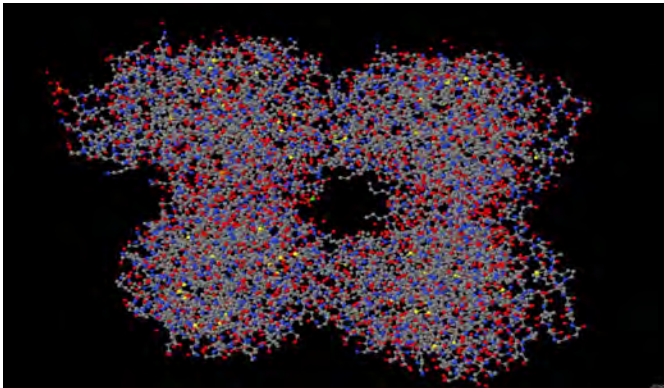
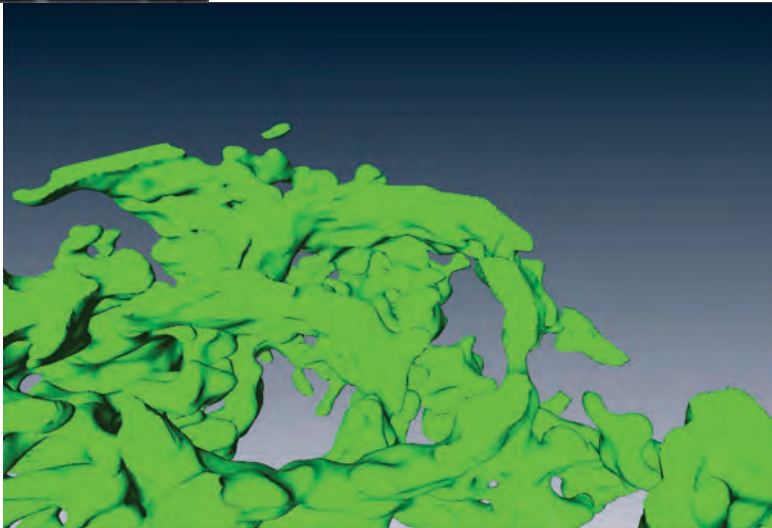


Ovalbumin Gels -> Protein Crystals





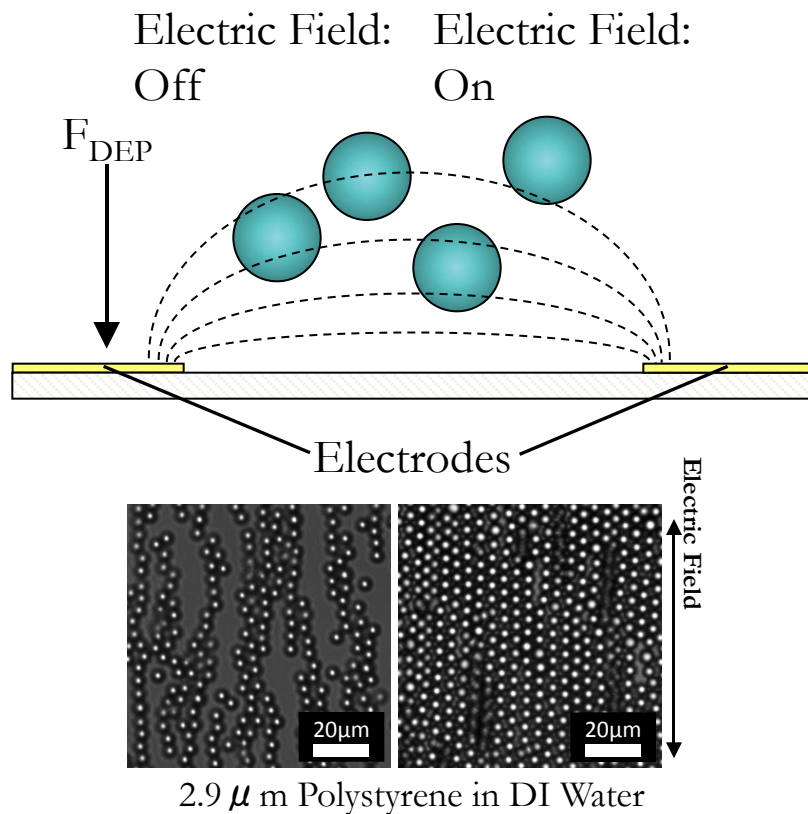
Need for Speed....



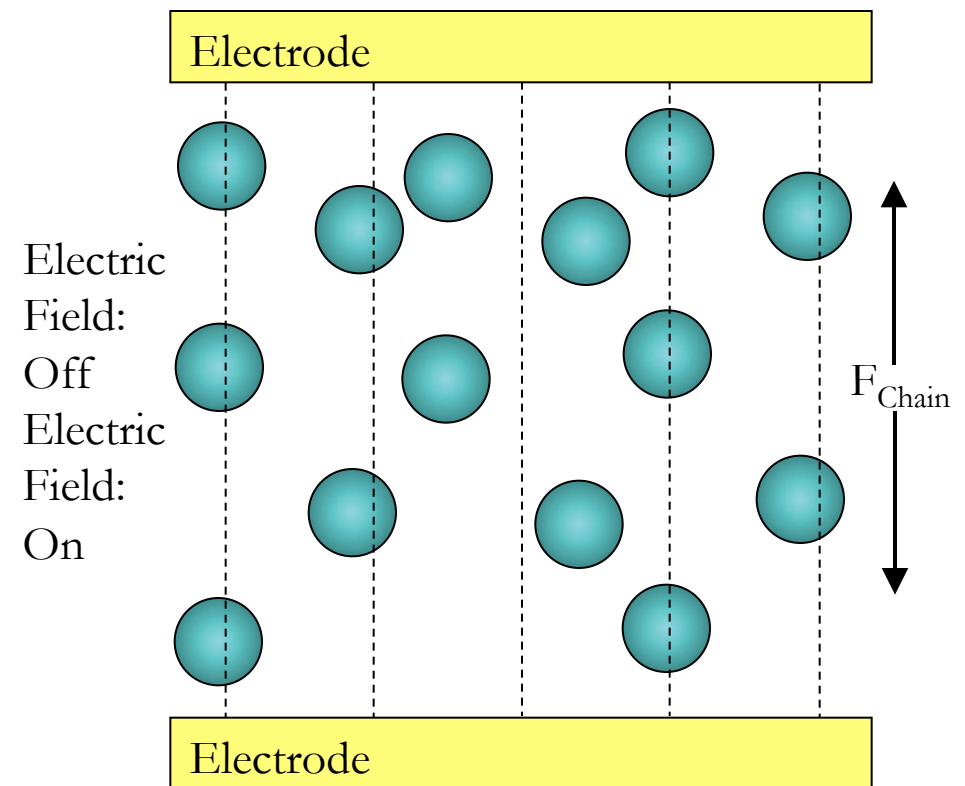
How Electric Field DSA Works

- Alternating current (AC) electric field induces a transient dipole
- Induced dipoles in particles interact to form structures

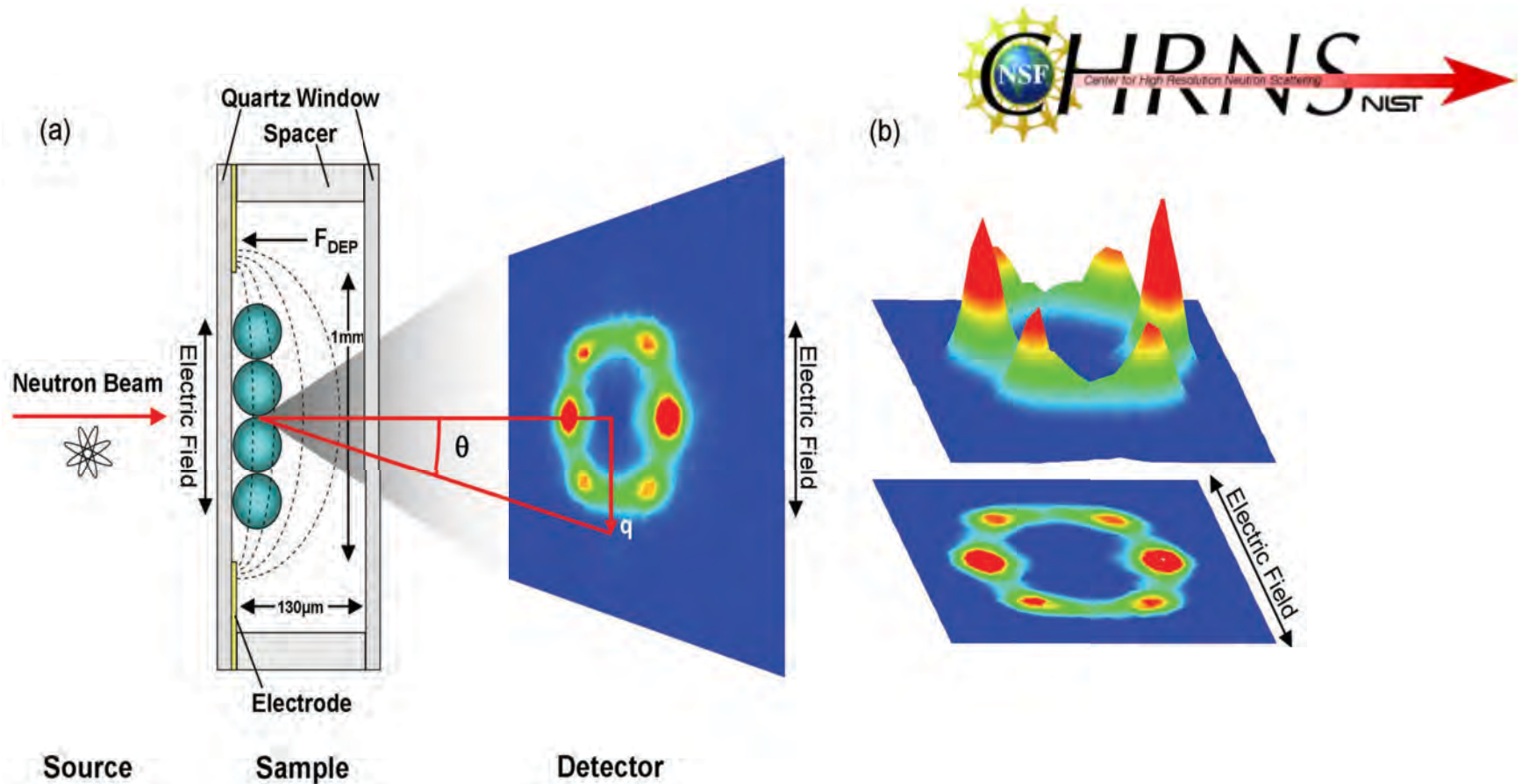
DSA Cell - Side View



DSA Cell - Top View



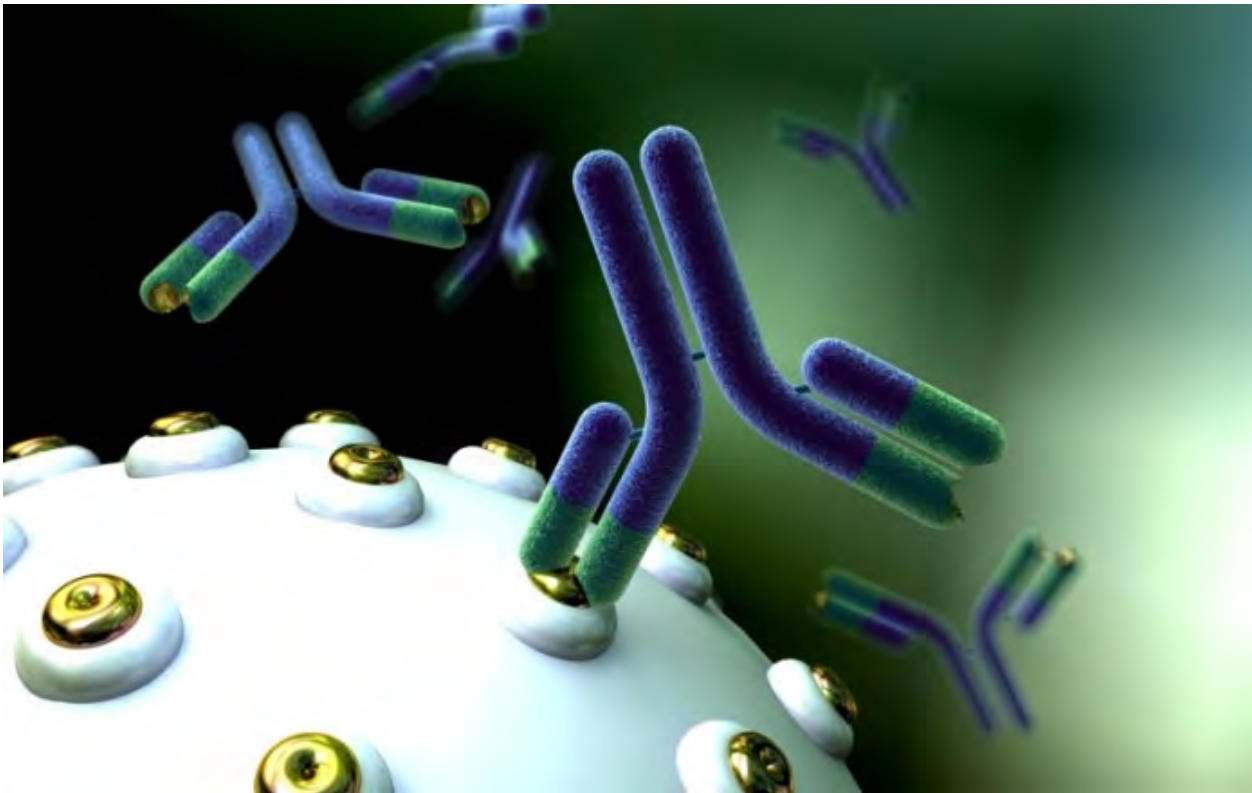
New Sample Environments: E-SANS



Directed self-assembly of colloidal crystals by dielectrophoretic ordering observed with small angle neutron scattering (SANS)[†]

Jason M. McMullan and Norman J. Wagner* Soft Matter 2010

Biotherapeutics: Next Generation of Pharmaceuticals



Importance of biotherapeutics: Unmet medical needs

- Immunological and allergic disorders as well as oncology-related abnormalities
- Structural specificity and low toxicity
- Several dozen MABs have been approved by the FDA for clinical use and several hundred are currently in development
 - New and exciting protein constructs have entered the pipeline (e.g. diabodies, MAB fragments, drug conjugates)



Delivery and Manufacturing (CMC or Developability) Issues

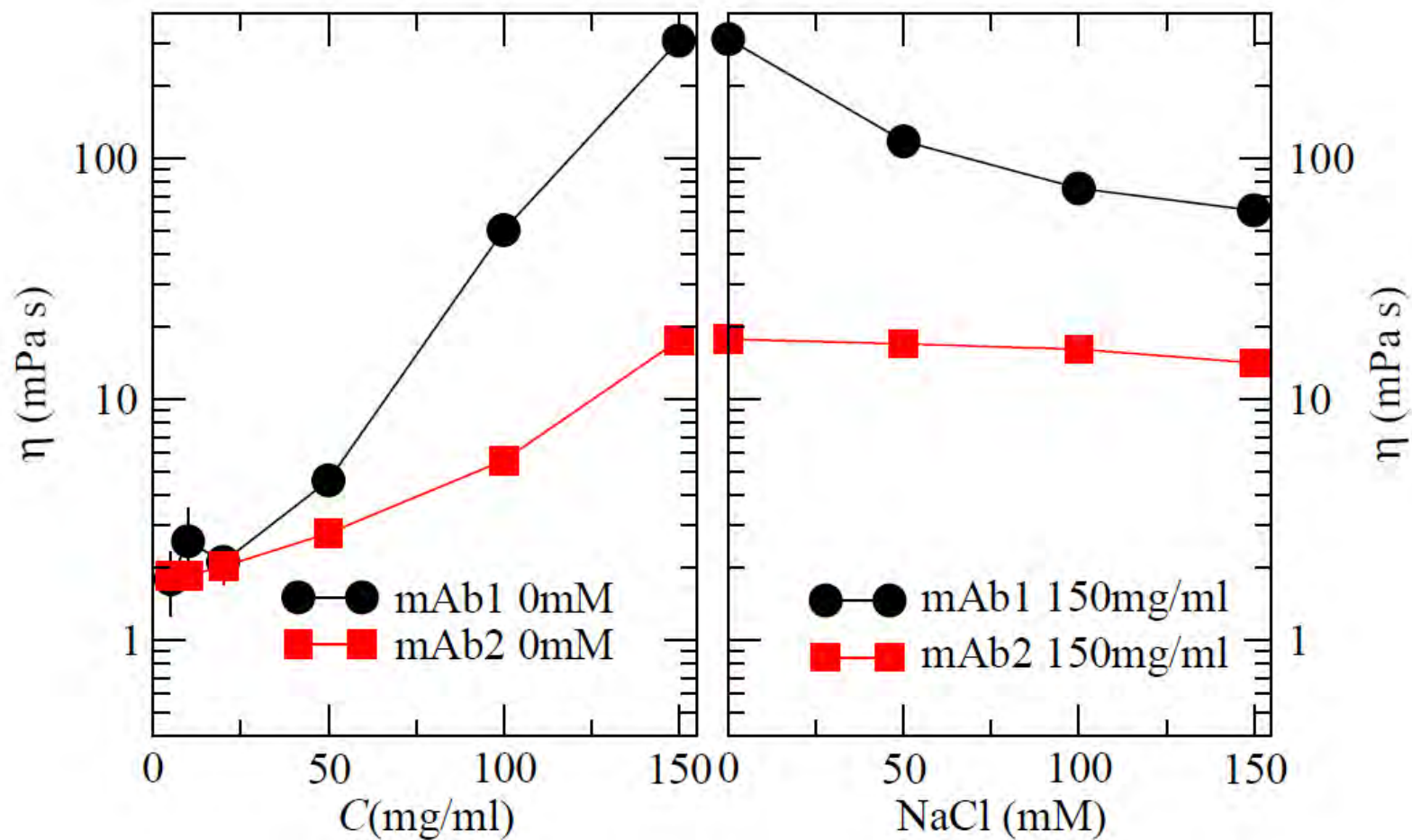
- More convenient subcutaneous delivery is desired for the clinical or home setting
- Smaller volumes (<1.5 mL) require larger concentrations for same effectiveness
- In some cases, larger concentrations lead to an undesirable viscosity
- Biopharmaceutical trend: even early stage development screens are now including techniques/methods to predict whether the candidates will exhibit elevated viscosities at high concentrations (light scattering techniques)
- Also manufacturing process steps are impacted, such as concentration, filtration and fluid transport



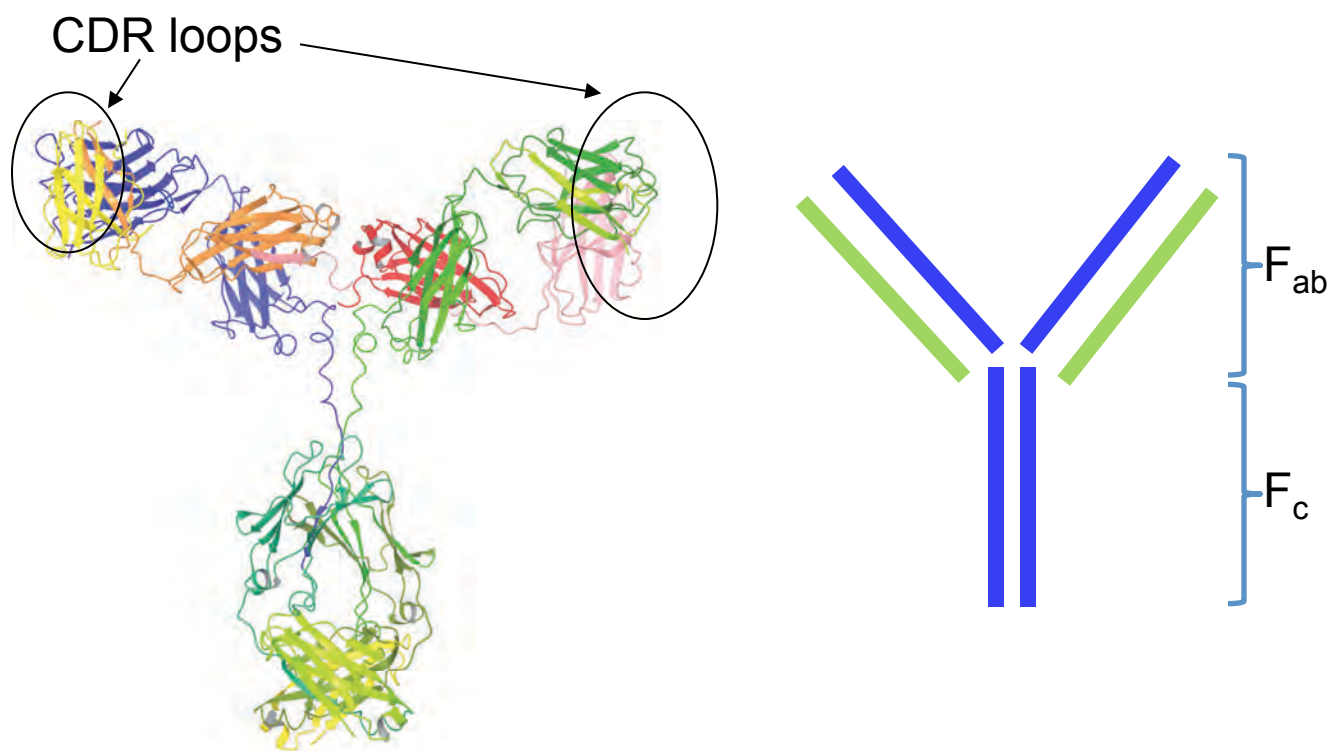
http://www.glassdoor.com/Photos/Genentech-Office-Photos-E274_P2.htm

<http://pramlintide.net/how-to-use-pramlintide/>

High Concentration MAb Viscosity



Genentech's MAb1 and MAb2 Comparison



MAb1 – more charged residues in the CDR loops

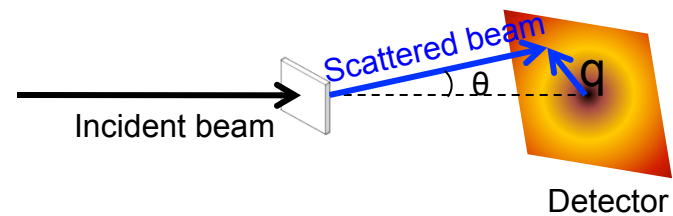
MAb2 – more polar or hydrophobic residues in CDR loops

MAB Cluster Characterization Procedure

Zero-Shear Viscosity vs. Concentration



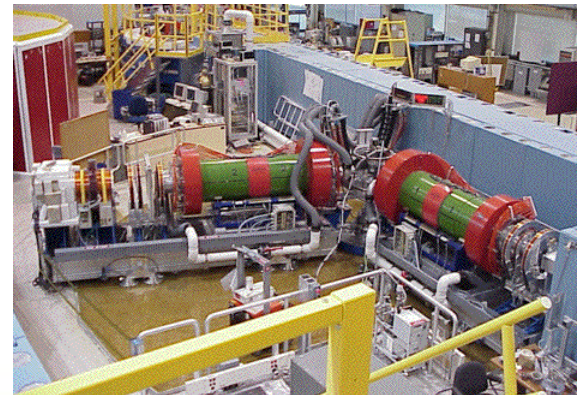
SANS/SAXS (Interaction Potential Types)



$$I(q) = \frac{N}{V} V_p^2 (\rho_s - \rho_p)^2 P(q) S(q) + bkg$$

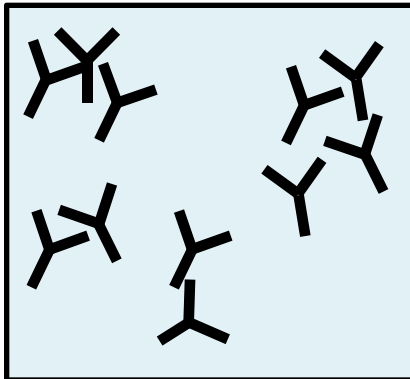


Neutron Spin Echo (Cluster Types)

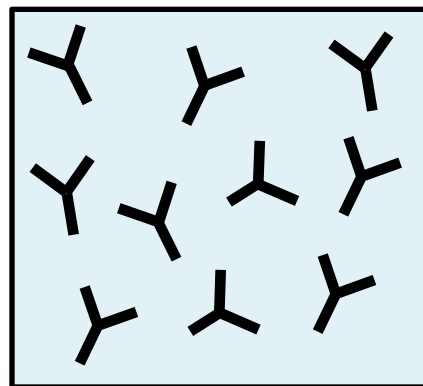


39

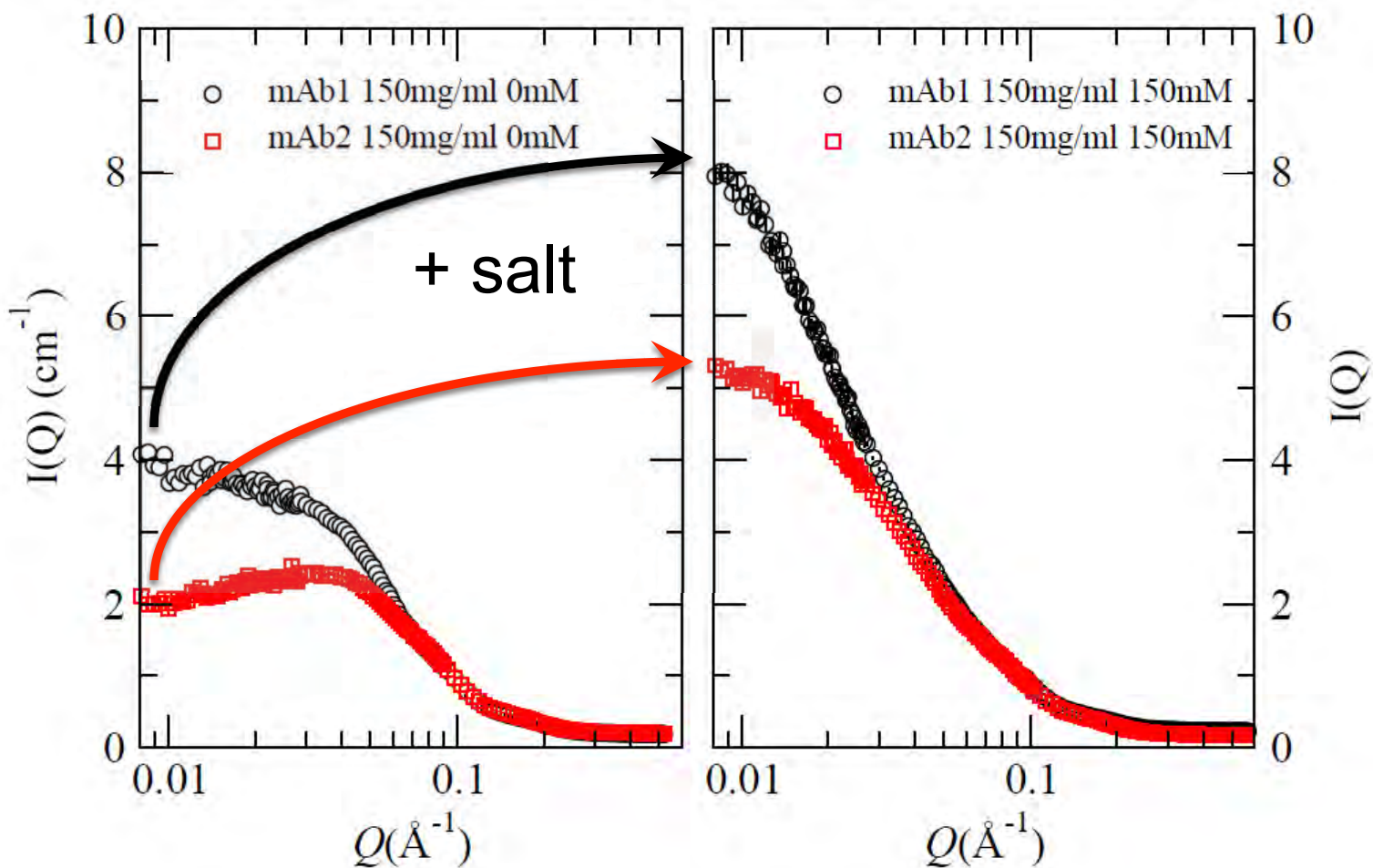
Clear Picture of MAb cluster types



OR



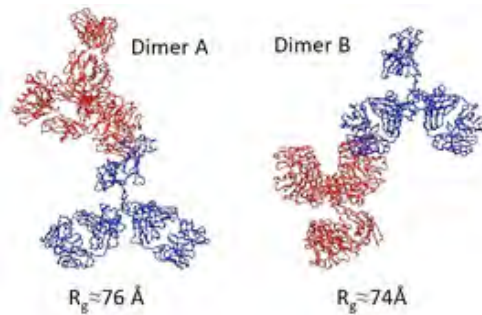
Connection Between Interactions and Scattering



Neutron spin echo results, dimeric clusters

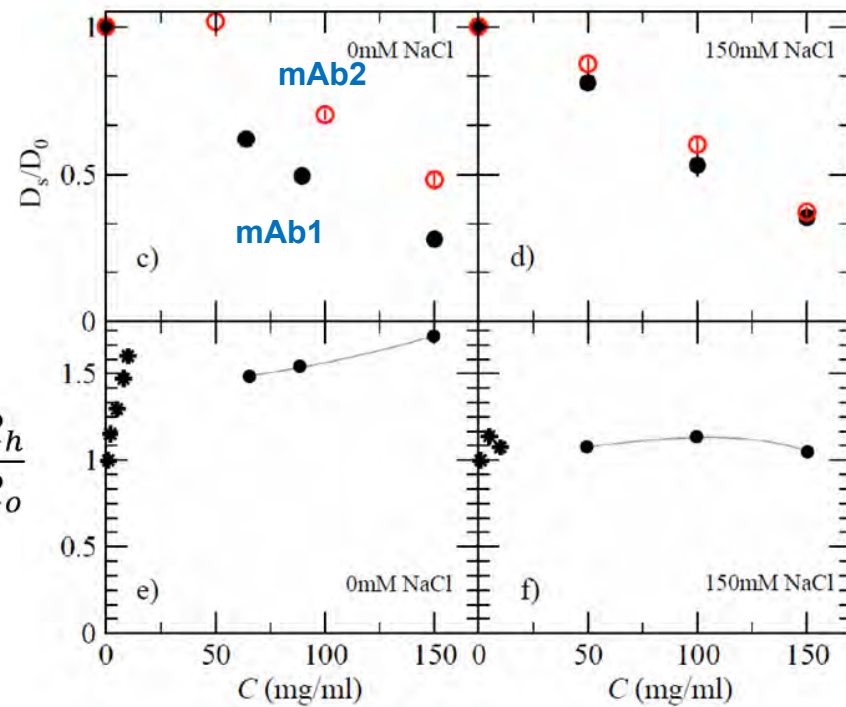
- Neutron spin echo (NSE) data:

Extended Dimers



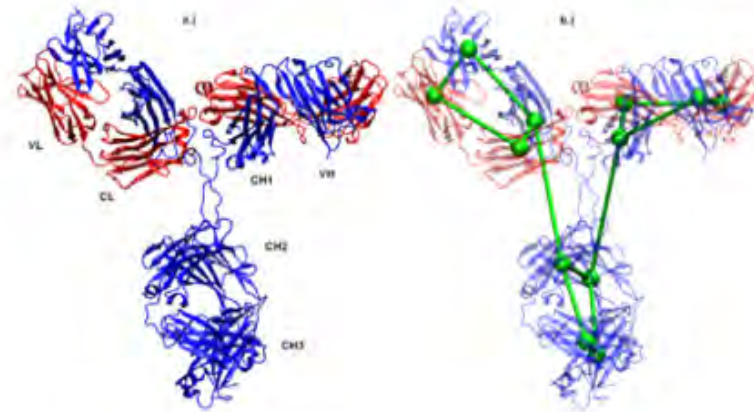
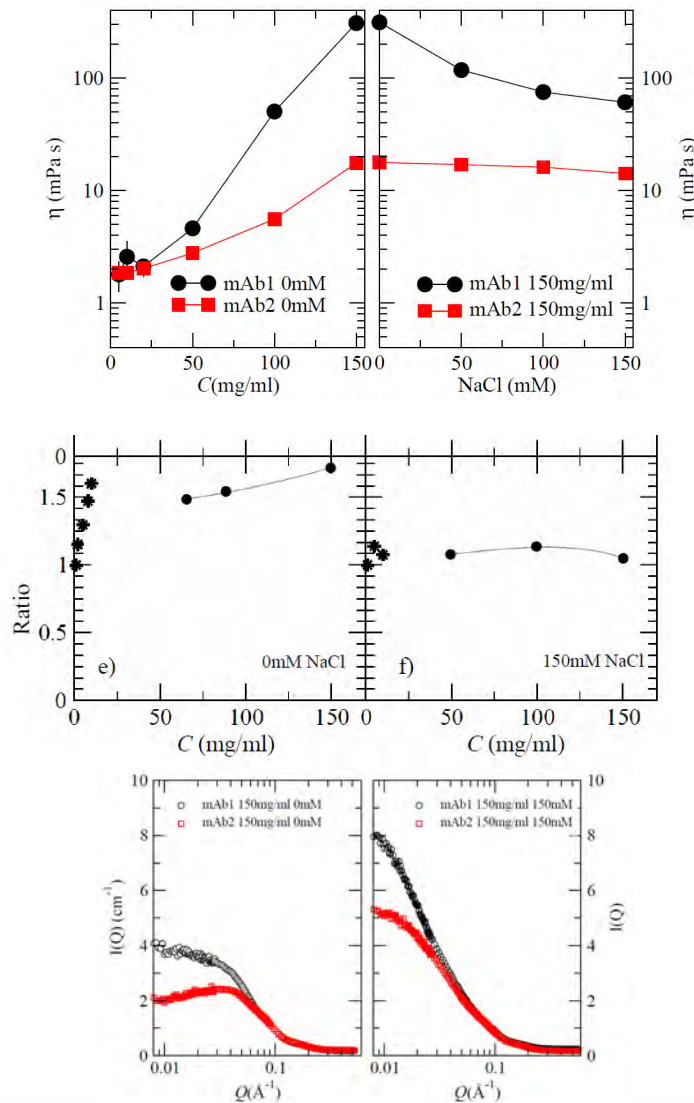
$$\frac{D_{S,mAb2}}{D_{S,mAb1}} \sim \frac{D_o}{D_s} \sim \frac{R_h}{R_o}$$

mAb1 cluster is about 1.7X that of mAb2 in 0mM NaCl case



Cluster Formation and Enhanced Viscosity Combining NSE and SANS

Genentech
A Member of the Roche Group



Eric J. Yearley, Isidro E. Zarraga*, Steven J. Shire, Thomas M. Scherer, Yatin Gokarn, Norman J. Wagner, Yun Liu*, "Small-Angle Neutron Scattering Characterization of Monoclonal Antibody Conformations and Interactions at High Concentrations", *Biophysical Journal*, 105, 720-731(2013)

Acknowledgements & Co-authors



Kate Gurnon
GE Research



Paul Butler
NCNR NIST



**Carlos López-
Barrón**
ExxonMobil



Lionel Porcar
ILL Grenoble



Aaron Eberle
ExxonMobil



Matt Helgeson
UCSB

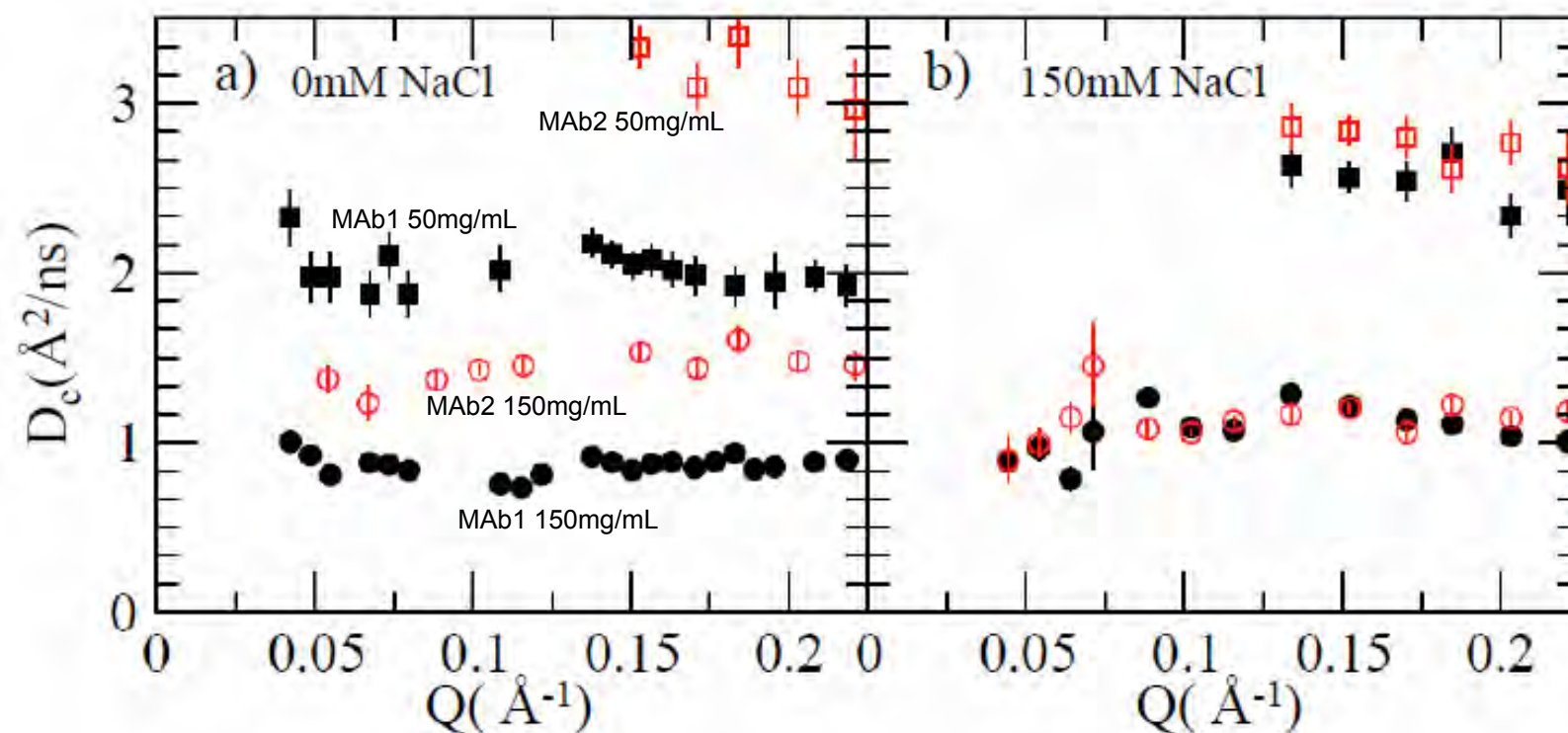


Florian Nettesheim
DuPont Analytical

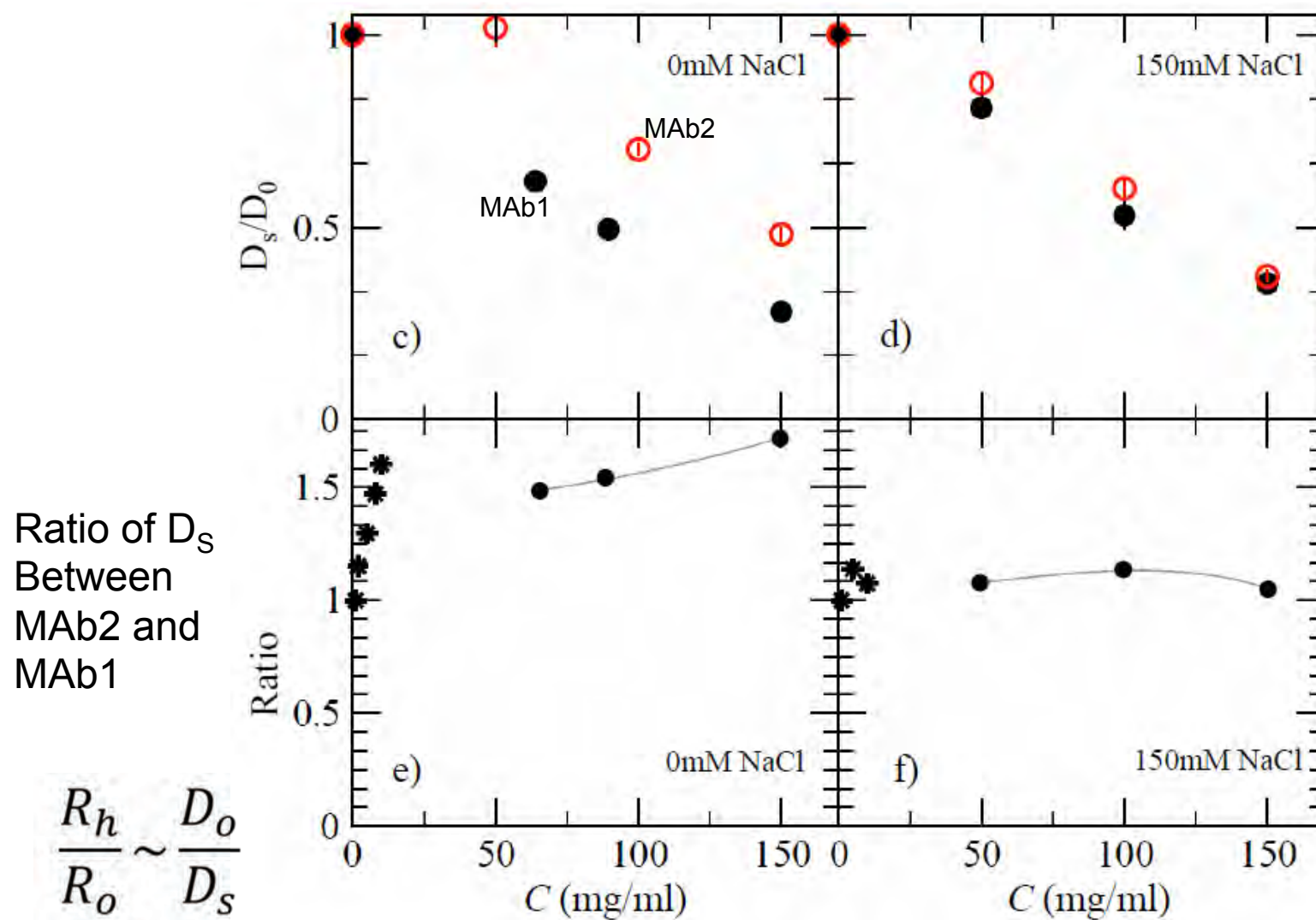


Matt Liberatore
CSM

MAb Neutron Spin Echo Data



MAb Neutron Spin Echo Data



Conclusions

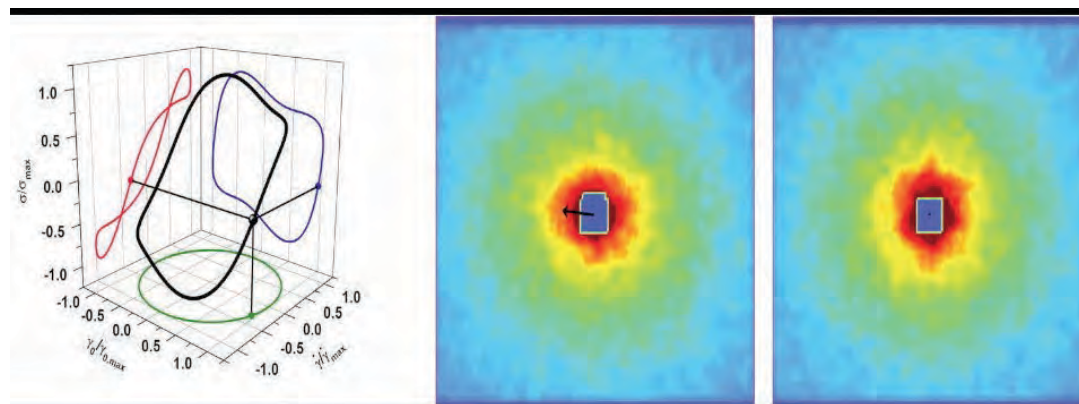
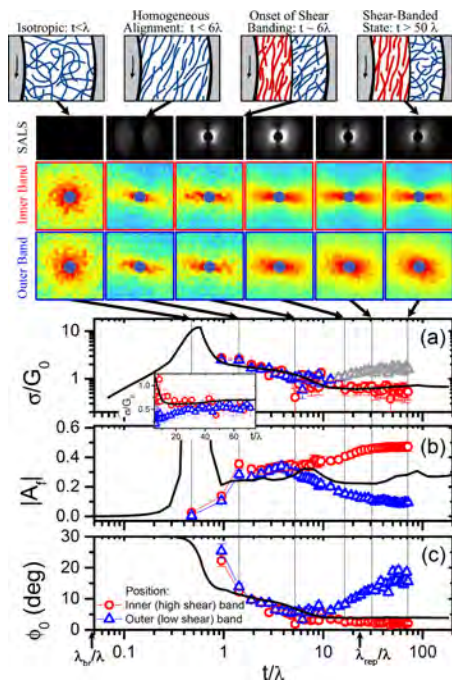
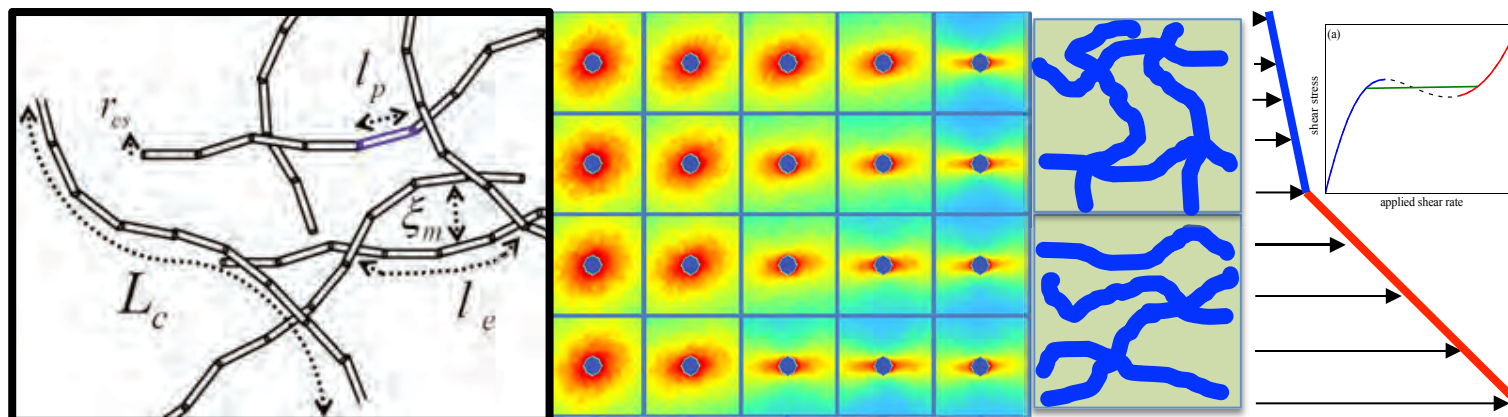
- SANS is a very useful tool to investigate the interaction types in solution
- NSE is a powerful tool to study the formation and types of dynamic clusters in solutions.
- MAb1 forms small clusters at low concentrations driven by an anisotropic attractive interaction
- Small clusters doesn't seem to grow with the increase of volume fraction.
- The large increase of viscosity of MAb1 is due to the formation of small dynamic clusters while MAb2 viscosity is dominated by the monomeric motions in solutions.
- What about SANS low-Q upturn in MAb1 150mg/mL at 150mM NaCl and the NSE data showing loss of long-lived dynamic clusters? Why doesn't the viscosity of MAb1 collapse to the levels of MAb2 with the addition of salt
 - One explanation: the viscosity decreases significantly (but not to the levels of MAb2) because the attractive electrostatic forces holding the cluster together is suppressed by the salt, but the ability of the MAb1 proteins to move closer to each other is enhanced due to the screening of the repulsion and increased in hydrophobic associations forming a larger, loose network (in comparison to MAb2)

Acknowledgements

- Yatin Gokarn and Rosalynn Tiang (Genentech Inc.)
- Lionel Porcar and Peter Falus (*ILL*)
- Michihiro Nagao and Antonio Faraone (*NIST Center for Neutron Research*)

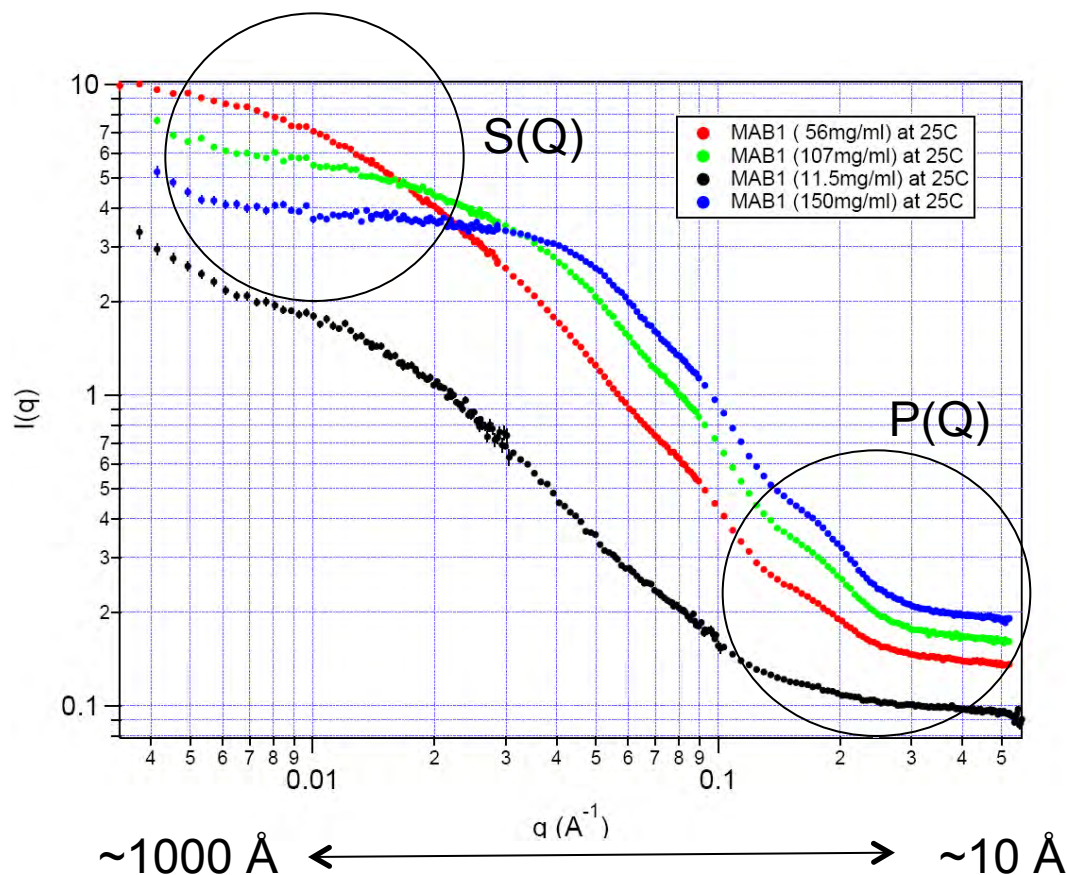


Conclusions & Acknowledgements



Gurnon et al. *ACS Macro Lett.* **2014**, 3, 276–280
 Gurnon et al. *JOVE* **2014**, 84, e51068
 Gurnon et al. *Soft Matter* **2014**, 10, 2889
 Lopez-Baron et al. *Phys. Rev. E.* **2014** 002300

Typical MAb SANS Patterns

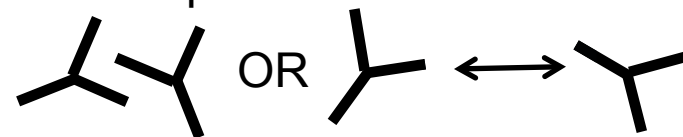


$$I(Q) \sim P(Q)S(Q)$$

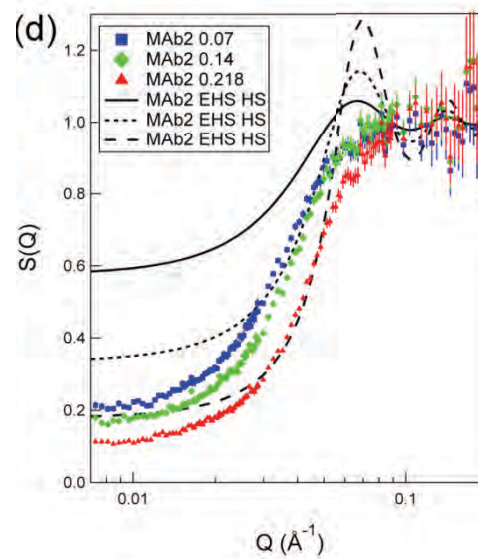
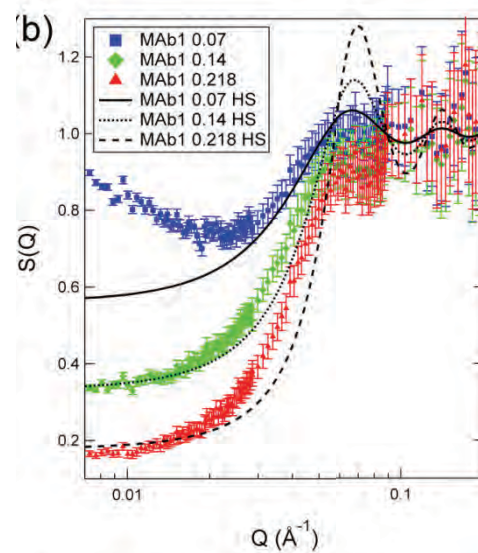
$P(Q)$ or form factor – gives information on the shape and size of a protein



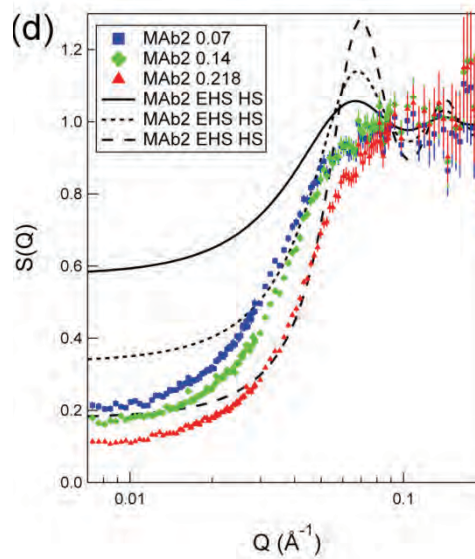
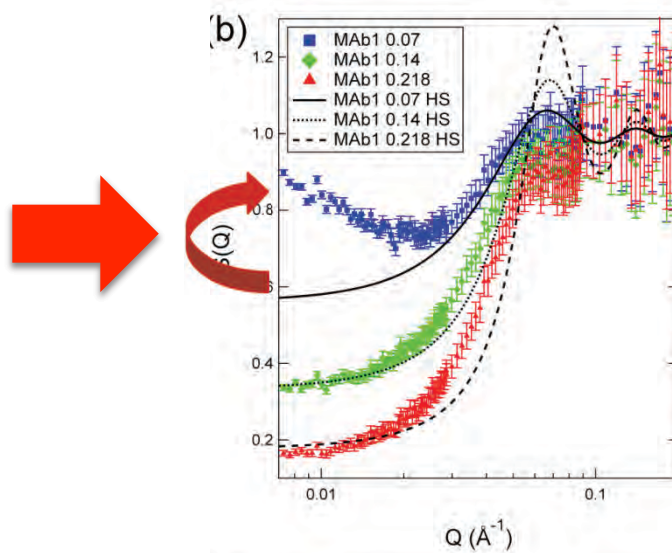
$S(Q)$ or structure factor – gives information on the interactions between proteins



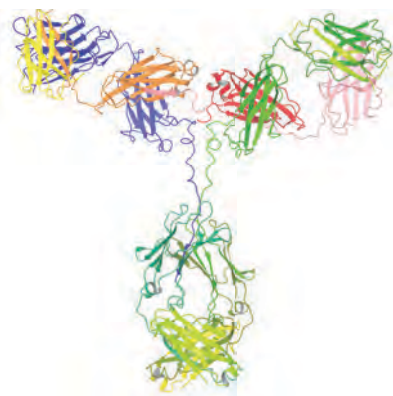
MAB Self-Associations



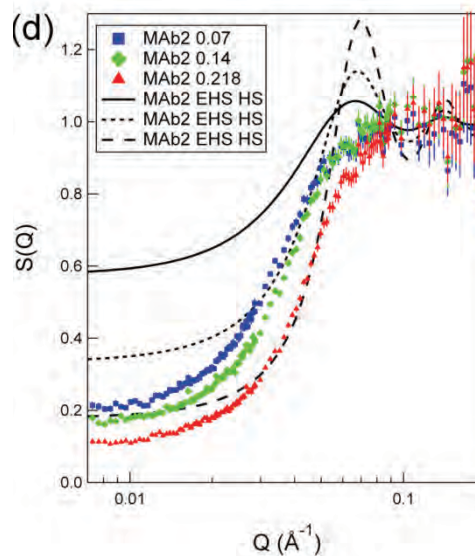
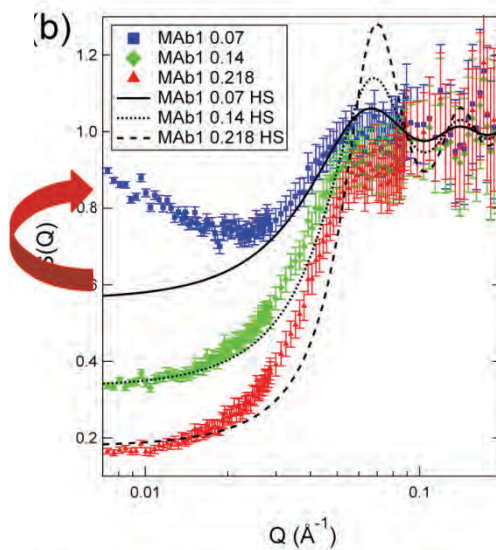
MAB Self-Associations



MAb Self-Associations



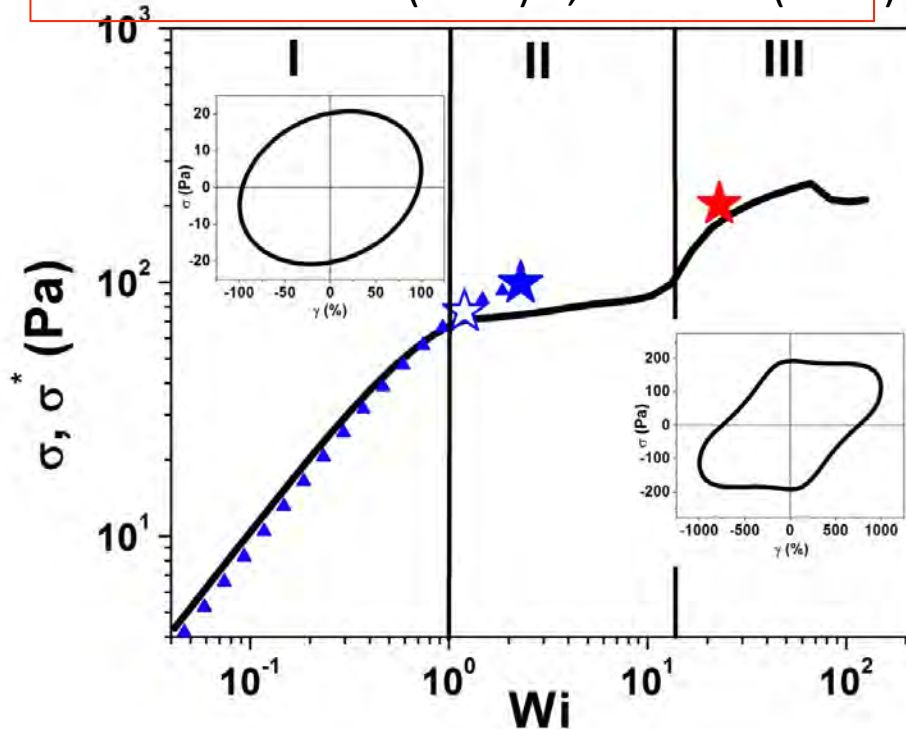
*Asymmetric
shape and
charge





Conclusions: LAOS of shear banding

Gurnon et al. *Soft Matter* 10, 2889 (2014)
ACS Macroletters (2014) 3, 276–280 (2014)



- **Region I** Stress-SANS Rule demonstrated for entangled flowing WLMs
- **Region II** Metastable states of flow-aligned, entangled WLMs with shear-induced concentration fluctuations as precursor to shear banding
- **Region III** flow-aligned, shear demixed WLMs with different SSR coefficient
- **LAOS with STR-SANS** are powerful tools to develop structure property relationships for complex fluids and to test nonequilibrium thermodynamic models

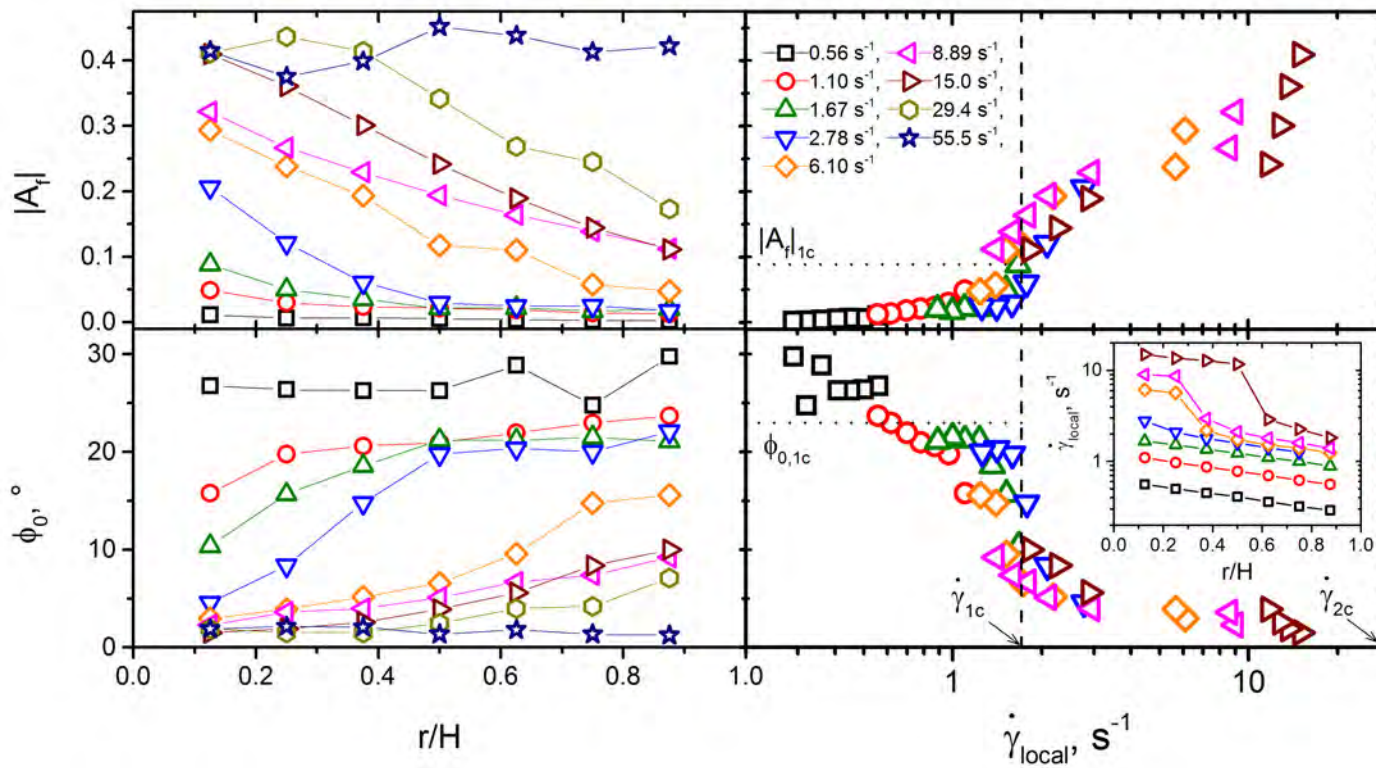
- 1,2 plane **STR-SANS** is available at the ILL Grenoble and at the NCNR NIST



- **RheoSALS** with temperature control is available from TA Instruments



SNAFUSANS-> no concentration gradients

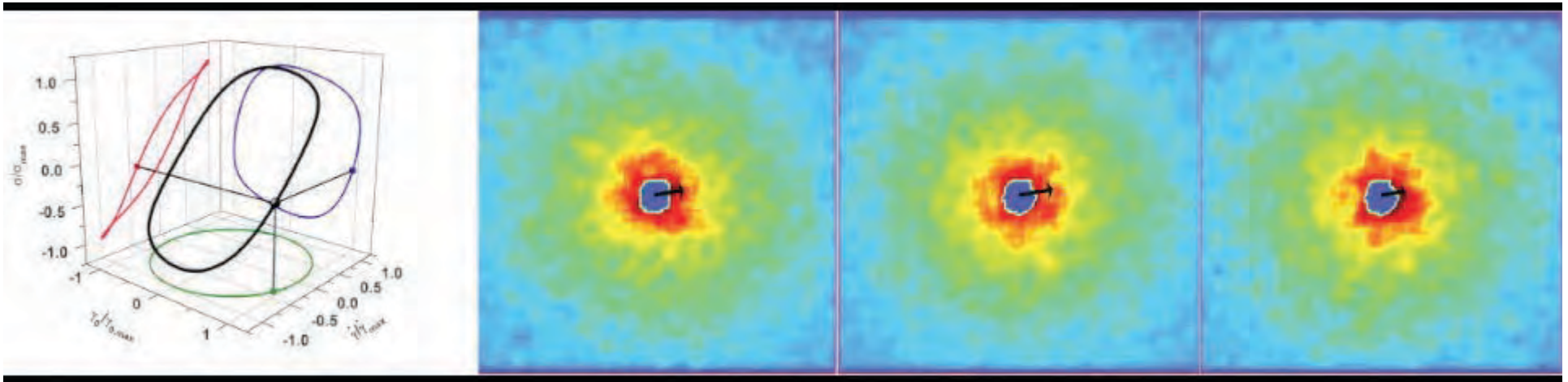


Nonlinear entangled WLM during LAOS

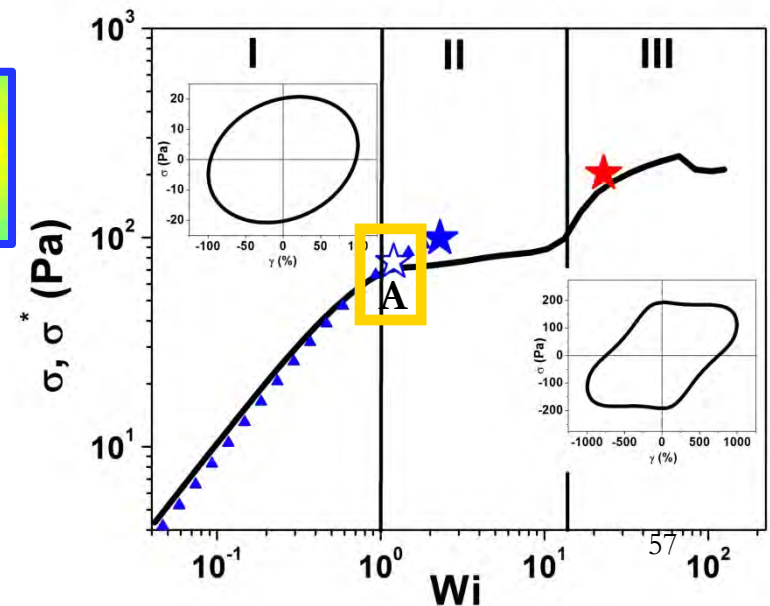
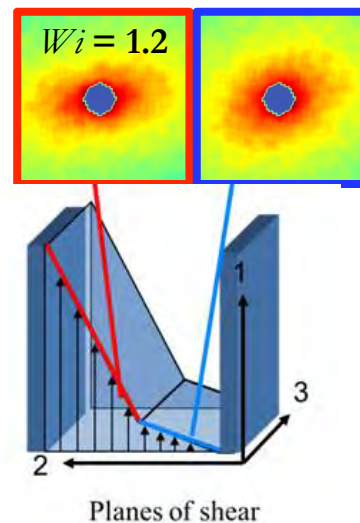
[$De = 0.23$, $Wi = 1.2$]



Arrows denote the average angle of orientation and the alignment factor at each condition given the SANS 2D scattering pattern.

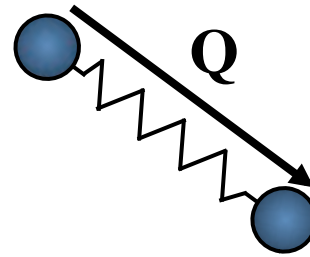


Gurnon et al. Soft Matter, 2014



Stress-SANS Rule

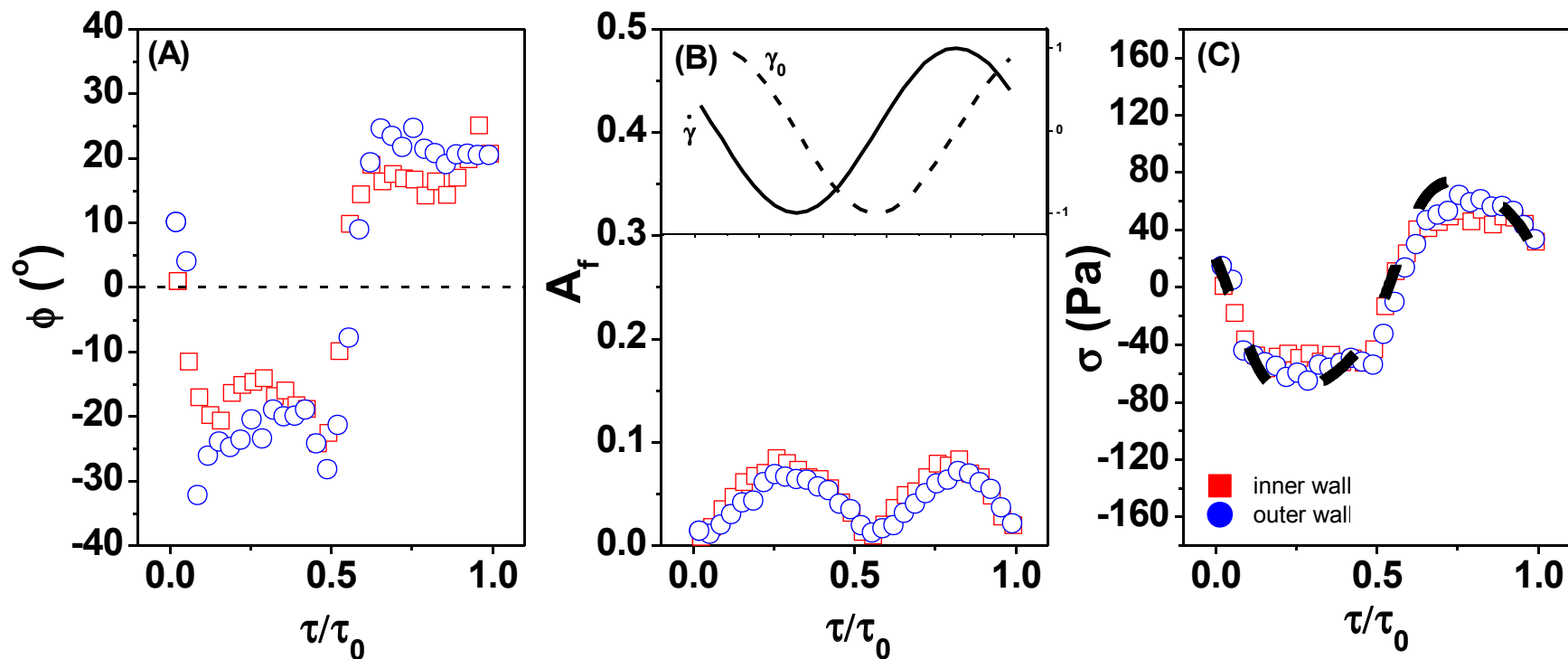
$$\sigma = G_0 \left(C A_f \right)^{1/2} \sin(2\phi)$$



$$\sigma \propto \langle \mathbf{Q}\mathbf{Q} \rangle$$



Good agreement for the local stress at both the inner and outer positions and the macroscopic stress response during rheology measurement.

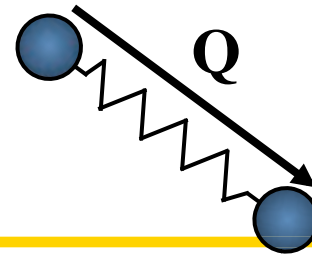


¹ L. M. Walker, N. J. Wagner, SANS Analysis of the Molecular Order in Poly(γ -benzyl L-glutamate)/Deuterated Dimethylformamide (PBLG/d-DMF) under Shear and during Relaxation. *Macromolecules* **29**, 2298 (1996/01/01, 1996).

² M. E. Helgeson, M. D. Reichert, Y. T. Hu, N. J. Wagner, Relating shear banding, structure, and phase behavior in wormlike micellar solutions. *Soft Matter* **5**, 3858 (2009).

Stress-SANS law

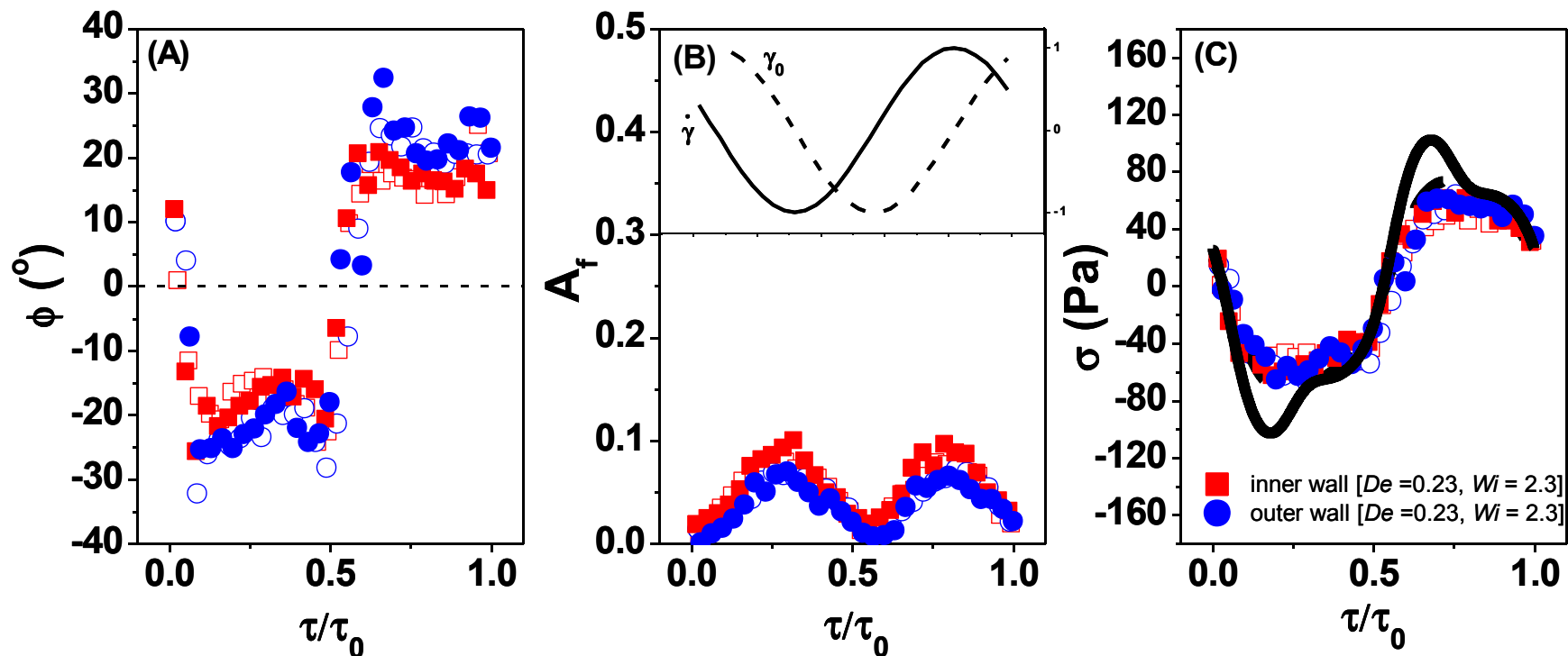
$$\sigma = G_0 \left(C A_f \right)^{1/2} \sin(2\phi)$$



$$\sigma \propto \langle \mathbf{Q} \mathbf{Q} \rangle$$



Neither the inner or outer positions neither capture the stress overshoot, the missing stress must be the result of larger length-scale structures.



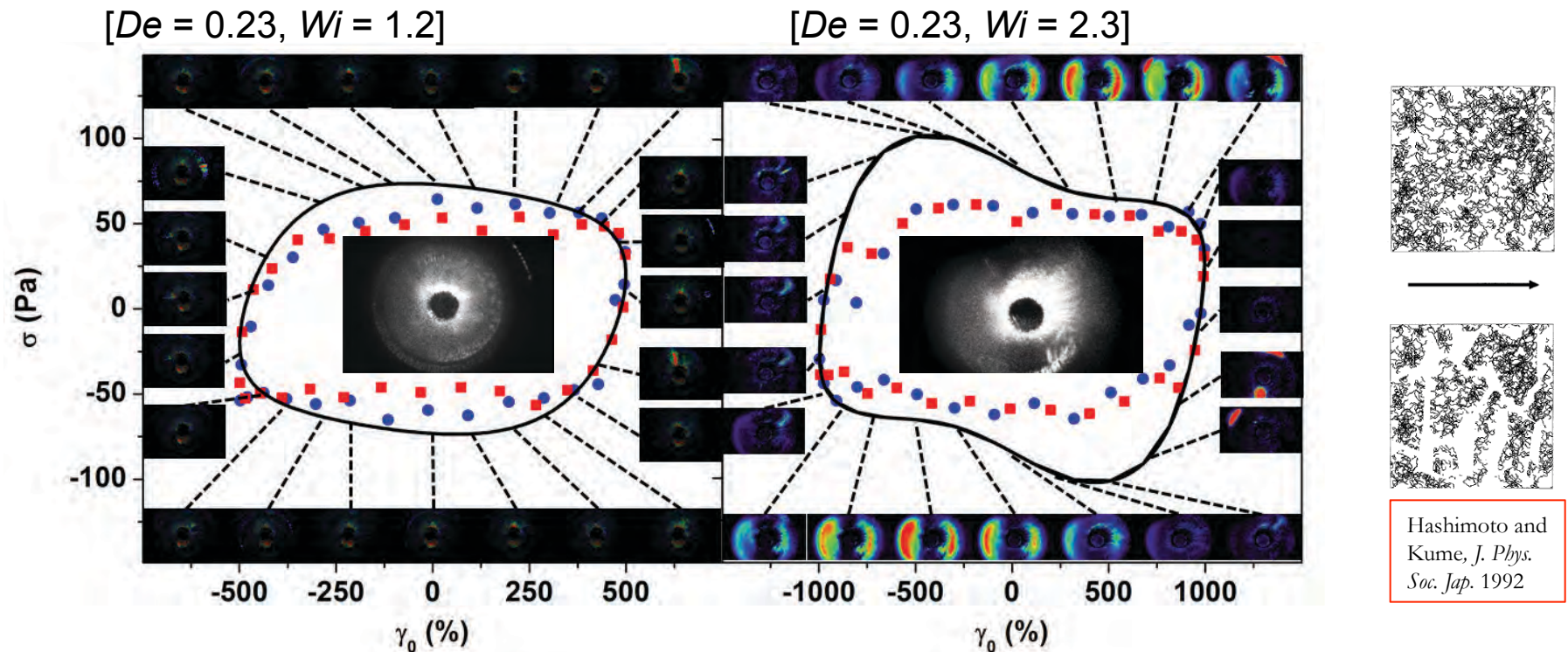
¹ L. M. Walker, N. J. Wagner, SANS Analysis of the Molecular Order in Poly(γ -benzyl L-glutamate)/Deuterated Dimethylformamide (PBLG/d-DMF) under Shear and during Relaxation. *Macromolecules* **29**, 2298 (1996/01/01, 1996).

² M. E. Helgeson, M. D. Reichert, Y. T. Hu, N. J. Wagner, Relating shear banding, structure, and phase behavior in wormlike micellar solutions. *Soft Matter* **5**, 3858 (2009).

³ R. H. Ewoldt, G. H. McKinley, On secondary loops in LAOS via self-intersection of Lissajous-Bowditch curves. *Rheol. Acta* **49**, 213 (Feb, 2010).

Evidence of supra-molecular microstructure

Rheo-Small Angle Light Scattering (SALS)



- **Butterfly patterns during SALS caused by concentration fluctuations**
- **LAOS rheology - stress overshoot corresponds with butterfly patterns in rheo-SALS which result from shear induced concentration fluctuations during LAOS.**
- **Shear banding microstructure origin is concentration fluctuations resulting in stress overshoot**

¹ E. Helfand & G. Fredrickson, Large Fluctuations in Polymer Solutions under Shear, PRL 62 (21) 2468 (1989)

² Y.T. Hu *et al.*, Shear thickening in low-concentration solutions of wormlike micelles I., JOR 42(5) 1185 (1998)

³ P. Thareja *et al.*, Shear-induced phase separation (SIPS) with shear banding in solutions of cationic surfactant and salt. *J. Rheol.* **55**, 60 1375 (Nov, 2011).

Gurnon, A. K., Godfrin, P. D., Wagner, N. J., Eberle, A. P. R., Butler, P., Porcar, L.
Measuring Material Microstructure Under Flow Using 1-2 Plane Flow-Small Angle Neutron
Scattering. *J. Vis. Exp.* (84), e51068, doi:10.3791/51068 (2014).

Measuring Material Microstructure Under Flow Using 1-2 Plane Flow-Small Angle Neutron Scattering

**A. Kate Gurnon¹, P. Douglas Godfrin¹,
Norman J. Wagner¹, Aaron P. R. Eberle^{1,2},
Paul Butler², and Lionel Porcar^{1,3}**

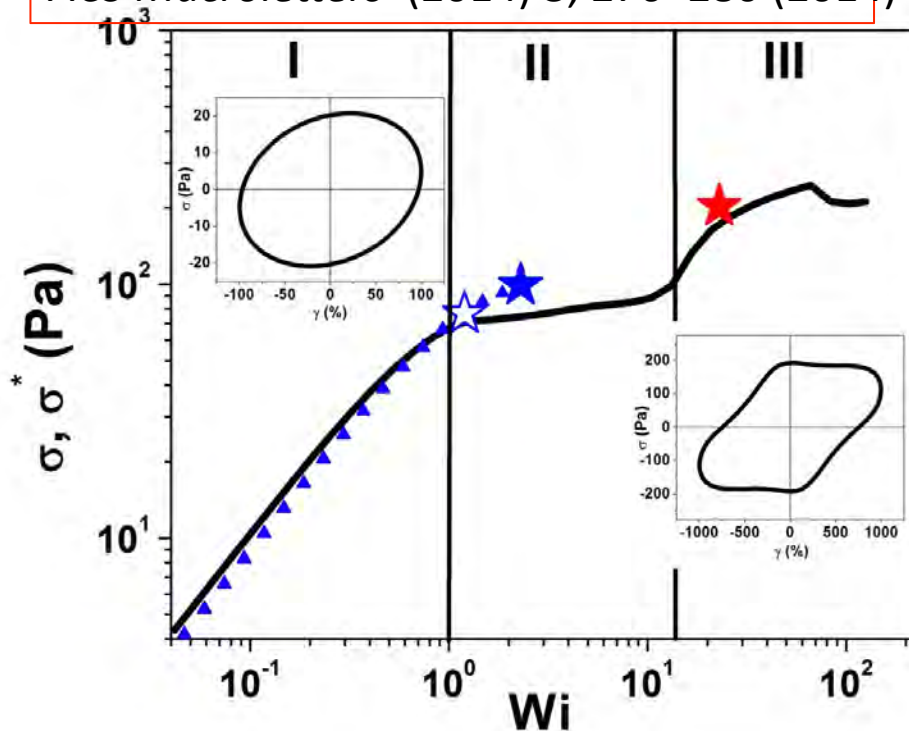
**¹Center for Neutron Science,
Department of Chemical, and
Biomolecular Engineering,
University of Delaware**

**²NIST Center for
Neutron Research,
National Institute of
Standards and Technology**

³Institut Laue-Langevin

Conclusions: LAOS of shear banding

Gurnon et al. *Soft Matter* 10, 2889 (2014)
ACS Macroletters (2014) 3, 276–280 (2014)



- **Region I** Stress-SANS Rule demonstrated for entangled flowing WLMs
- **Region II** Metastable states of flow-aligned, entangled WLMs with shear-induced concentration fluctuations as precursor to shear banding
- **Region III** flow-aligned, shear demixed WLMs with different SSR coefficient
- **LAOS with STR-SANS** are powerful tools to develop structure property relationships for complex fluids and to test nonequilibrium thermodynamic models

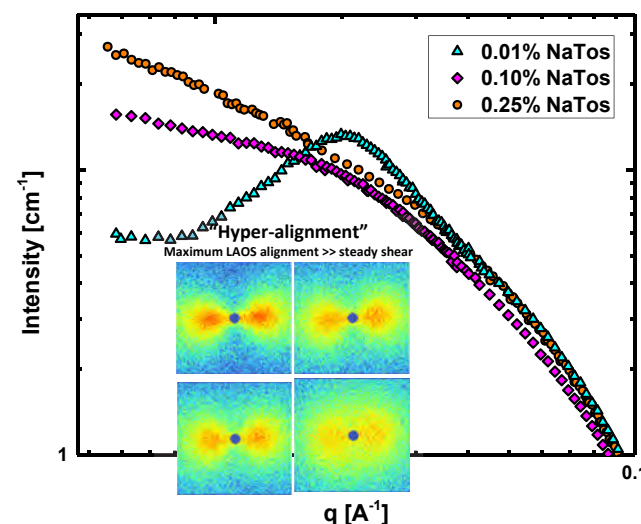
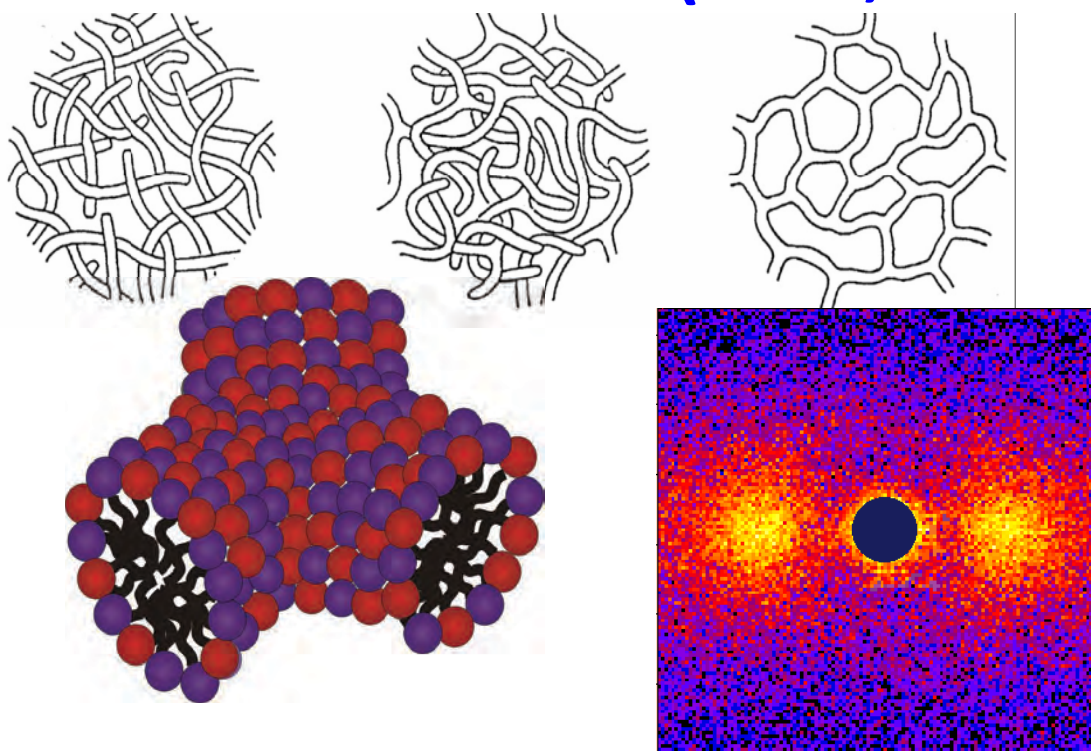
- 1,2 plane **STR-SANS** is available at the ILL Grenoble and at the NCNR NIST



- **RheoSALS** with temperature control is available from TA Instruments



Effects of Micellar Branching: Michelle Calabrese (this session) & Poster # BP3.02 (Tues, 3:30 Summit II)

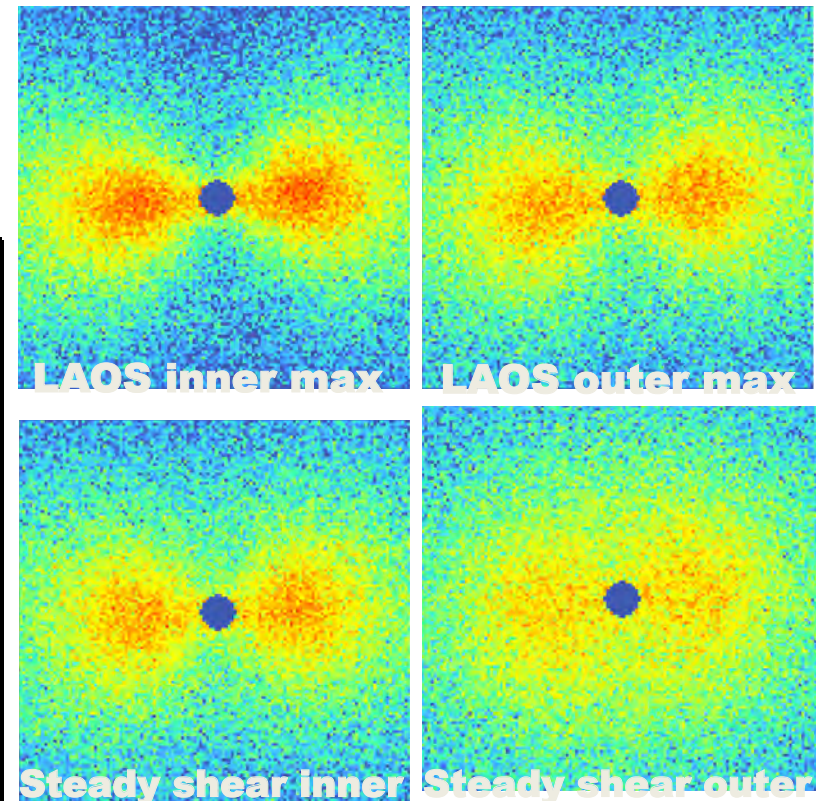
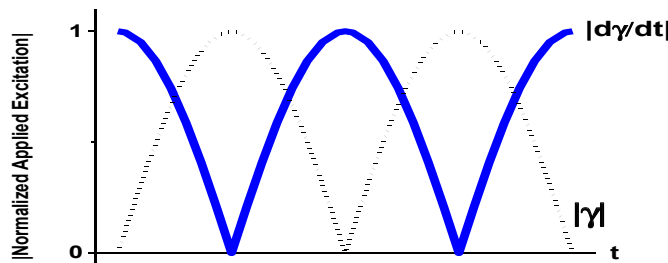


Thareja, P., Hoffmann, I.H., Liberatore, M.W., Helgeson, M.E., Hu, Y.T., Gradzielski, M., and Wagner, N.J., "Shear-induced phase separation (SIPS) with shear banding in solutions of cationic surfactant and salt". *Journal of Rheology*. **55**(6): p. 1375-1397 (2011).

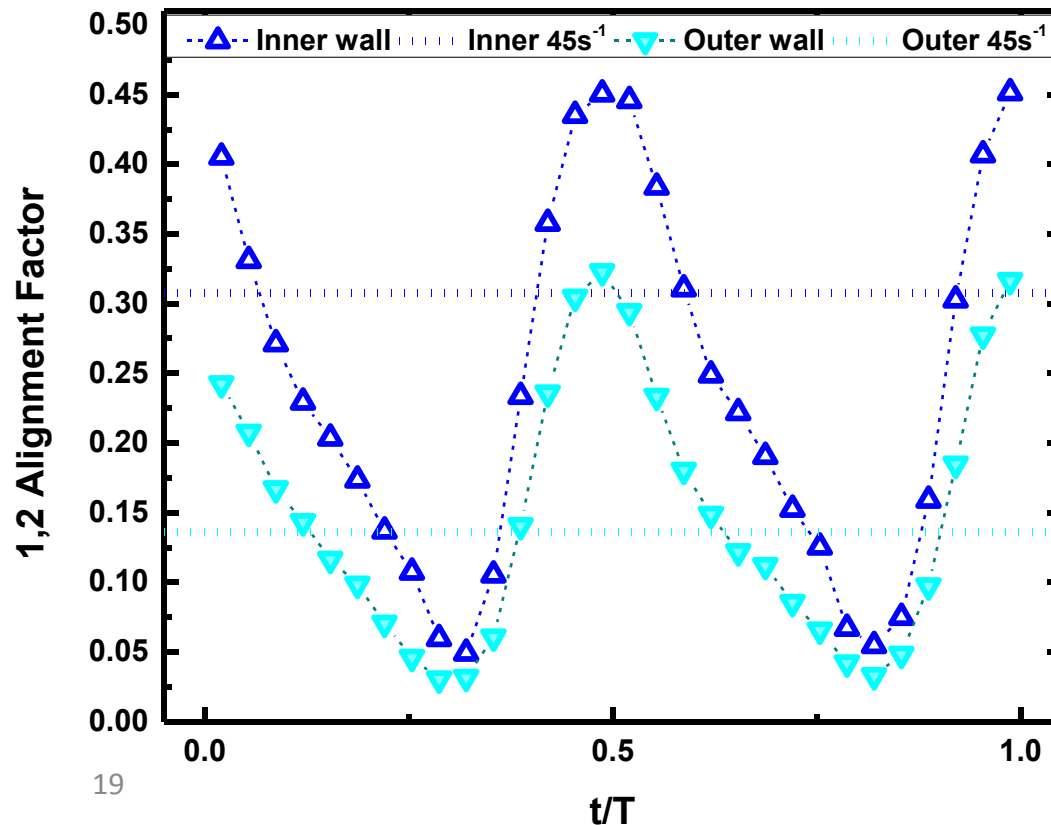
High Branching – low frequency, moderate shear rate

“Hyper-alignment”

Maximum LAOS alignment \gg steady shear



Degree of hyper-alignment is
magnified by branching



Conclusions

Low Branching

Interaction peak

Shear banding

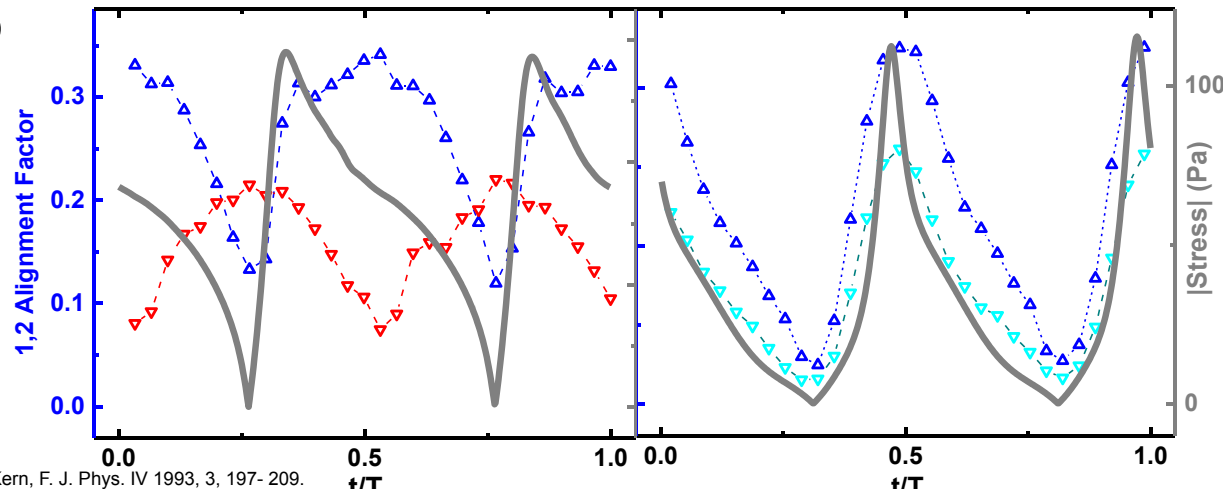
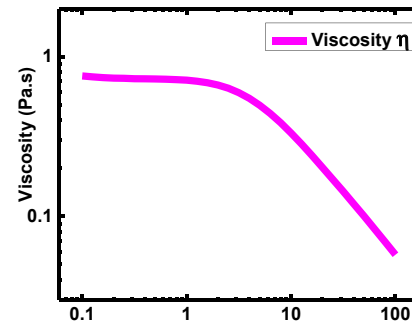
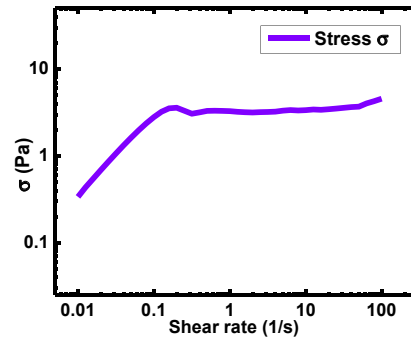
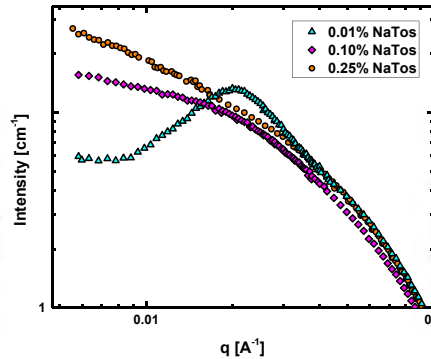
→ steady shear

Simultaneous
elastic, **viscous**

responses

across gap

→ LAOS



High Branching

Screened interactions

Shear thinning only

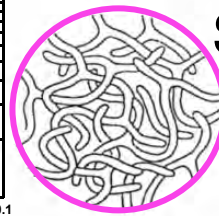
→ inhibits banding

Viscous response

only across gap

→ inhibits material

stratification

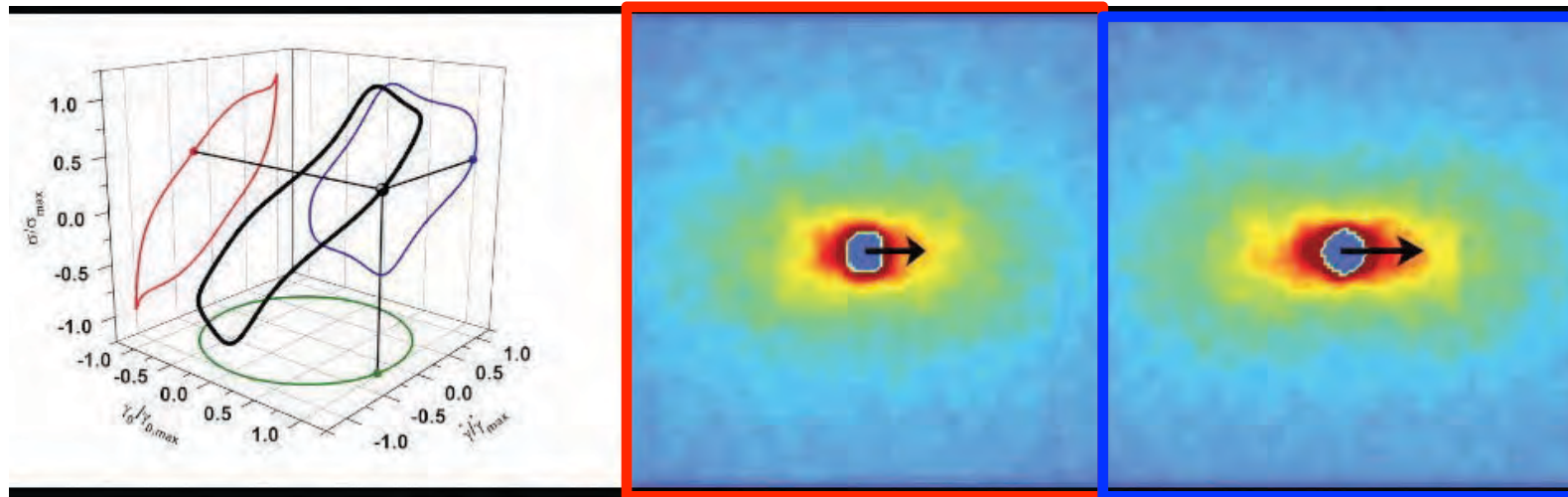


Disentangled high shear state of WLMs

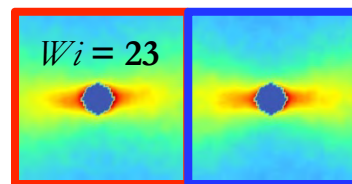
[$De = 2.3$, $Wi = 23$]

Please click on the movie below to play it:

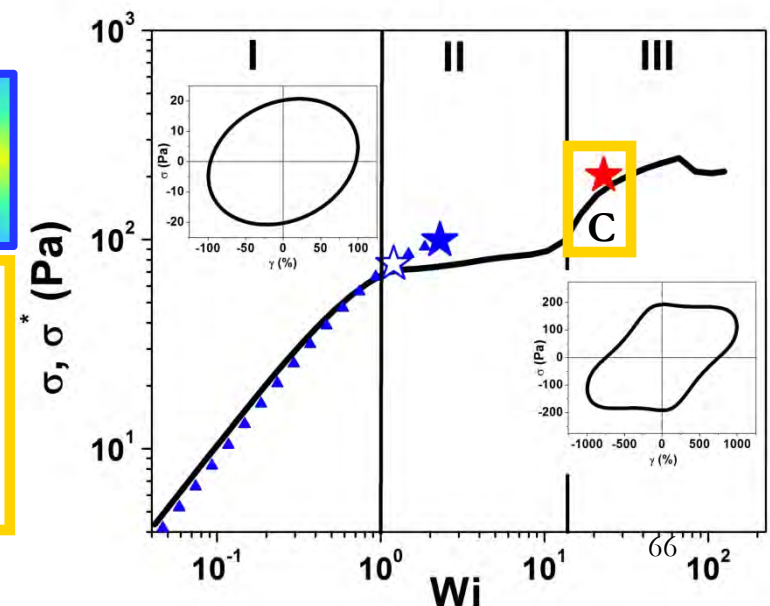
SANS arrow's magnitude and direction defines the degree of alignment and angle of orientation respectively.



Microstructure at two positions across the gap for comparable steady shear Wi .

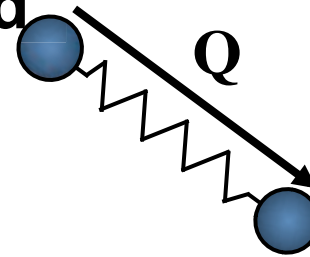


For LAOS of equivalent Wi as region III, a highly aligned, oriented microstructure persists throughout the oscillatory cycle. The materials is largely shear thinning and less viscoelastic than the previous two conditions.

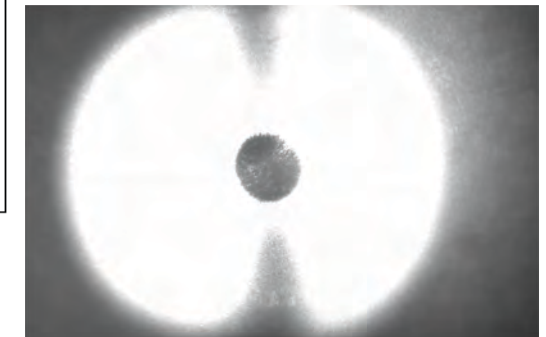
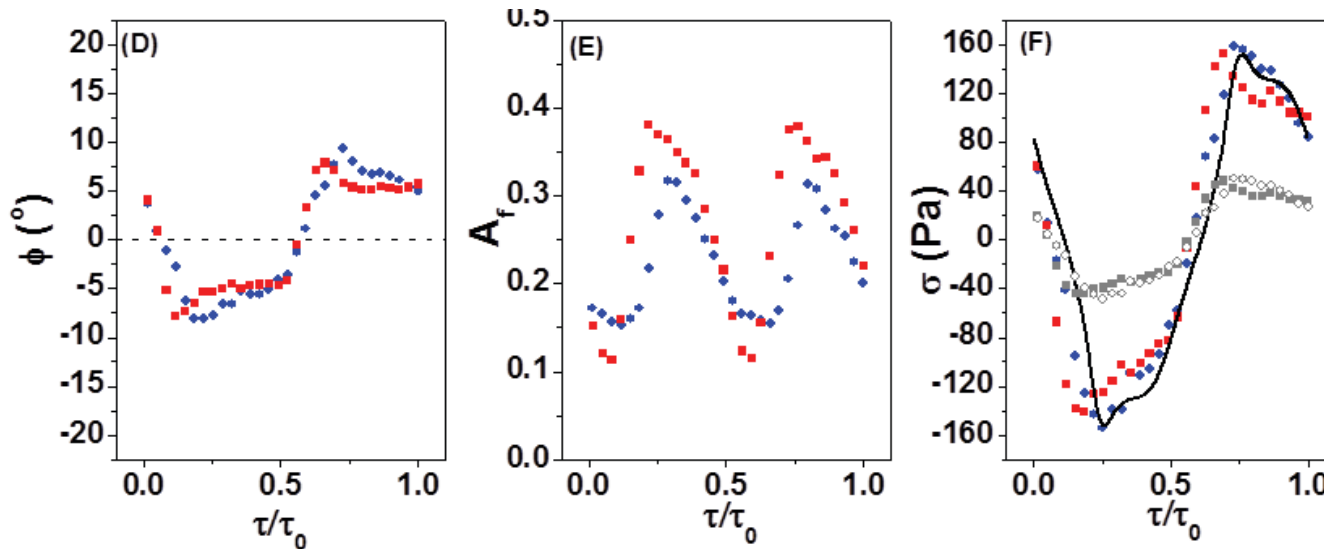


LAOS stress of the disentangled high shear state of WLMs

[$De = 2.3$, $Wi = 23$]



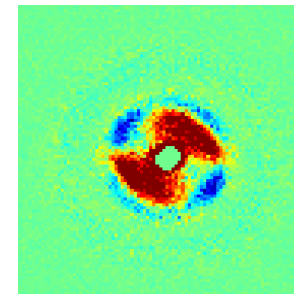
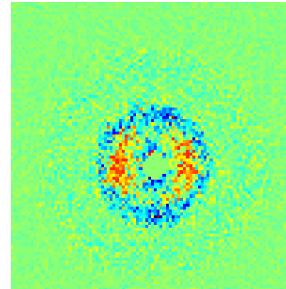
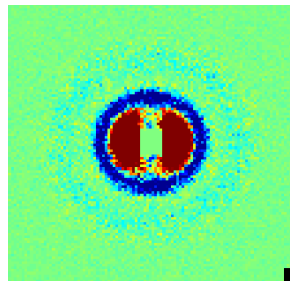
$$\sigma \propto \langle QQ \rangle$$



The stress-SANS rule using the segmental microstructure fails to predict the rheology stress however, the rheo-SALS experiments show a persistent butterfly pattern during the oscillation. Evidence of a supra-molecular state that cannot relax during the oscillation cycle indicates that shear induced demixing occurs during LAOS.



Kate Gurnon: Wed: 5:00-5:15pm **533h** Continental 6, Hilton
Rheology and Microstructure of Concentrated, Near Hard-Sphere Colloidal Dispersions Under Steady Shear and Large Amplitude Oscillatory Shear in All Three Planes of Shear



Wed. 12:30-1:00 PM *Golden Gate 8 (Hilton)*
Thomas Baron Award Lecture: Shear Thickening & Gelation in Colloidal Dispersions - Nonequilibrium States and Their Applications in Personal Protective Equipment



Understanding the nonlinear shear rheology of complex fluids - including polymers, self-assembling solutions, colloids and nanoparticle suspensions - is advanced by directly measuring the microstructure(s) responsible for the stress under deformation. Rheo-optics, direct visualization, rheo-NMR, and light and x-ray scattering under flow are among the various methods applied to a wide variety of model and industrial systems to aid in the development of structure-property relationships and often, to rationalize seemingly anomalous rheological behavior. These methods are often system specific, however, and a quantitative, robust, and broadly applicable method capable of measuring the full three-dimensional microstructure remains an experimental challenge. Indeed, some of the more interesting nonlinear effects, such as shear-banding and shear-induced phase transformations, where the flow-field and microstructure are intimately coupled, require the ability to resolve the microstructure both with spatial and time resolution.

In this presentation we review a robust and broadly applicable method using neutron scattering to measure the microstructure in all three planes of flow, and with spatial and time-resolution. Neutron scattering has a distinct advantage as most materials are amenable to study by neutron scattering, unlike x-Ray and light scattering. Further, truly unique experiments are possible by selective isotopic substitution, which allows probing components in a mixture by contrast matching. We have addressed this challenge by developing a Couette geometry to access the 1-2 (velocity-velocity gradient plane of flow) by small angle and ultra-small angle neutron scattering. Further, spatial resolution of order 100 microns is achieved by an aperture that scans across the flow. Combined with a now commercial, rheo-SANS Couette geometry that enables radial (velocity-vorticity) and tangential (velocity gradient-vorticity) measurements, these instruments provide the first measurements of microstructure in all three projections of the flow and thus, reconstructing the full, three dimensional flowing microstructure. Further, time dependent deformations that are often used to test physically-based constitutive models, such as flow start-up and large amplitude oscillatory shear (LAOS), are probed by stroboscopically synchronizing the deformation field and the scattered neutron collection through time stamping and binning methods. Finally, neutron scattering is an absolute scattering method such that local chemical composition can also be measured under flow. This enabled determining such effects as shear-induced concentration gradients. These instruments are now available for use by the community at the Institute Laue Langevin in Europe and at the NIST Center for Neutron Research in the U.S.

Recent results for the shear-crystallization of self-assembled block copolymer micelles in ionic liquids under LAOS, the shear banding of worm-like micelles under start-up flow, and the time-dependent microstructure of shear thickening colloidal dispersions and colloidal gels under LAOS are presented to demonstrate the breadth of the method and how these measurements provide fundamental microstructural data essential for understanding the rheology, as well as for critically testing rheological constitutive models of these complex fluids.

Experimental System

6 wt% cetylpyridinium chloride/sodium salicylate
([NaSal]/[CPyCl]=0.5) in 0.5M NaCl/D2O brine

Linear viscoelastic response:

- Nearly Maxwellian behavior

$$G'(\omega) = \frac{G_0(\lambda\omega)^2}{1+(\lambda\omega)^2}$$

$$G''(\omega) = \frac{G_0(\lambda\omega)}{1+(\lambda\omega)^2} + \eta_\infty \omega$$

Rehage & Hoffman, Mol. Phys. **74**, 933 1991

Relaxation time:

$$\lambda = 0.42 \text{ s}$$

Plateau modulus:

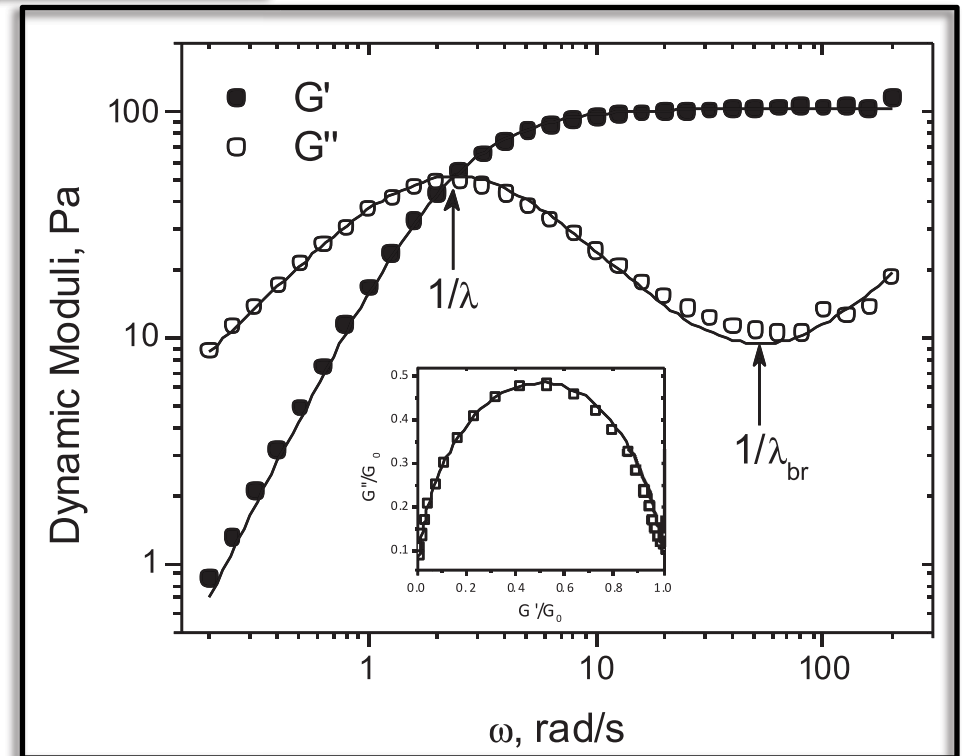
$$G_0 = 103.2 \text{ Pa}$$

Breakage time:

$$\lambda_{br} = 0.0019 \text{ s}$$

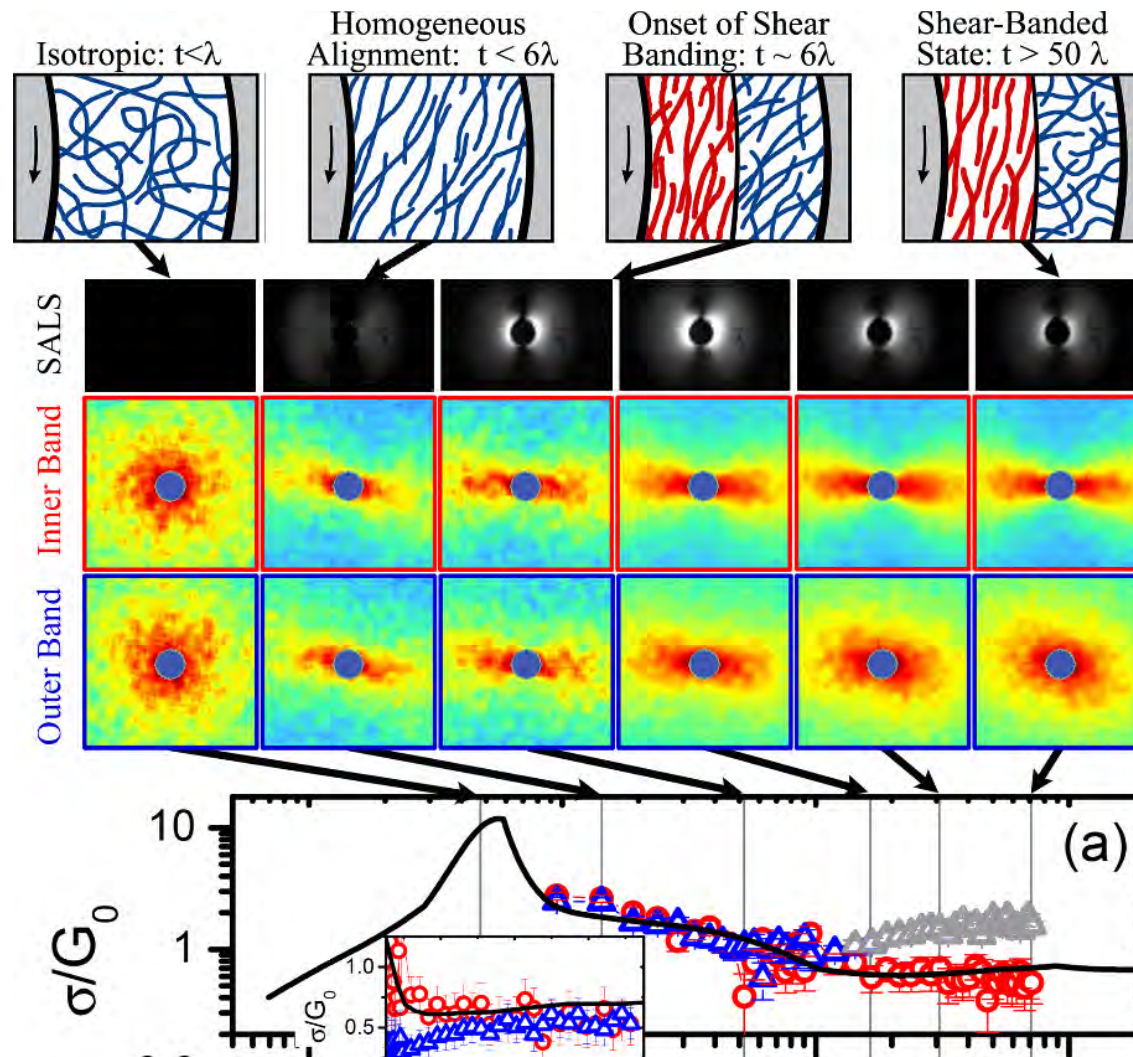
Reptation time¹:

$$\lambda_{rep} = \lambda^2 / \lambda_{br} = 9.2 \text{ s}$$



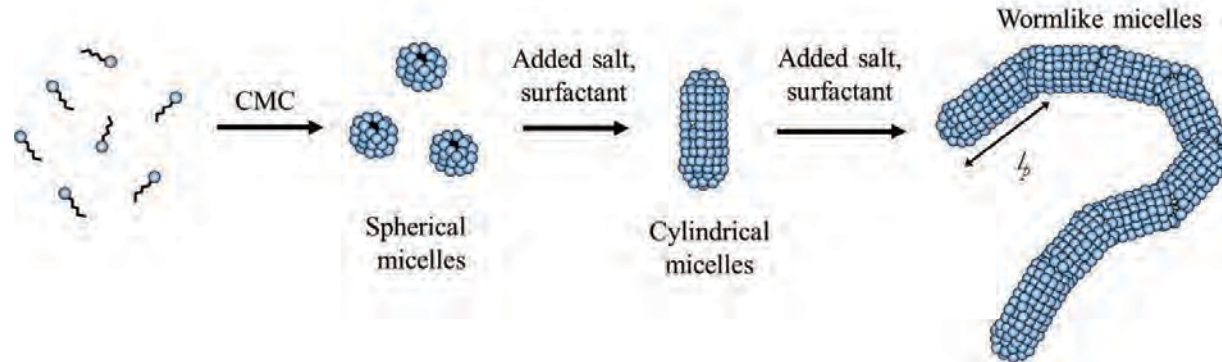
¹Cates, J. Phys.: Condens. Matter **8**, 9167, 1996

Conclusions for start-up flows of WLMs



Wormlike Micellar solutions (WLMs)

WLM formation with ionic surfactants:

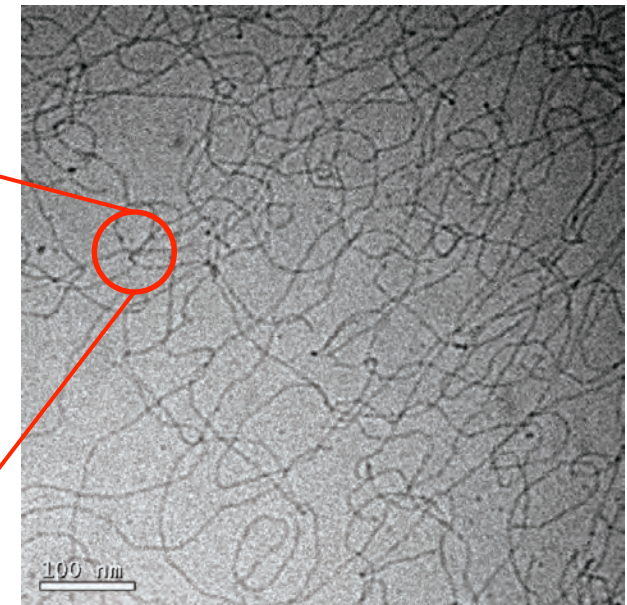


Relevant length scales in WLMs:

- Contour Length, L_c
- Entanglement length, l_e
- Mesh size, κ_M
- Persistence length, l_p
- WLM radius, r_{cs}



Schubert et al., Langmuir **19**, 4079, 2003

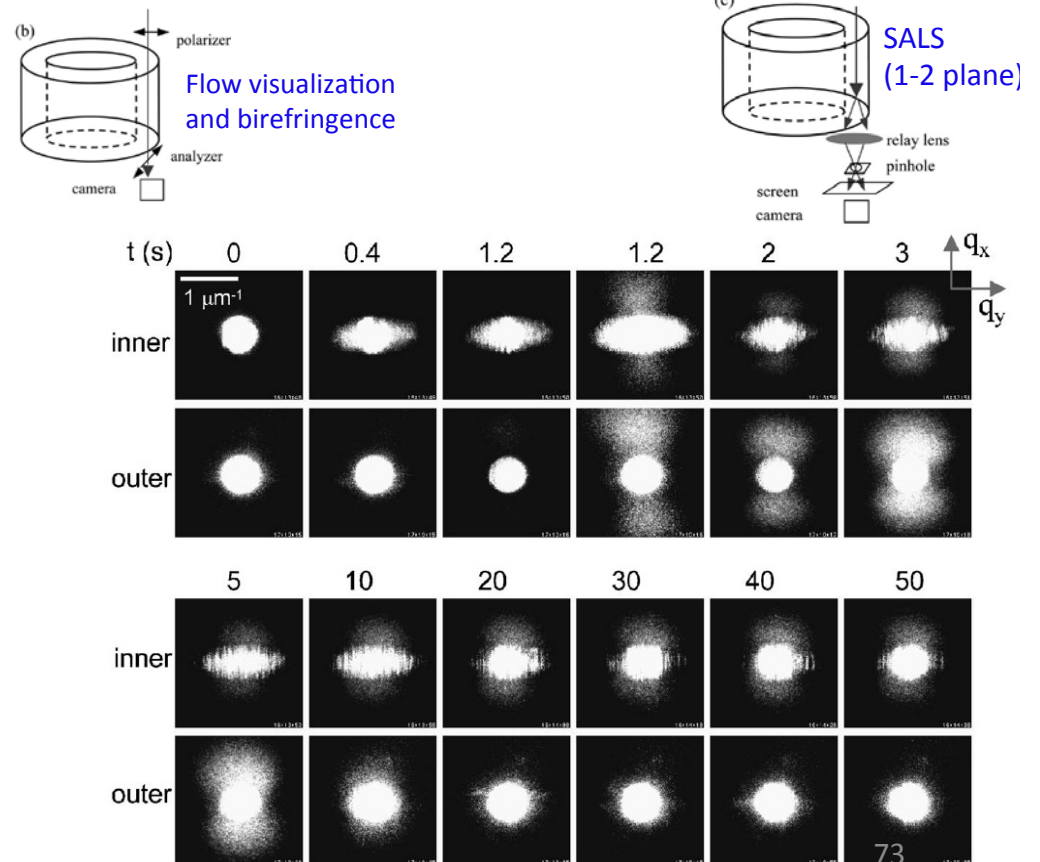
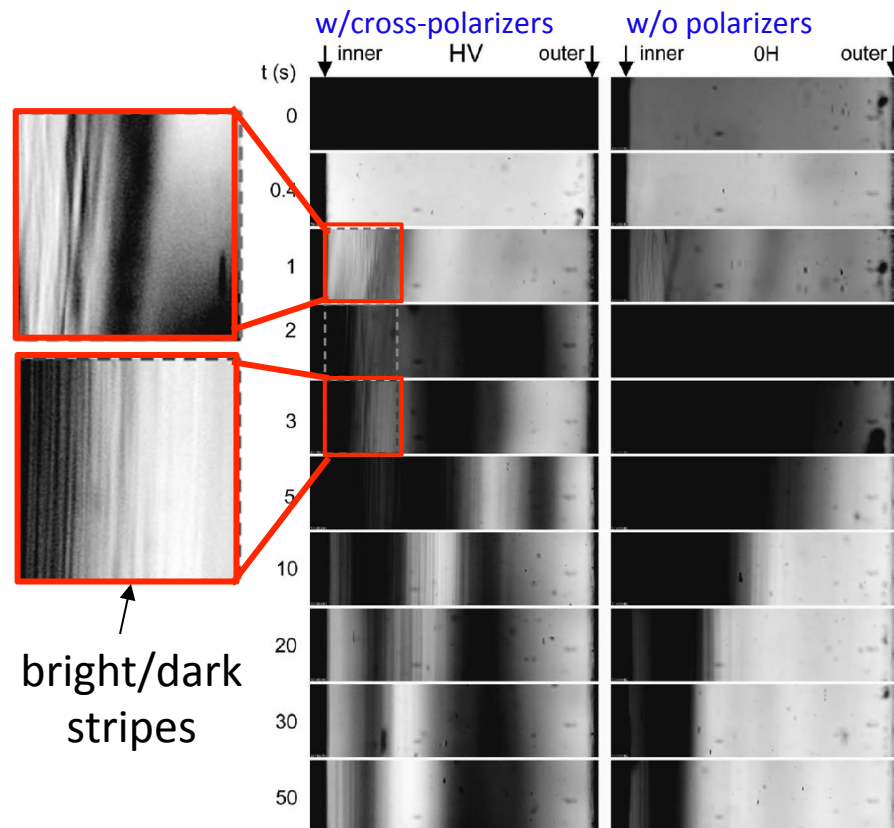
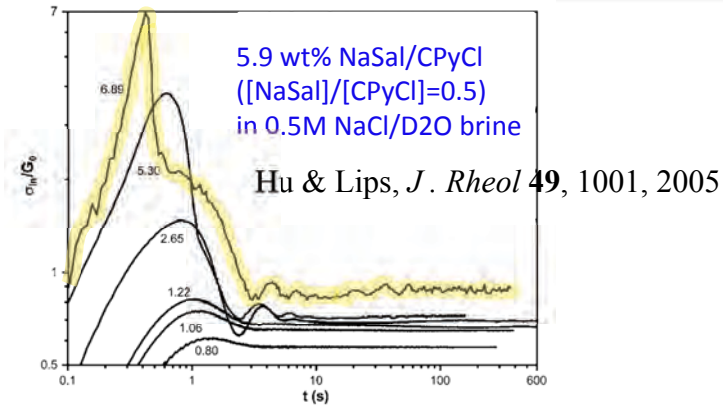


Length scales have been and can be obtained from birefringence, linear rheology and small-angle neutron scattering

Start-up shear flow (Previous Work)

Flow visualization and SALS:

- Before the stress peak: **homogenous** sample with **no scattering**.
- After peak: **bright/dark stripes** appear are neither spatially nor temporally fixed. Butterfly SALS patterns appear in both bands.
- After stress “shoulder”: Decrease in scattering. **Butterfly disappear** in outer band. The banded state is established.



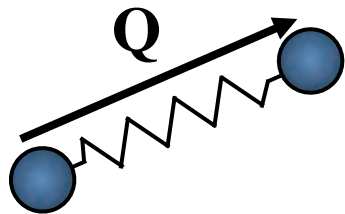
The Giesekus-diffusion (G-D) model¹¹: Shear banding and constitutive models

$$\nabla \tau_p = - \underbrace{\frac{1}{\lambda} \left(\mathbf{I} + \frac{\alpha}{G_0} \tau_p \right) \cdot \tau_p}_{\text{polymeric stress}} + 2G_0 \dot{\gamma} + \underbrace{D_\tau \nabla^2 \tau_p}_{\text{"diffusion"}} \rightarrow \tau = \tau_p + \underbrace{\eta_\infty \dot{\gamma}}_{\text{"solvent"}}$$

Bead-spring chains with anisotropic friction:

α : drag-orientation coupling parameter

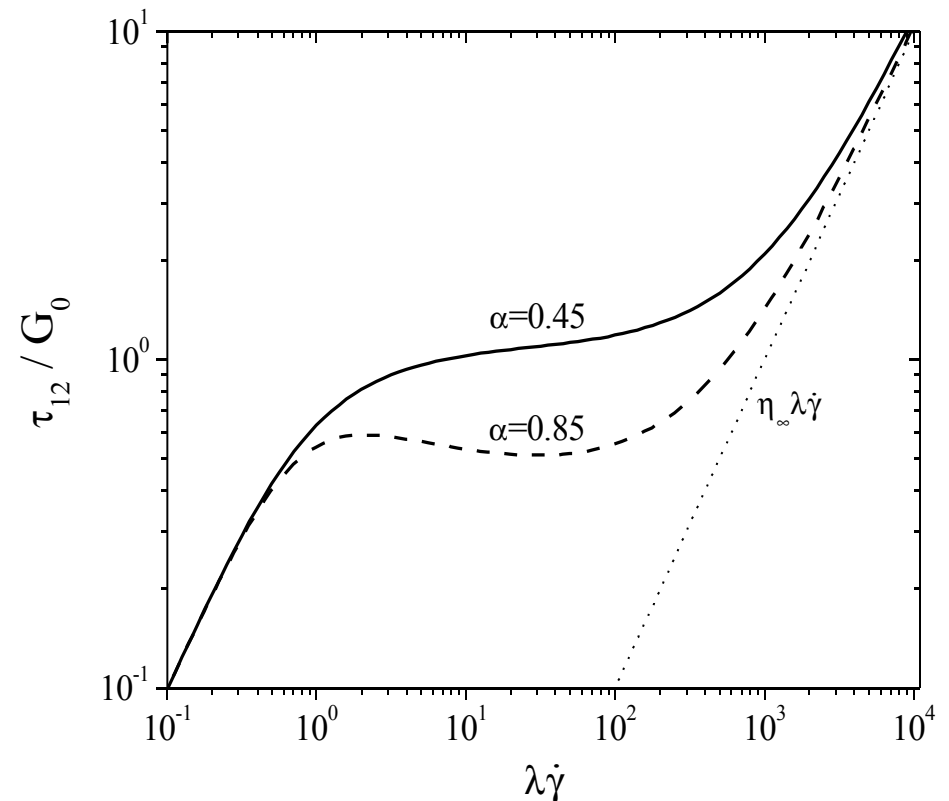
$$\zeta^{-1} = \frac{1}{\zeta} \left((1-\alpha)\mathbf{I} + \frac{\alpha H}{k_B T} \langle \mathbf{Q}\mathbf{Q} \rangle \right)$$



$\alpha < 0.5 \rightarrow$ monotonic

$\alpha > 0.5 \rightarrow$ non-monotonic

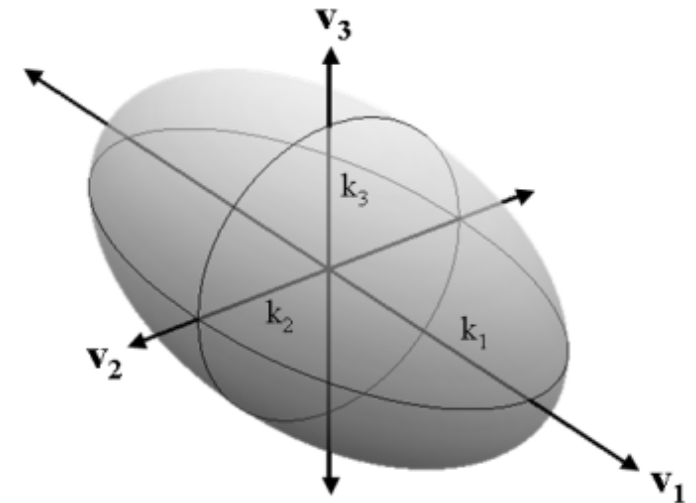
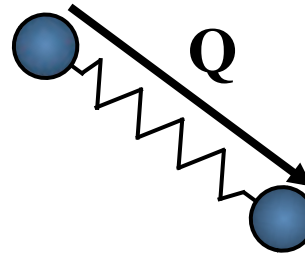
Model couples non-monotonic stress to anisotropic drag through α .



Linking rheology and orientational order

Kramers relation: $\langle \mathbf{Q}\mathbf{Q} \rangle = \mathbf{I} + \tau_p$

$$\text{Order tensor: } \mathbf{S} = \frac{\langle \mathbf{Q}\mathbf{Q} \rangle}{\text{tr} \langle \mathbf{Q}\mathbf{Q} \rangle} - \frac{1}{3} \mathbf{I}$$



Scalar parameters²:

- Orientation angle: $\cot(2\phi_0) = 2 \left(\frac{S_{22} - S_{11}}{S_{12}} \right)$

$$A_f = 3(k_1 + k_2) = 3(S_{11} + S_{22}) = \frac{\tau_{11} + \tau_{22}}{3G_0 + \tau_{11} + \tau_{22}}$$

- Alignment factor:

[1] H. Giesekus (1982) J. Non-Newt. Fluid Mech., 11(1-2): 69-109.

[2] Helgeson *et al.* (2009) Journal of Rheology, 53(3): 727-756.

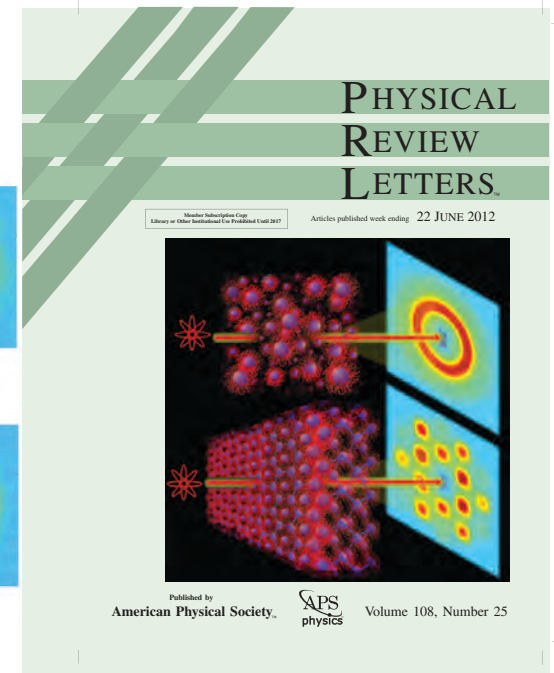
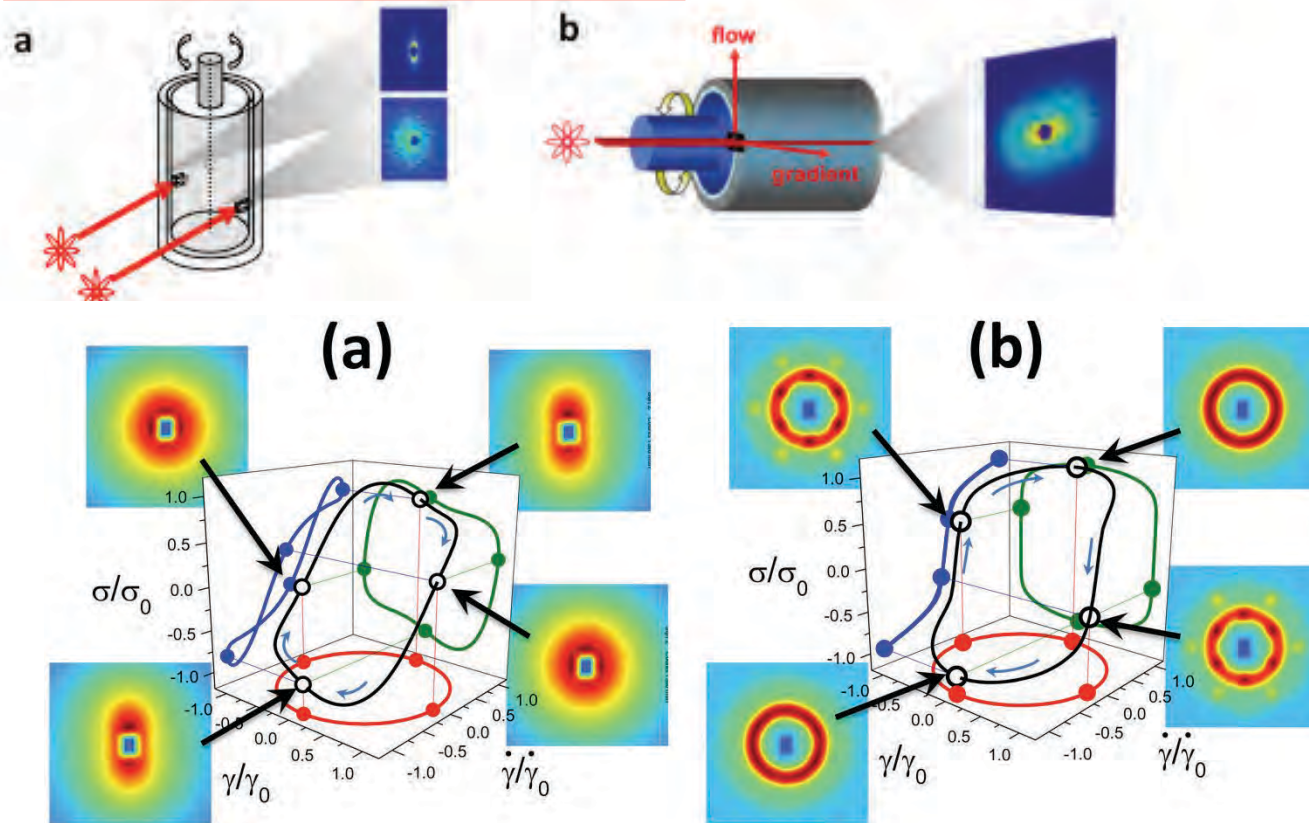
Flow-SANS and Rheo-SANS Applied to Soft Matter

Aaron P.R. Eberle & Lionel Porcar

Curr. Opin. Coll. Int. Sci. **17** (2012) 33-43

SOR Rheology Bulletin, July 2012

Lopez-Barron et al. , PRL 108 258301 (2012)



Goal:



Directly prove or refute the current scientific hypothesis concerning the local microstructural evolution of WLMs that leads to shear banding.

Acknowledgements & Co-authors



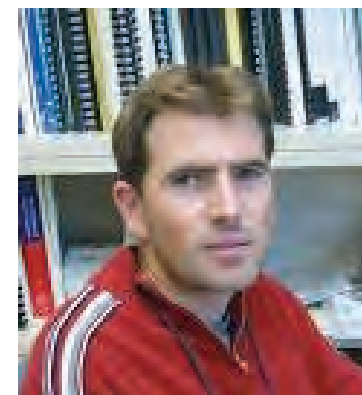
Kate Gurnon
PhD Student UD



Paul Butler
NCNR NIST



Carlos López-Barrón
ExxonMobil



Lionel Porcar
ILL Grenoble



Aaron Eberle
ExxonMobil



Matt Helgeson
UCSB



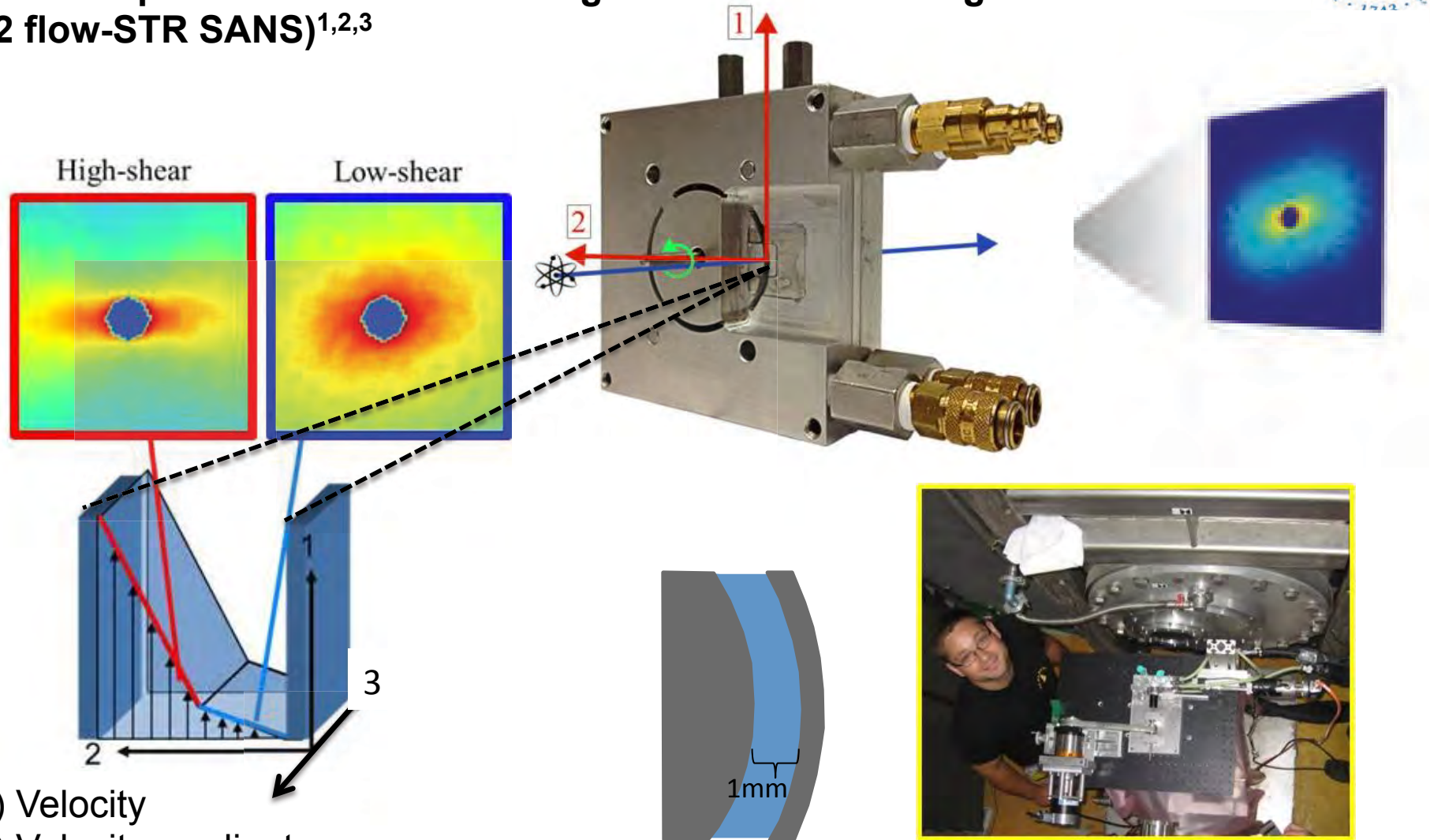
Florian Nettesheim
DuPont Analytical



Matt Liberatore
CSM

New sample environment: shear cell

SpatioTemporal Resolved Small Angle Neutron Scattering
(1-2 flow-STR SANS)^{1,2,3}



- (1) Velocity
- (2) Velocity gradient
- (3) Vorticity



Aaron Eberle

[1] A. Eberle and L. Porcar (2012) *Current Opinion in Colloid and Interface Science* 17(1): 33-43.

[2] [A. Kate Gurnon](#), P. Douglas Godfrin, Norman J. Wagner, Aaron P. R. Eberle, Paul Butler, Lionel Porcar JOVE 2014

[3] M. Liberatore et al. *Phys. Rev. E* **73**, 020504 (2006).

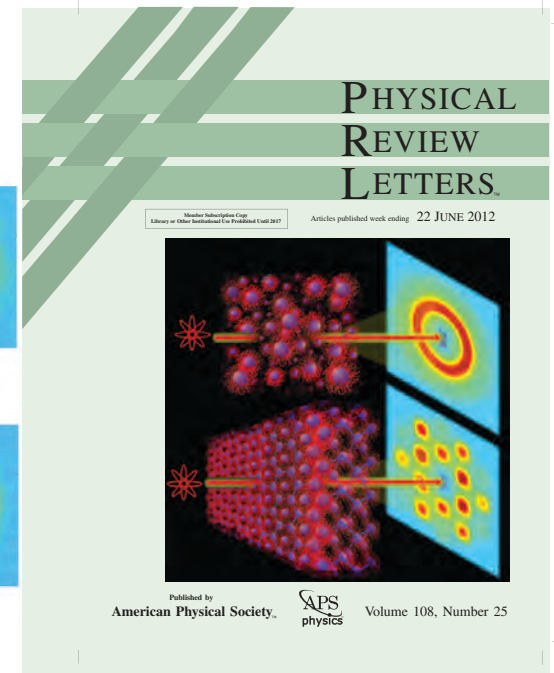
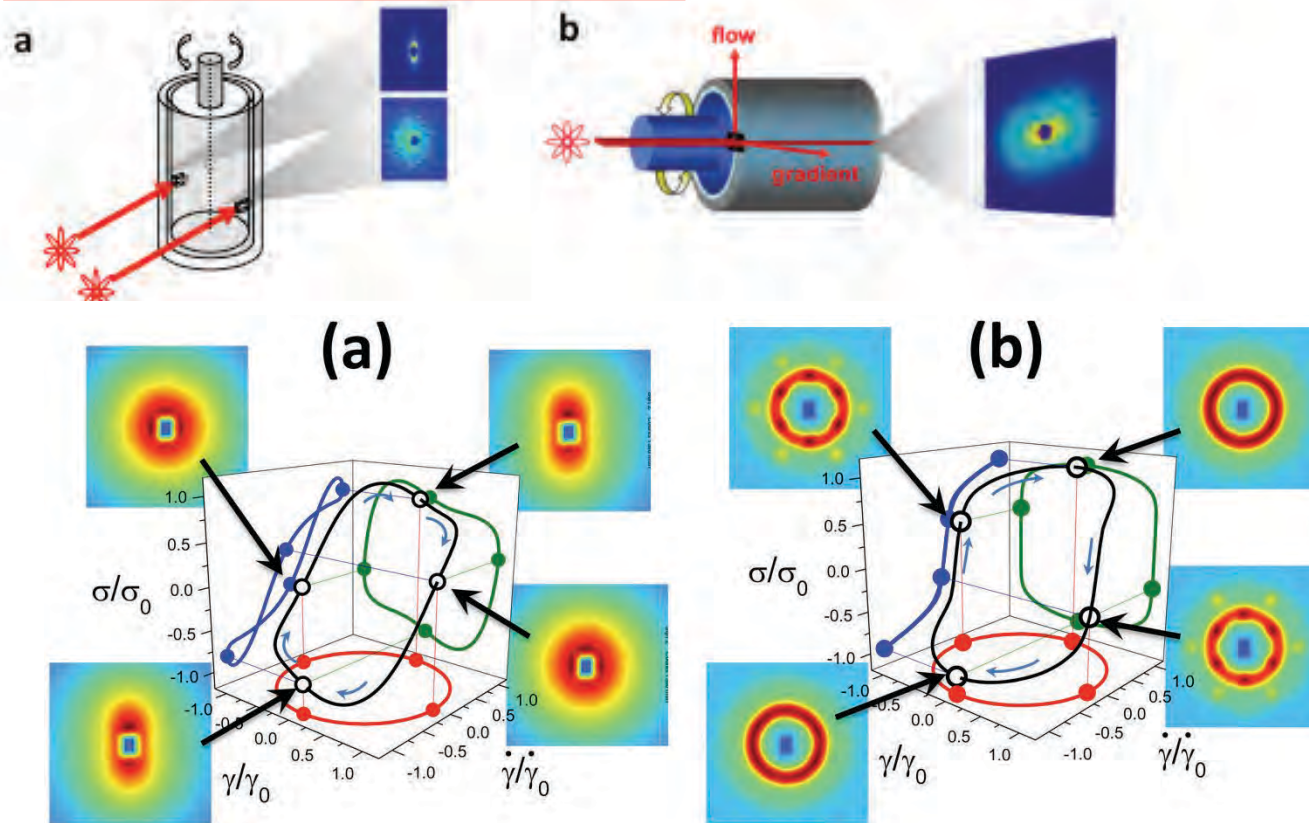
Flow-SANS and Rheo-SANS Applied to Soft Matter

Aaron P.R. Eberle & Lionel Porcar

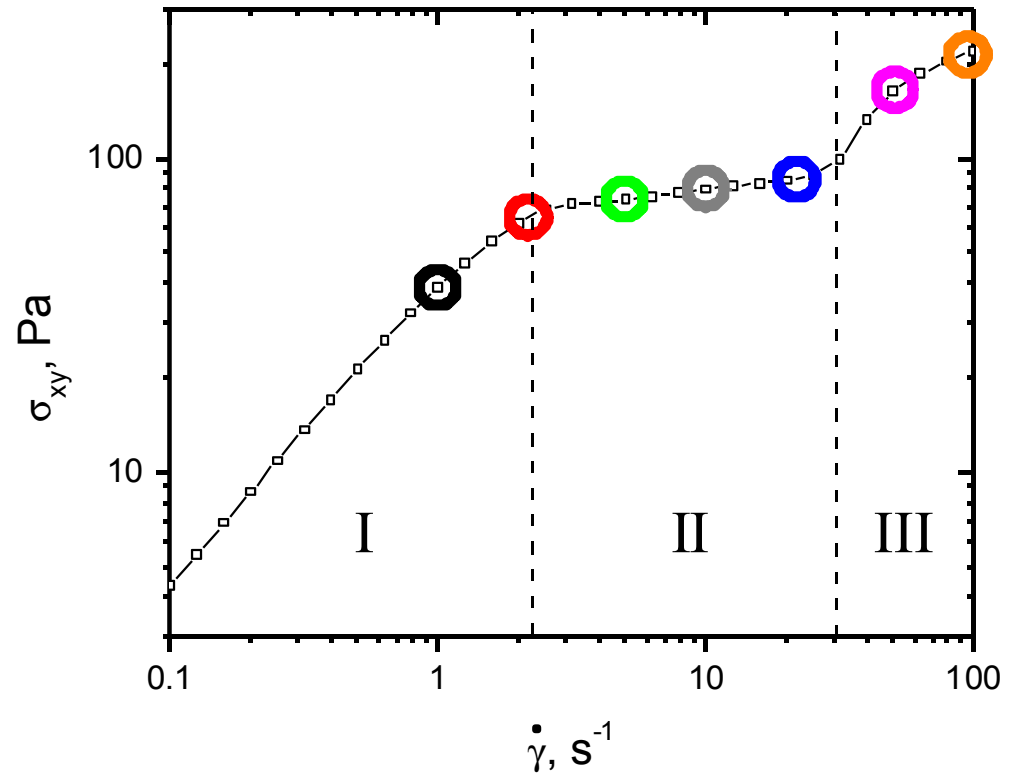
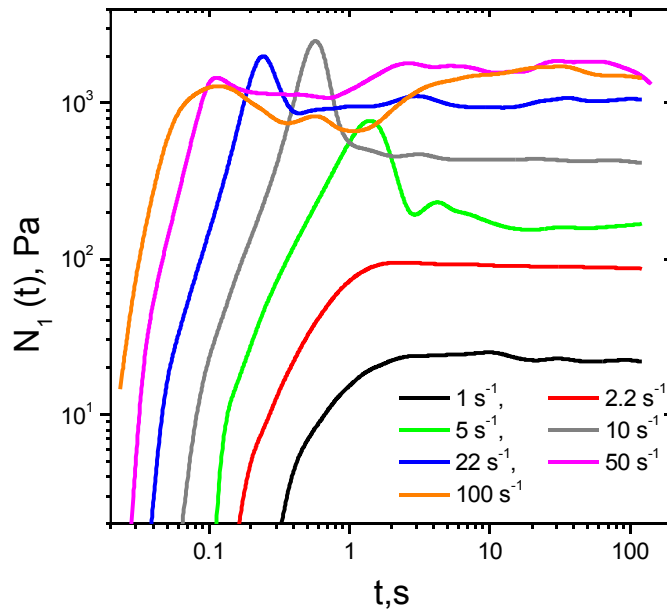
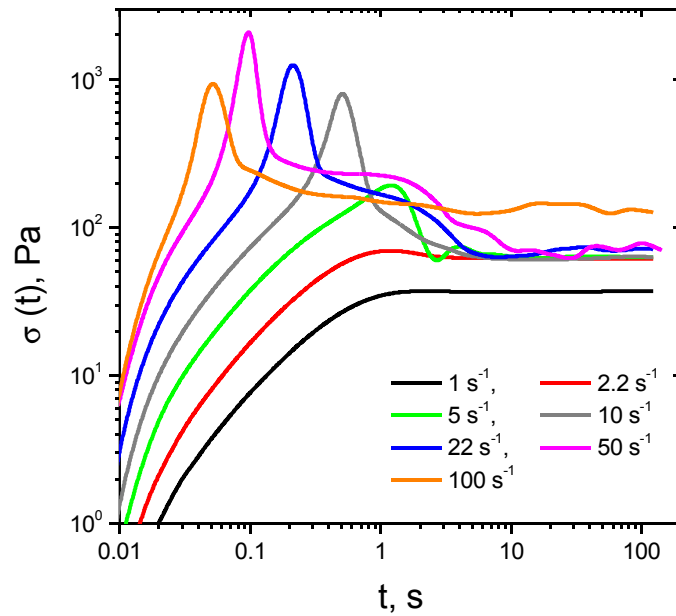
Curr. Opin. Coll. Int. Sci. **17** (2012) 33-43

SOR Rheology Bulletin, July 2012

Lopez-Barron et al. , PRL 108 258301 (2012)



Transient (start-up) flow

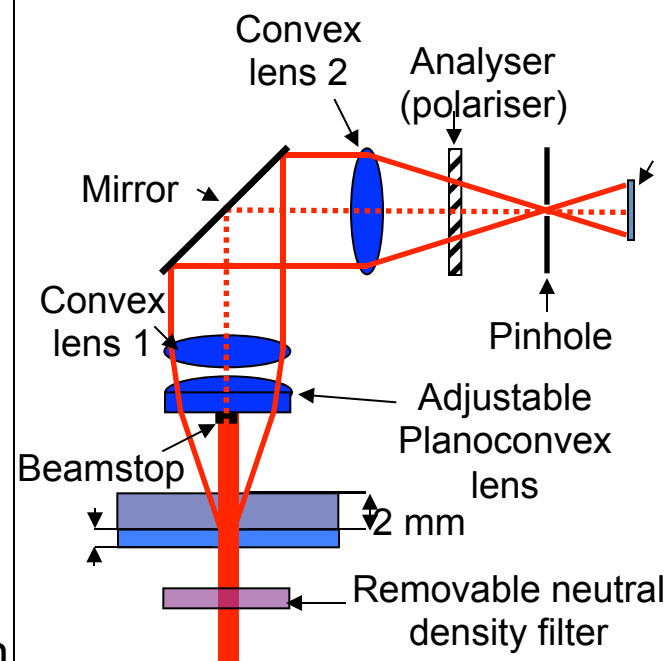
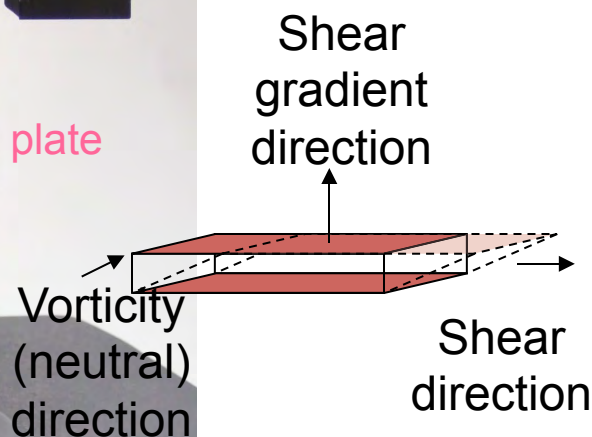
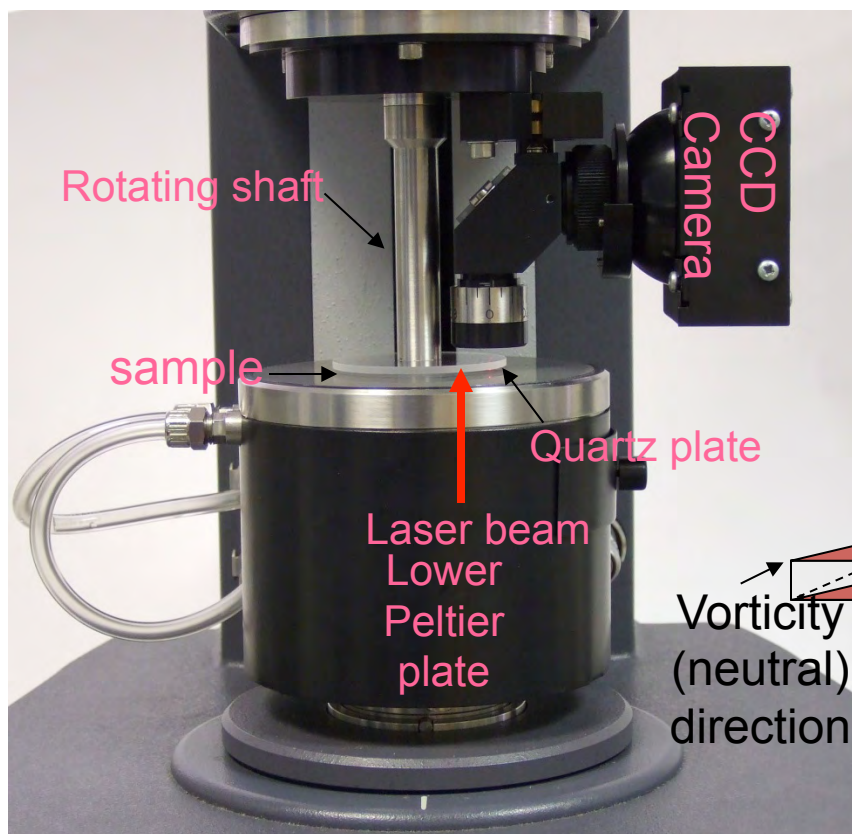


Stress and Normal stress **overshoots** appear in shear **region II**



Thareja et al. JOR 2012

Rheo-SALS Experimental set up



<http://www.tainstruments.com>

Incident light travels in the **shear gradient** direction, so that the scattering is in the plane of the **shear** and **vorticity** directions.

Butterfly Patterns & Shear Induced Concentration Fluctuations in Polymer Solutions

Thareja et al. JOR 2012

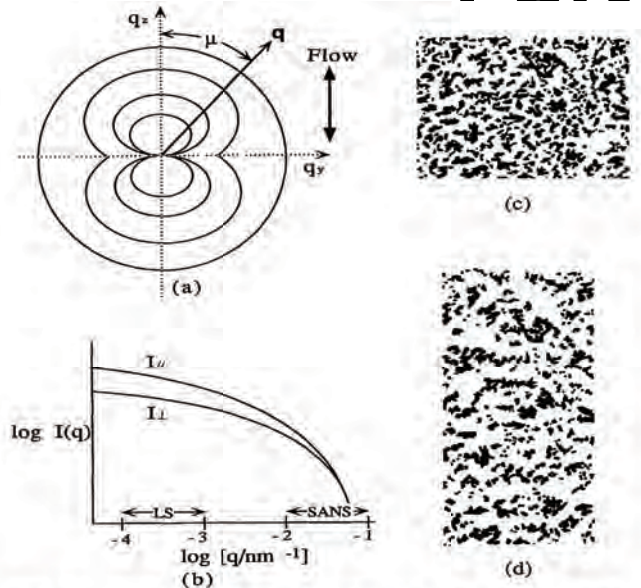
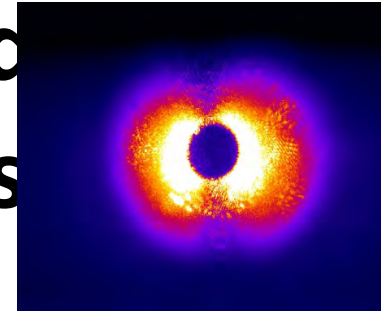
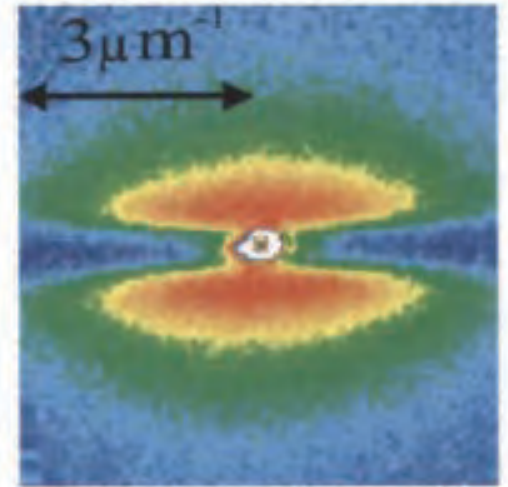


Fig. 4. Sketches of butterfly pattern (a), the intensity distributions $I_{\parallel}(q)$ and $I_{\perp}(q)$ (b), the clusters (the dark regions containing more entanglements and less subjected to deformation) in the quiescent state or at $\dot{\gamma} < \dot{\gamma}_c$ (c) and at $\dot{\gamma} > \dot{\gamma}_c$ (d).

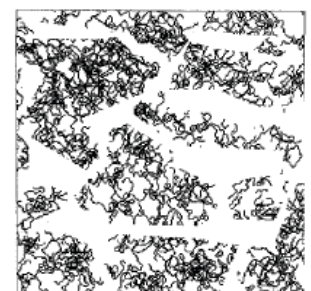
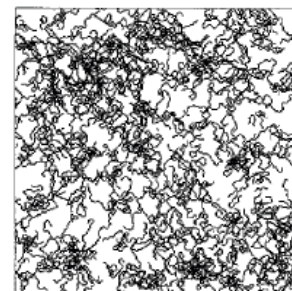
- Predicted for heterogeneous polymer networks by Bastide, Leibler and Prost, *Macromol.* 1990

- Extended to explain shear-induced concentration fluctuations in polymer solutions by Hashimoto and Kume, *J. Phys. Soc. Jap.* 1992

- Observed for shearing wormlike micelles by van Egmond (1997) and others...

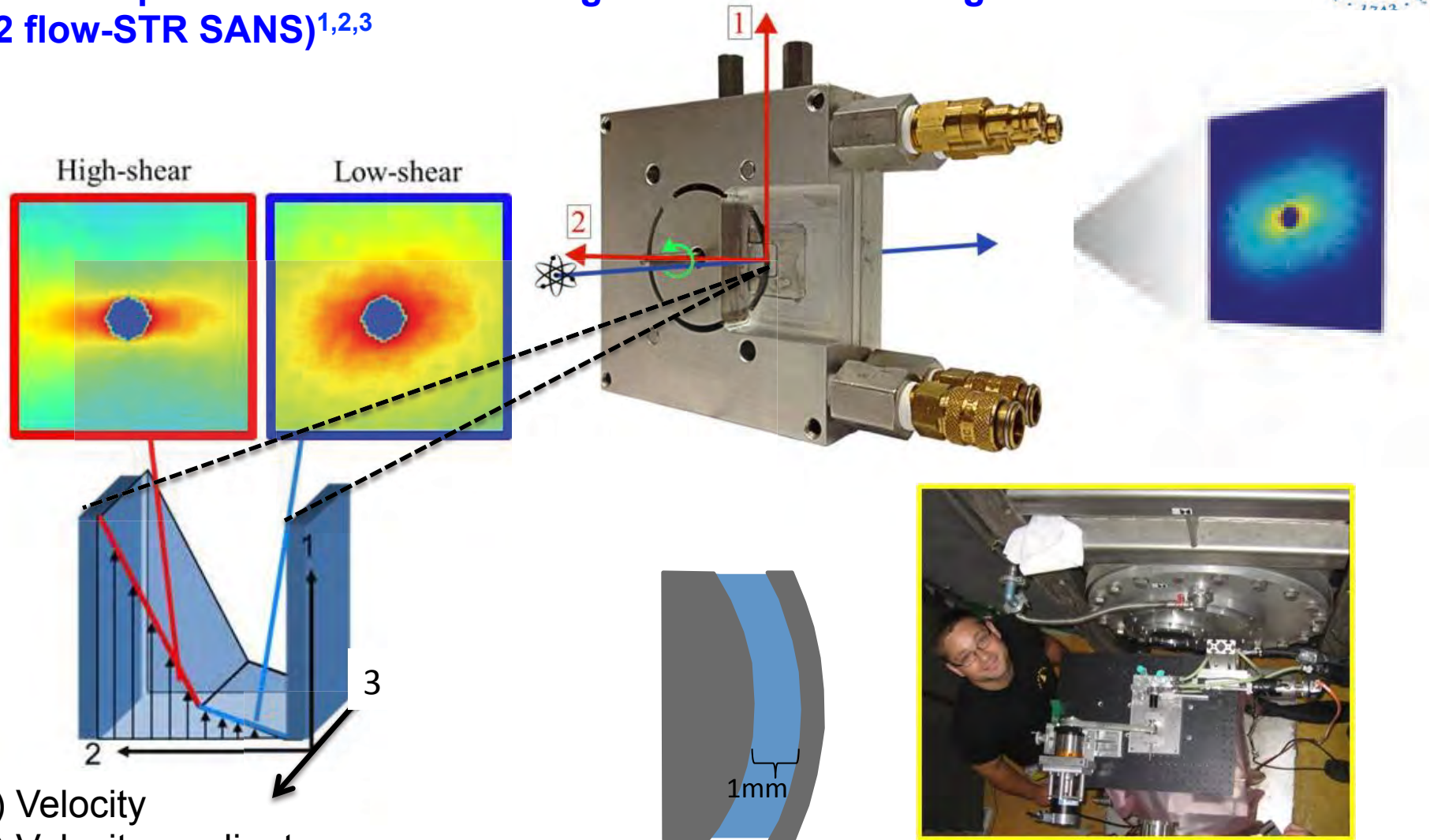


Hashimoto and Kume, *J. Phys. Soc. Jap.* 1992



New sample environment: shear cell

SpatioTemporal Resolved Small Angle Neutron Scattering
(1-2 flow-STR SANS)^{1,2,3}



- (1) Velocity
- (2) Velocity gradient
- (3) Vorticity



Aaron Eberle

[1] A. Eberle and L. Porcar (2012) *Current Opinion in Colloid and Interface Science* 17(1): 33-43.

[2] [A. Kate Gurnon](#), P. Douglas Godfrin, Norman J. Wagner, Aaron P. R. Eberle, Paul Butler, Lionel Porcar JOVE 2014

[3] M. Liberatore et al. *Phys. Rev. E* **73**, 020504 (2006).